Physics Lib

VOLUME 41 SECOND SERIES NUMBER 4

THE PHYSICAL REVIEW

PUBLISHED BY THE

AMERICAN INSTITUTE OF PHYSICS
INCORPORATED

UNDER THE EDITORIAL SUPERVISION OF THE

AMERICAN PHYSICAL SOCIETY

BOARD OF EDITORS

Managing Editor, JOHN T. TATE, University of Minnesota, Minneapolis
Assistant Editor, J. W. BUCHTA, University of Minnesota, Minneapolis
K. F. HERZFELD, A. W. HULL, F. W. LOOMIS, A. J. DEMPSTER, DAVID M. DENNISON, J. C. SLATER, R. C. GIBBS, E. O. LAWRENCE, J. H. VAN VLECK

AUGUST 15, 1932

Energies of Cosmic-Ray Particles — CARL D. ANDERSON 405
Scattering of X-Rays from Solids — ALLEN W. COVEN 432
Sum Rules for Atomic Transition Probabilities — J. P. VINTI 433
Multiplet Splitting and Intensities of Intercombination Lines. Part I. — HOBE C. WOLFE 448
Isotope Shift in Hyperfine Structure — JENNY E. ROSENTHAL AND G. BREIT 459
Isotope Separations in the Infrared Absorption Spectrum of HCl and the Possible Existence of a Chlorine Isotope of Mass 39 — J. D. HARDY AND G. B. B. M. SUTHERLAND 471
Spectra of Na II, III, and IV in the Extreme Ultraviolet — BRUCE B. VANCE 480
Absorption Spectrum of Benzene in the Region of 6.75μ — S. SILVERMAN 486
Theory of the Faraday Effect in Molecules — ROBERT SERBER 489
Experiments on the Nature of Ferromagnetism — FRANCIS BITTER 507
Thermoelectric Power of Single Crystal Bismuth near the Melting Point — ADOLF SOMMER 516
Acoustic Resonator Interferometer: II. Ultrasonic Velocity and Absorption in Gases — J. C. HUBBARD 523
Mutual Impedance of Grounded Wires above the Surface of the Earth — RONALD M. FOSTER 536
Letters to the Editor — 551
Frequency of Resonance Radiation — S. A. KNIPP 551
Use of Argon in the Ionization Method of Measuring Cosmic Rays — ARTHUR H. COMPTON AND JOHN J. HOPFIELD 560
Strain and Magnetic Orientation — LEWI TONKS AND K. J. SIXTUS 560
Electrons as Cosmic Rays — W. F. G. SWANN 560
Book Reviews — 562
Current Literature of Physics

THE AMERICAN INSTITUTE OF PHYSICS INCORPORATED
41 EAST 50th STREET, NEW YORK, N. Y.

THE AMERICAN PHYSICAL SOCIETY

OFFICERS OF THE SOCIETY

President:	W. F. G. Swann	Bartol Research Foundation, Philadelphia, Pa.
Vice-President:	Paul D. Foote	The Gulf Companies, Pittsburgh, Pa.
Secretary:	W. L. Severinghaus	Columbia University, New York City
Treasurer:	G. B. Pegram	Columbia University, New York City
Editor:	John T. Tate	University of Minnesota, Minneapolis, Minn.
Local Secretary for the Pacific Coast:	L. B. Loeb	University of California, Berkeley, Calif.

THE PHYSICAL REVIEW

Published by the American Institute of Physics under the editorial supervision of the American Physical Society. Four volumes annually, six issues per volume.

First series. From July 1, 1893, to January 1, 1913, the Review was conducted by Edward L. Nichols, Ernest Merritt and Frederick Bedell, with the financial support of Cornell University. The first four volumes were issued annually; subsequent volumes, semi-annually; thirty-five volumes in all.

Second series. On January 1, 1913, the Review was transferred to the American Physical Society as announced on the first page of the new series which was then begun. Since then it has been conducted by a Board of Editors elected by the Society. Volumes 1-38 are semi-annual, beginning in January and July of each year from 1913 to 1931. Volumes 1-33 contain six issues each. Volumes 34-38 twelve issues. Beginning with Volume 39 there will be four volumes per year of six issues each.

Contributors are referred to page 2 of the advertisements for further information.

Annual subscription, throughout the Postal Union, $12.00 in advance.

General index, 1893-1920, $4.00 in advance.

Back Volumes. Volumes 1-38, $9.00 per volume; Volume 39, $4.50; Back Numbers, $1.50 per copy for issues prior to July 1, 1929 (Vols. 1-33), $.75 per copy for issues subsequent thereto. Postage is free if remittance accompanies order; otherwise postage is extra. No bound volumes can be supplied. The Review offers to purchase a limited number of First Series, Vol. 1, No. 1 (at $2.00 each); Second Series, Vol. 7, No. 1, January 1916; Vol. 7, No. 2, February 1916; Vol. 7, No. 4, April 1916; and Vol. 7, No. 5, May 1916 (at $2.00 each).

Advertisements. Rates will be supplied by the Editor on request. Copy for each number must be received at Minneapolis two weeks prior to the dates of issue; old copy is used until new copy is received. Send electrotypes direct to printers, George Banta Publishing Co., Menasha, Wis.

Discount of ten percent is allowed to members of the American Physical Society on purchase of back numbers.

Changes of Address and Complaints of failure to receive the Review, in the case of members of the Physical Society, should be addressed to the Treasurer; in the case of other subscribers, to the Editorial Secretary. New copies can be sent free in response to complaints of non-delivery only if notice of non-delivery is received within three months of date of issue.

Manuscripts for publication should be submitted to the Editor, Physical Review, University of Minnesota, Minneapolis, Minn.

Proof and all correspondence concerning papers in process of publication should be addressed to the Editorial Secretary, American Institute of Physics, 11 East 38th Street, New York, New York.

Subscriptions, renewals, and orders for back numbers should be addressed to the Editorial Secretary, American Institute of Physics, 11 East 38th Street, New York, New York.

Entered at the post office at Menasha, Wis., as second class matter.
Acceptance for mailing at special rate of postage provided for in section 1103, Act of October 3, 1917, authorized September 6, 1926.

Second Series *August 15, 1932* *Vol. 41, No. 4*

THE

PHYSICAL REVIEW

Energies of Cosmic-Ray Particles

By CARL D. ANDERSON

California Institute of Technology

(Received June 28, 1932)

Cloud chamber photographs of cosmic-ray tracks in a magnetic field up to 17,000 gauss are shown. On the assumption that the particles producing the tracks are travelling downward through the chamber rather than upward, particles of positive charge appear as well as electrons. From the specific ionization along the track it is concluded that the positives are protons, and are not nuclei of charge greater than unity. No evidence is uncovered demanding the introduction of a neutron for cosmic-ray phenomena. Eight examples of associated tracks are shown. Energies range from below 10^6 electron-volts to values in a few cases of the order of 10^9 electron-volts. Energy values for 70 tracks are listed. The scattering of cosmic particles in traversing a 6.0 mm lead plate is measured.

AN AUTOMATIC, vertical Wilson expansion chamber operating in a strong magnetic field up to 21,000 gauss was designed for a study of the high-energy corpuscles associated with cosmic rays. The expansion chamber itself is 15 cm in diameter and has a depth of 2 cm. The axis of the piston lies in a horizontal plane in order to effect the most favorable position for photographing the cosmic-ray tracks. The magnetic field was found by direct measurement to be homogeneous to within 10 percent throughout the volume of the chamber. Photographs are taken through a hole in the pole piece of the magnet along the lines of force, thus revealing a particle deflected by the magnetic field as an arc of a circle on the photographic film. A description of the apparatus will follow in a later publication.

A brief discussion of the results has been published jointly with Professor R. A. Millikan,[1] to whom the writer is indebted for suggesting the investigation and cooperating in planning it, and whose keen interest throughout the course of the work has been of the greatest value.

Of the 3000 photographs taken to date, 62 show cosmic-ray tracks of length sufficient for energy measurements, 19 of which are here reproduced with addition of 3 photographs taken for test purposes. The photographs are 7/10 full size. The dark back ground in several of the photographs is due to light scattered by the back wall of the expansion chamber.

[1] Millikan and Anderson, Phys. Rev. **40**, 325 (1932).

In the test photograph of Fig. 2 appear tracks in air of the secondary electrons ejected by gamma-rays from Ra. Figs. 3 and 4 show alpha-particle trajectories.

The remainder of the tracks shown, Figs. 5–23, are ascribed to cosmic rays because of their high energy. Cosmic-ray tracks are in all cases readily distinguishable from alpha-particle tracks due to the very much greater specific ionization of the latter.

Positively Charged Particles

A charged particle will be deviated by the magnetic field into an arc of a circle. The sense of rotation in the chamber as viewed in the photographs will be clockwise for a particle of negative charge, and counter-clockwise for one of positive charge. The sign of the charge can be ascertained only if the

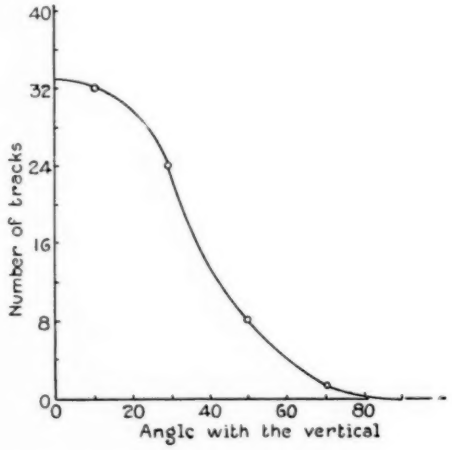

Fig. 1. The number of tracks per unit solid angle as a function of the angle with the vertical. Only those tracks are included whose curvature in the magnetic field is sufficiently small to allow a determination of the direction to be made. Therefore no electrons of energy less than 100×10^6 volts are included. This space-distribution in showing a large percentage of nearly vertical tracks differs from that reported by Skolbeltzyn.[2]

direction of motion of the particle is known. It is assumed here that the particles are traveling downward through the chamber. The small degree of scattering to be expected for high-energy particles, combined with the known fact that the rays come in from above, appears to justify this assumption. In Fig. 1 it is seen that the cosmic-ray tracks prefer the vertical direction over the horizontal indicating that backward or large angle scattering is infrequent.

In many instances on the above assumption as to the direction of motion, the tracks are deviated in a sense to indicate the presence of positively charged particles as well as electrons.

[2] Skobeltzyn, C. R. **194,** 118 (1932).

Fig. 2.

Fig. 3.

Fig. 2. 12,000 gauss. A test photograph showing tracks in air of secondary electrons ejected by gamma-rays from Ra, filtered through 2.5 cm of steel. The energies of the electrons range from 10^6 electron-volts down.

Fig. 3. 12,000 gauss. An α-particle trajectory of 3.85 cm range photographed in air.

Fig. 4.

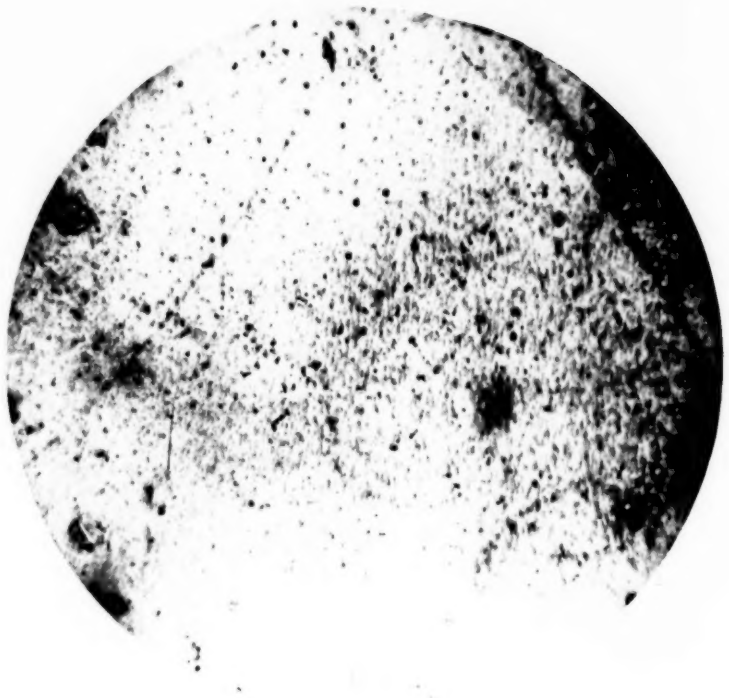

Fig. 5.

Fig. 4. 12,000 gauss. An α-particle trajectory photographed in helium, showing range of 10 cm.

Fig. 5. 17,000 gauss. A pair of associated tracks; at the left an electron of 120×10^6 volts energy, at the right a porton of 130×10^6 volts energy. Since protons and electrons, for a given velocity, have an equal specific ionization, then from the measurements of E. J. Williams and F. R. Terroux (Proc. Roy. Soc. **A126,** 300 (1929–30)) on the ionization by β-particles, the 120×10^6 volt-proton here is expected to ionize about $2\frac{1}{2}$ times as heavily as the electron.

Fig. 6.

Fig. 7.

Fig. 6. 17,000 gauss. A group of three tracks; at the left an electron of 30×10^6 volts energy, at the right probably a proton of 400×10^6 volts energy. The center track, perhaps a proton of 150×10^6 volts energy, lies in a different plane from the other two, and because of its length there is a difficulty in associating it with the other two. The probability of its appearing here by chance is, however, very slight. A small scattering is noted in the center track.

Fig. 7. 12,000 gauss. A proton of 20×10^6 volts energy and an electron of about 400,000 volts energy.

Fig. 8.

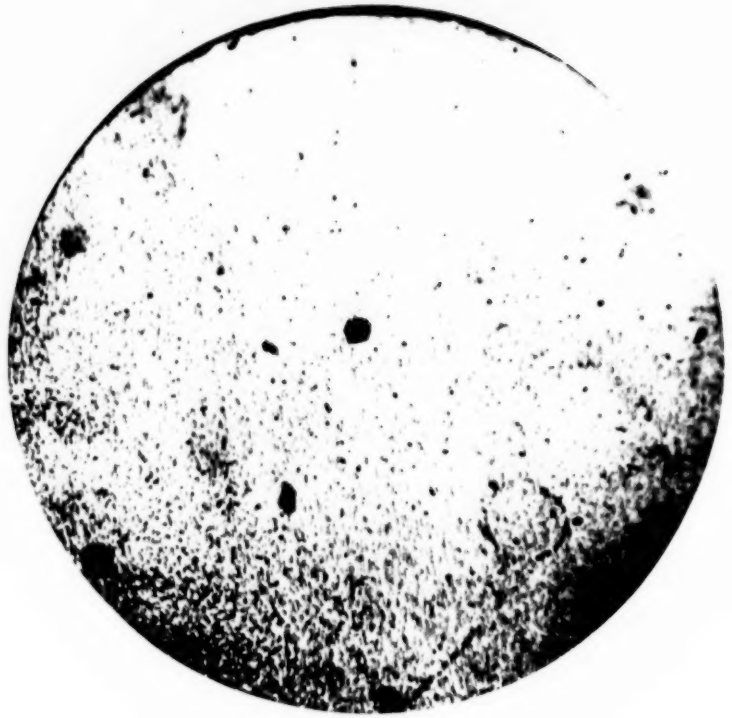

Fig. 9.

Fig. 8. 12,000 gauss. A plate of lead 6.0 mm thick extends horizontally across the chamber. Below the lead appear two tracks, one apparently a proton of about 100×10^6 volts energy, the other an electron of 11.4×10^6 volts energy which passes out through the 0.5 cm glass wall. Above the lead another electron enters through the glass wall, or perhaps the same electron after having been deflected into the chamber again by the magnetic field. It suffers a deflection of 80° upon striking the lead surface. Its energy is 8.2×10^6 volts. The assumption that the same electron re-entered the chamber above the lead is borne out by the fact that an energy loss of 3.0×10^6 volts is to be expected for an electron traversing the 0.5 cm glass wall twice as shown in the figure. The angle of divergence of the two associated tracks below the lead is 25°. (The track above the lead appears double due to a double reflection of the light before entering the camera.)

Fig. 9. 12,000 gauss. Two electrons of energy about 180×10^6 volts and 2×10^6 volts respectively.

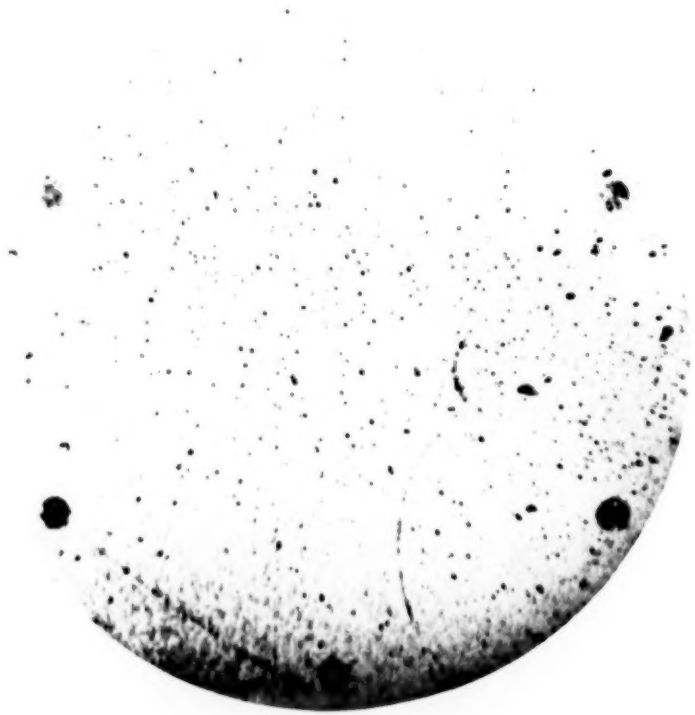

Fig. 10.

Fig. 11.

Fig. 10. 12,000 gauss. Two associated electrons moving upward through the chamber, of energy 170×10^6 volts and 11×10^6 volts respectively. A large angle scattering from the glass wall is noted.

Fig. 11. 12,000 gauss. An electron of 27×10^6 volts energy and probably a proton of 450×10^6 volts energy though the curvature here is small. A slight scattering is apparent.

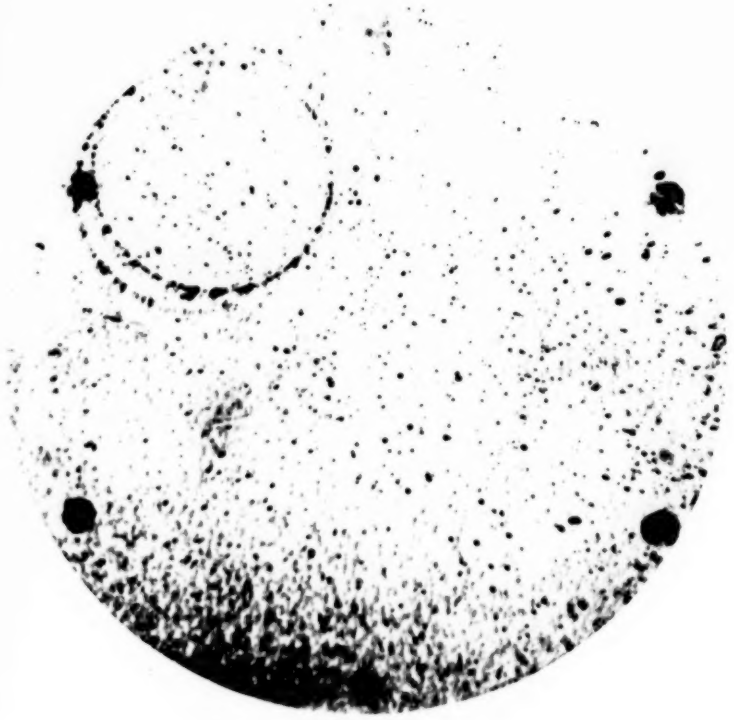

Fig. 12.

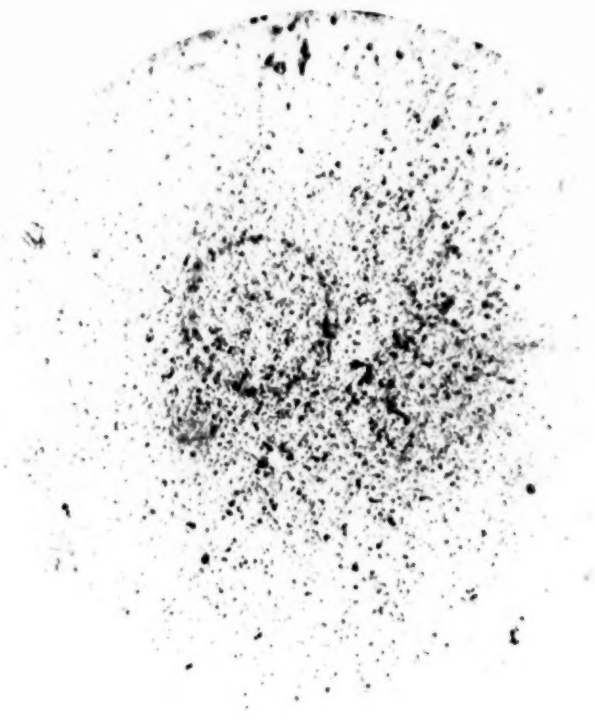

Fig. 13.

Fig. 12. 12,000 gauss. An electron of 8×10^6 volts energy. It is seen to make over $1\frac{1}{2}$ complete revolutions in the chamber. The displacement of the track from left to right is quantitatively explained by the fact that the magnetic field is 10 percent stronger at the center than at the edge of the chamber.

Fig. 13. 17,000 gauss. An electron of 7×10^6 volts energy.

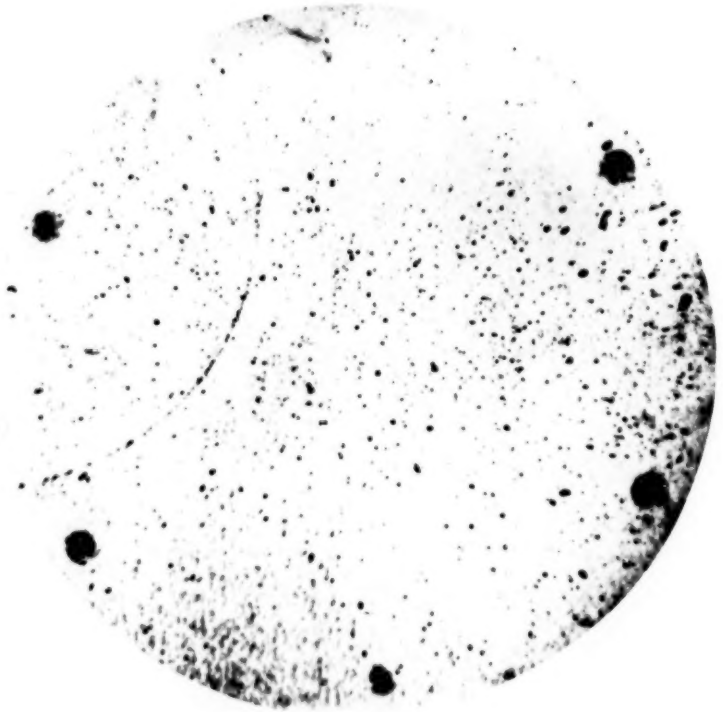

Fig. 14.

Fig. 15.

Fig. 14. 12,000 gauss. An electron of 18×10^6 volts energy.

Fig. 15. 12,000 gauss. An electron of 4.6×10^6 volts energy emerging from the lower surface of the lead. No track is seen entering the lead thus indicating a photon encounter. Above the plate to the left is another electron of 9×10^6 volts energy.

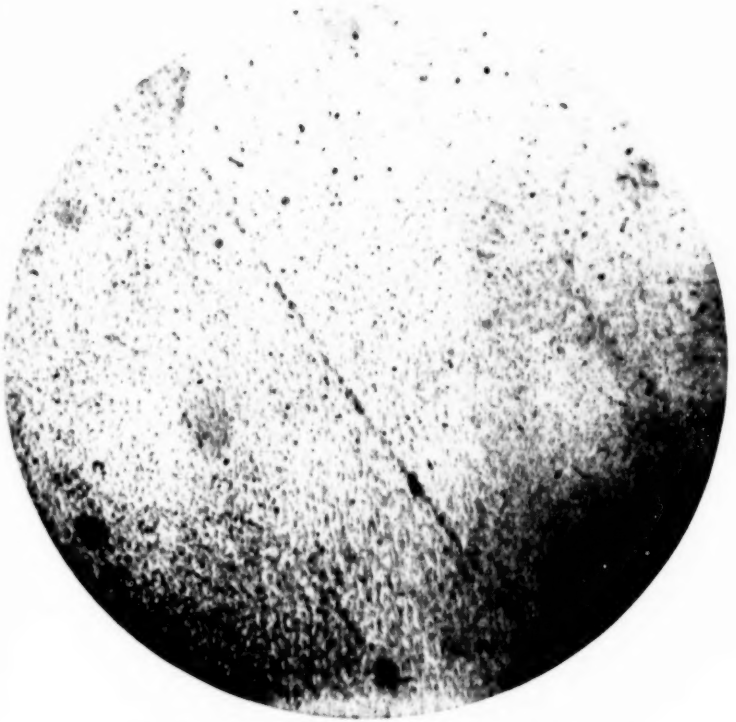

Fig. 16. 12,000 gauss. A proton of 30×10^6 volts energy.

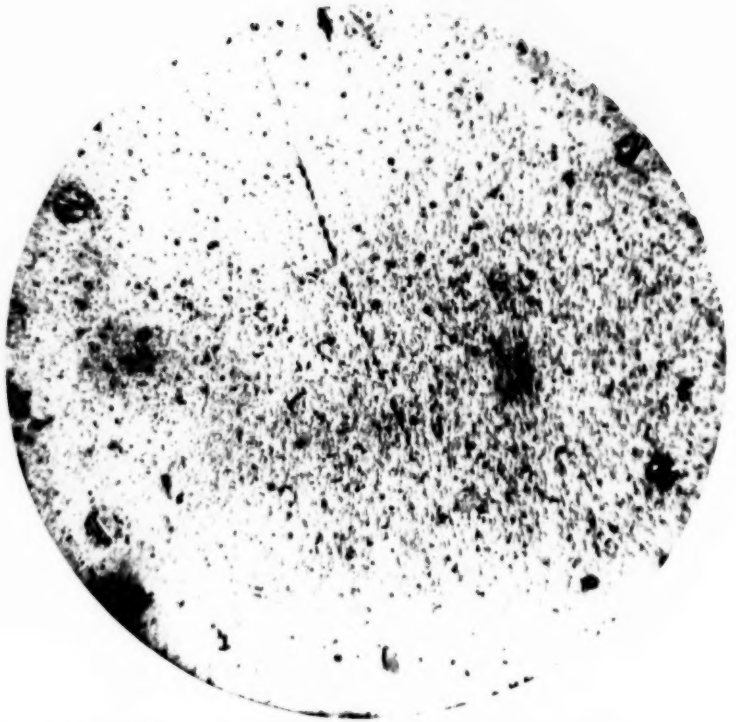

Fig. 17. 17,000 gauss A proton of 130×10^6 volts energy, slightly scattered.

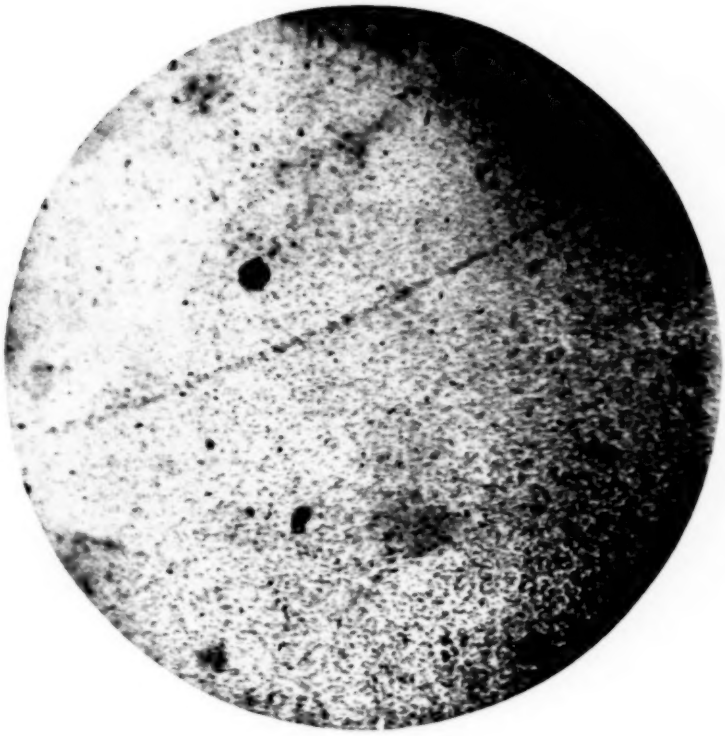

Fig. 19. 12,000 gauss. A proton of 40×10^6 volts energy.

Fig. 18. 17,000 gauss. A proton of 450×10^6 volts energy.

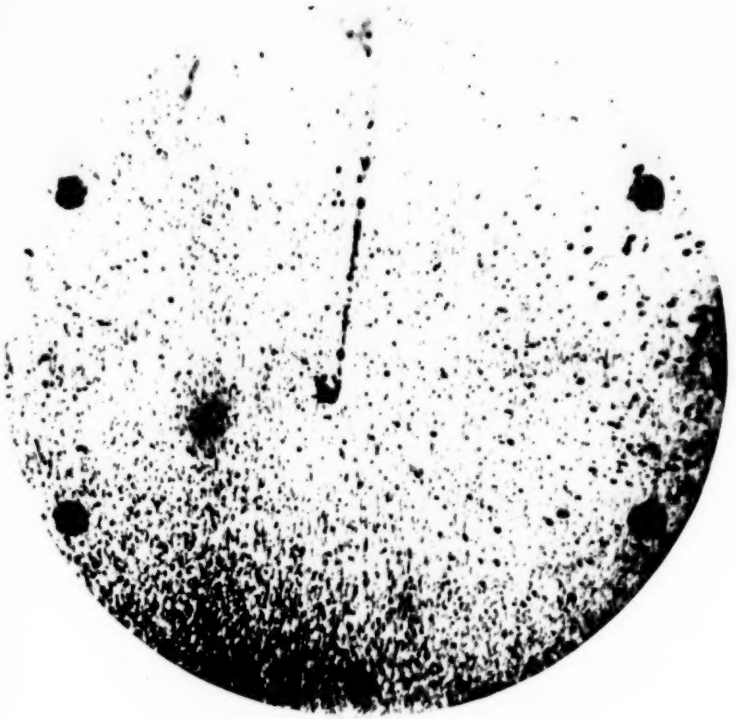

Fig. 20.

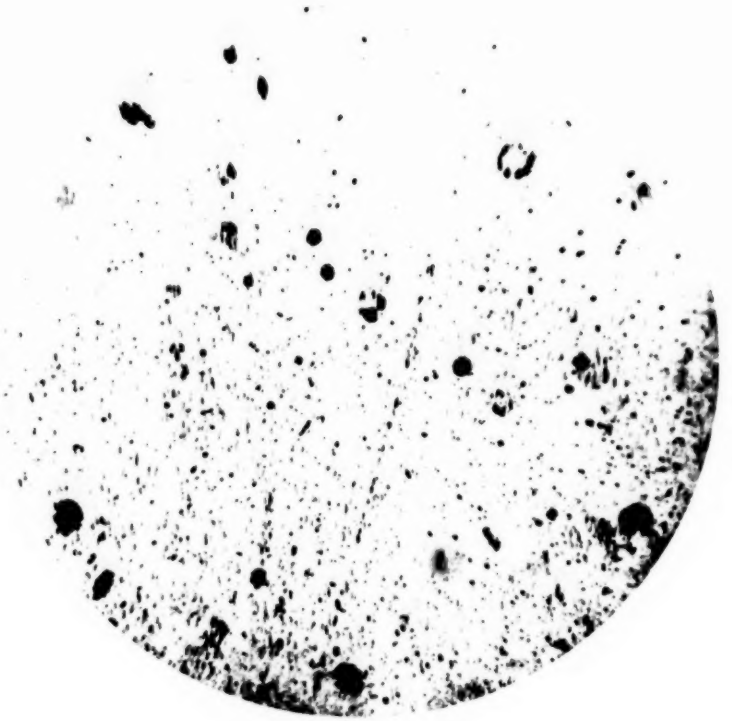

Fig. 21.

Fig. 20. 12,000 gauss. A particle of doubtful sign of charge. If an electron, the minimum energy is 600×10^6 volts, if a proton, the minimum energy is 400×10^6 volts. A close encounter with an electron takes place in the wall in which about 400,000 volts energy is transferred to the electron, shown by the small circle at the lower end of the track.

Fig. 21. 12,000 gauss. A high-energy particle of uncertain sign, photographed in helium. The energy, whether the particle is assumed to be an electron or a proton, exceeds 10^9 volts.

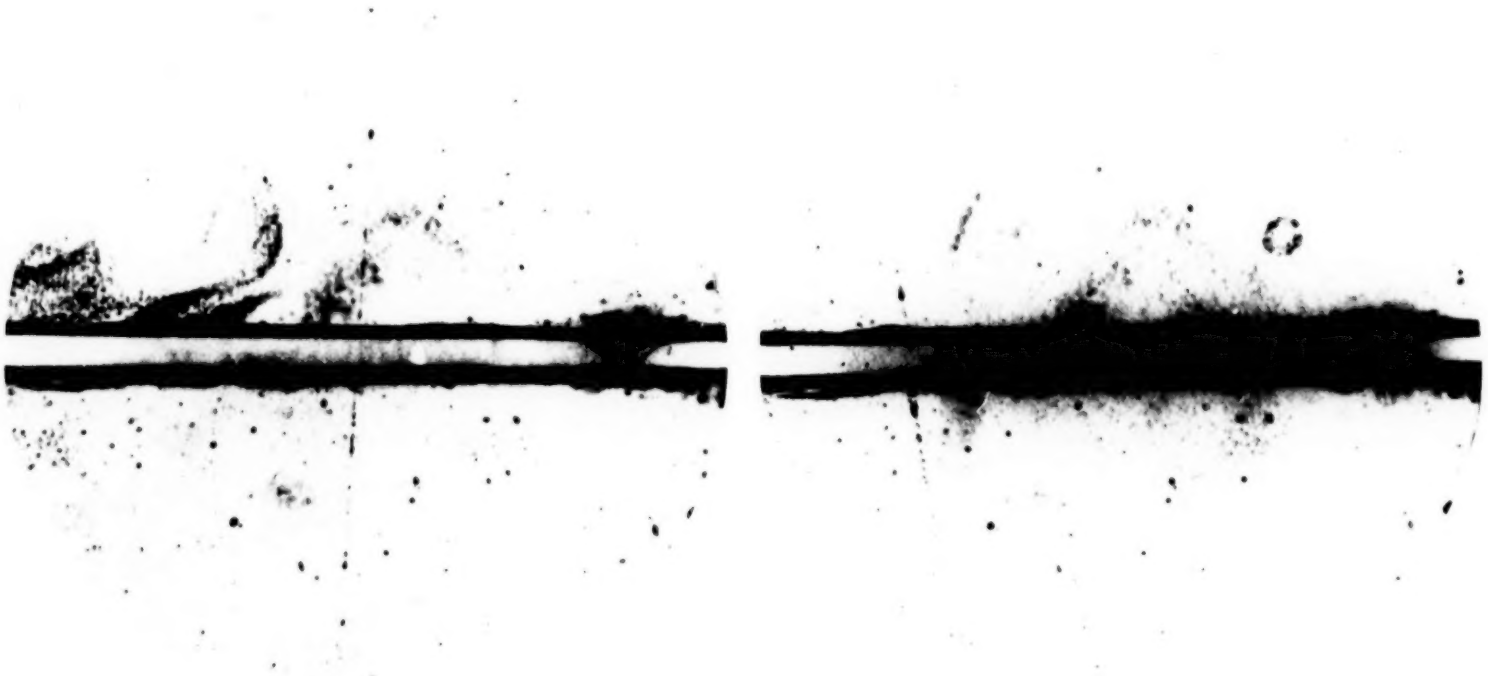

Fig. 22. Fig. 23.

Fig. 22. 12,000 gauss. A particle of uncertain sign of charge of energy exceeding 200×10^6 volts if a proton is assumed and exceeding 600×10^6 volts if an electron is assumed. In traversing the 6.0 mm lead plate it suffers a deflection of 0.5 degrees as measured in the plane of the chamber.

Fig. 23. 12,000 gauss. A particle of uncertain sign of charge of energy exceeding 100×10^6 volts if a proton is assumed and exceeding 450×10^6 volts if an electron is assumed. The deflection in traversing the 6.0 mm lead plate is 0.8 degrees. A double scattering, however, is indicated by the sidewise displacement of the portion of the track below the lead as compared to that above the lead.

Specific Ionization

A few tracks photographed in an atmosphere of helium with 5 percent air show about 14 ion pairs per cm at standard pressure, a value close to that found for electrons of about 10^6 volts energy from Ra gamma-rays, which show about 13 ion pairs per cm in the same gas. The specific ionization for an electron remains practically independent of its energy for energies ranging from about 300,000 volts to several hundred million volts. For a given velocity, protons and electrons ionize the same, and for high energies where the velocities of both the electrons and the protons are of the order of the velocity of light it becomes impossible to distinguish electrons from protons by their ionization. Only at lower energies where the proton velocities are appreciably less than the velocity of light will protons show an appreciably greater specific ionization than electrons of the same energy. Nuclei of higher atomic charge would, for a given velocity, produce many more ions per cm, the specific ionization being to a first approximation proportional to the square of the charge on the nucleus.

The specific ionization along the tracks showing positives is in most instances not much greater than that for the electrons. It is concluded, therefor; that the positives can only be protons, and cannot themselves represent nuclei of higher atomic number than unity.

The projection of whole nuclei by the penetrating radiation produced in the bombardment of beryllium with alpha-particles has been reported in recent experiments. For the explanation of this fact, on the basis of the conservation laws, Chadwick[3] postulates a neutron. For the interpretation of the cosmic-ray effects so far observed such a neutron is not demanded on the basis of the energy-momentum arguments which apply in the experiments of Chadwick. Further work will show if the associated tracks of cosmic rays represent an effect similar, but on a higher energy scale to the disintegration tracks photographed by Feather[4] in the neutron experiments, though the frequent occurrence of electron tracks in the cosmic-ray experiments seems to indicate a different type of phenomenon.

A possibility to be borne in mind is that, in rare cases, the tracks of curvature that indicate positives might be in reality electrons scattered backwards by the material underneath the chamber and are traversing it from bottom to top. Precise data on the specific ionization of the low-energy positives will distinguish, however, between downward positives and upward negatives.

Associated Tracks

A well-known characteristic of the cosmic tracks is their tendency to occur in groups.[5,6,7] Of the 55 photographs showing cosmic tracks, 7 show double tracks and 1 shows three tracks.

[3] Chadwick, Nature **129,** 312 (1932).
[4] Feather, Proc. Roy. Soc. **A136,** 709 (1932).
[5] Skobelzyn, Zeits. f. Physik **54,** 686 (1929).
[6] Auger and Skobelzyn, C. R. **189,** 55 (1929).
[7] Locher, Phys. Rev. **39,** 883 (1932).

In general, for paired tracks, the energy of one of the associated pair is considerably less than that of the other, in some instances 10^6 volts and less. One of the associated pair is also in all cases definitely an electron.

The associated tracks have been assumed to be due to the simultaneous ejection by a photon of two particles from an atomic nucleus.[1]

Another effect which may give rise to associated tracks is a close encounter between a cosmic particle and an electron. Fig. 20 is an example of an encounter of this type, the encounter taking place in the wall. For such an encounter where an electron of high energy (energy$\gg mc^2$) produces a secondary track, giving to the secondary electron an energy E, the angle θ between the primary and secondary electron is given by $\tan\theta=(2mc^2/E)^{1/2}$. The two tracks of Fig. 10 might represent an effect of this type, the relation above being satisfied within experimental uncertainty. The possibility also exists that a proton may by direct impact give to an electron energy sufficient to produce a secondary track. It is pointed out, however, that on the basis of the conservation laws, due to the relatively large proper mass of a proton, it is difficult to explain the associated tracks as a binary collision between a proton and an electron because of the prohibitively high energy which would have to be assigned to the proton in this case to account for the electron energies observed. To produce an electron of 100×10^6 volts would require a proton energy of 10^{10} volts. In both Figs. 8 and 11 one of the associated pair has a curvature to indicate a positive, and therefore, if these curvatures are correctly measured these cases cannot represent such encounters. Even if these are incorrectly measured and are in reality electrons then for Fig. 11 the value of θ calculated for an energy of 27×10^6 volts is 11°, which would agree with the angle indicated by the photograph within experimental uncertainty. But for the case of Fig. 8, the calculated value of 17° and the measured value of 25° are in conflict. Again the associated pair of Fig. 5 can not possibly be interpreted as due to a binary collision. The hypothesis of simple binary collisions is inadequate to account for all the associated tracks. Furthermore, encounters of this type in which a large amount of energy is transferred to an electron are not to be expected frequently, and the abundance of associated tracks coupled with the fact that positives as well as electrons appear, is strong evidence that the associated tracks represent a quite different phenomenon, i.e., the ejection of two particles from a nucleus.

Scattering of the Cosmic Particles

Certain of the tracks, Figs. 11 and 17, show sudden though very small deflections identical in appearance with the deflections observed in alpha-particle tracks due to nuclear encounters, but which are to be expected in the gas only rarely on the basis of the present scattering laws for high energy electrons or protons. The deflections in some instances represent scattering from the walls of the chamber. An example of large angle scattering from a lead surface is shown in Fig. 8. In Fig. 10 another instance of large angle scattering is shown, the electron being scattered by the glass wall of the chamber.

Experiments are now in progress to study the scattering of cosmic particles in lead. Figs. 22 and 23 show particles traversing 6.0 mm of lead, the angle of scattering being in each case readily measurable.

Energies

The energies of the cosmic particles as determined from the radii of curvature of the tracks range from values below 10^6 electron-volts to, in a few cases, values of the order of 10^9 electron-volts. The greater part of them, however, have energies below 500×10^6 volts.

Precautions were taken to reduce to a minimum the effects of air movements in the expansion chamber which tend to distort the tracks. The energies of the higher energy tracks, i.e., protons of energies of the order of 500×10^6 volts and electrons of the order of 10^9 volts, can be determined only roughly due to the small curvature in the magnetic field.

Table I. *Energy distribution.*

Number of electrons	Number of protons	Energy range in electron-volts
2	0	Below 10^6
4	0	From 10^6 to 10×10^6
6	1	" 10×10^6 to 20×10^6
4	1	" 20×10^6 to 30×10^6
3	3	" 30×10^6 to 50×10^6
1	3	" 50×10^6 to 100×10^6
5	5	" 100×10^6 to 200×10^6
4	2	" 200×10^6 to 300×10^6
5	2	" 300×10^6 to 400×10^6
1	4	" 400×10^6 to 500×10^6
3	3	" 500×10^6 to 700×10^6
2		" 700×10^6 to 1000×10^6

Table II. *Energies of the associated tracks in electron-volts.*

Group 1	Proton	130×10^6	See Fig. 5
	Electron	120×10^6	
	Electron	30×10^6	
Group 2	Probably proton	150×10^6	See Fig. 6
	Probably proton	400×10^6	
Group 3	Probably proton	450×10^5	See Fig. 11
	Electron	27×10^6	
Group 4	Proton	20×10^6	See Fig. 7
	Electron	4×10^5	
Group 5	Probably proton	$\sim100\times10^6$	See Fig. 8
	Electron	11×10^6	
Group 6	Electron	170×10^6	See Fig. 10
	Electron	11×10^6	
Group 7	Electron	180×10^6	See Fig. 9
	Electron	2×10^6	
Group 8	Electron	4×10^5	See Fig. 20
	Electron or proton	$\sim400\times10^6$	

Table I gives the distribution in energy of the electrons and protons. The number of protons and the number of electrons in various energy ranges are listed. It is to be noted that there may be many more electrons in the energy range below 10^6 volts than those listed. Since this includes the energy region of radio-activity, it is impossible to distinguish between electrons from radio-active sources and low-energy electrons due to cosmic rays. Therefore only those very low-energy electrons which are associated with other cosmic-ray tracks, and are definitely to be attributed to cosmic rays are listed in Table I.

There are in addition 5 tracks whose sign of charge is doubtful due to the lack of an appreciable curvature in the magnetic field. For these it is possible only to assign a lower limit to the energy, i.e., 450×10^6 volts on the supposition that they are electrons and 100×10^6 volts on the supposition that they are protons. There is one track, Fig. 21 to which an energy in excess of 10^9 volts must be assigned whether it is assumed a proton or electron.

In Table II are given the energies of the 8 groups of associated tracks.

I wish to thank Mr. Seth H. Neddermeyer for assistance in the measurement of the photographs.

Scattering of X-Rays from Solids

By ALLEN W. COVEN
Ryerson Laboratory, The University of Chicago

(Received July 5, 1932)

The total scattering of the $K\alpha$ radiation of molybdenum from powdered crystals of KCl, NaF, and MgO has been observed with an ionization chamber whose window subtended several degrees of angle at the scatterers. The scattering from NaF and MgO was found to be approximately the same as that from neon. The scattering from KCl was found to be approximately the same as that from argon. The intensities of the diffracted portion of the scattered rays from the crystals have been calculated and found to be distributed along the F^2/Z curves, thus agreeing with Jauncey's relation between gas and crystal scattering, $S_g = S_c + F^2/Z$. The sums of the diffracted intensities plus diffuse intensities have been found to follow the gas scattering curves, in agreement with Compton's formula for the scattering from a monatomic gas, $S_g = (f^2/Z) + (1 - f^2/Z^2)/R^3$. The method of measurement may be used to determine values of the structure factor for the atom at rest.

I. INTRODUCTION

A. H. COMPTON[1] has shown that the intensity of x-rays scattered from a monatomic gas or vapor is given by

$$S_g = f^2/Z + (1 - f^2/Z^2)/R^3 \tag{1}$$

where S_g is the scattered intensity relative to the value given by the Thomson theory of scattering.[2] f is an average atomic structure factor for the atom at rest, Z is the number of electrons in the atom, and $1/R^3$ is the Breit-Dirac factor. R has the value $1 + (h/mc\lambda)\text{vers}\,\phi$, where ϕ is the angle of scattering. G. E. M. Jauncey[3] has developed a theory of the scattering of x-rays from solids in which Eq. (1) is included as a factor in the scattered intensity. In the special case of scattering from a simple cubic crystal consisting of atoms of one kind Jauncey's theory gives[4]

$$S_c = \frac{f^2 - F^2}{Z} + \frac{1 - f^2/z^2}{R^3} = S_g - \frac{F^2}{Z} \tag{2}$$

where F is the atomic structure factor at the temperature of the crystal. Eq. (2) connects the diffuse scattering from a crystal with the scattering from a monatomic gas of the same kind of atoms as those in the crystal. The term F^2/Z represents a correction for the effect of interference between atoms in the crystal.

The energy per second emitted in a diffraction line by one of the particles in an aggregation of powdered crystals is given by[5]

[1] A. H. Compton, Phys. Rev. **35**, 925 (1930).
[2] J. J. Thomson, *Conduction of Electricity through Gases*, 2d Ed., p. 326.
[3] G. E. M. Jauncey, Phys. Rev. **37**, 1193 (1931).
[4] G. E. M. Jauncey and G. G. Harvey, Phys. Rev. **37**, 1203 (1931).
[5] A. H. Compton, *X-Rays and Electrons*, p. 130.

$$P = \frac{In^2\lambda^3 pF'^2 e^4(1 + \cos^2 2\theta)dV}{8(\sin\theta)m^2c^4}, \tag{3}$$

where θ is the glancing angle of incidence on a crystal plane, p is the number of planes, F' is the structure factor for the crystal, n is the number of atoms per cm^3, I is the intensity of the primary beam, and dV is the volume of the particle. If the diffracted rays are measured at a distance r with an ionization chamber whose window has a length L which is short compared to $r \sin\theta$, then the energy per second entering the ionization chamber is

$$P_s = PL/2\pi r \sin 2\theta.$$

Thomson's classical theory[2] gives the intensity scattered from the $nZdV$ electrons in one of the powdered crystal particles to be

$$I_s = \frac{InZe^4(1 + \cos^2\phi)dV}{2m^2c^4r^2}, \tag{4}$$

and therefore the energy entering the ionization chamber is equal to AI_s, where A is the area of the chamber window. To get the energy per second in a diffraction line in the units corresponding to S_g and S_c of Eqs. (1) and (2) we take the ratio of P_s to AI_s. We then have

$$\frac{P_s}{AI_s} = \frac{n\lambda^3 pLrF'^2}{8\pi ZA \sin\theta \sin 2\theta}.$$

But the atomic structure factor F in Eq. (2) has a value $F'/2$ for a simple cubic crystal consisting of atoms of one kind. Substituting $2F$ for F' in the above expression, we then have for the energy in a powdered crystal line where the crystals are of the simple cubic type and contain similar atoms

$$\frac{P_s}{AI_s} = \frac{n\lambda^3 pLr}{2\pi A \sin\theta \sin 2\theta} \cdot \frac{F^2}{Z}. \tag{5}$$

If the ionization chamber window is of such width as to subtend several degrees of angle at the scatterer, there will be several diffraction lines entering the chamber at large angles of scattering where the lines are close together, and probably more than one line at each of the smaller scattering angles if the scattering crystals have a grating constant that is not too small. The total diffracted energy entering the chamber is then equal to the sum of the energies in the lines and may be expressed as

$$S_d' = \sum\left(\frac{n\lambda^3 pLr}{2\pi A \sin\theta \sin 2\theta} \cdot \frac{F^2}{Z}\right). \tag{6}$$

The total scattered intensity entering the ionization chamber is the sum of the diffuse and the diffracted intensities. Using previously measured values of F, Eq. (6) may be used to calculate the diffracted portion of the scattering and this portion may then be added to measured values of the diffuse scattering to get values of the total scattered intensitites. Values of S_d' are in terms

of energy so the corresponding quantity representing the diffuse scattering will be represented by the area under the curve of diffuse intensity between the limits of the $(\sin \phi/2)/\lambda$ ordinate corresponding to the angle subtended by the ionization chamber window. Hence we may divide each value of S_d' by a value dx, which is the length of the ordinate corresponding to the range of scattering angle subtended by the ionization chamber window and add the quotient to the intensity of diffuse scattering at the value of the ordinate corresponding to the position of the middle of the window. The total scattered intensity is thus represented by

$$S_t = S_c + S_d'/dx = S_c + S_d, \tag{7}$$

where S_d is equivalent to S_d'/dx. If the total scattering from a powdered crystal aggregation is measured with an ionization chamber whose window subtends several degrees of angle at the scatterer, a distribution of intensity equivalent to that given by Eq. (1) is observed.

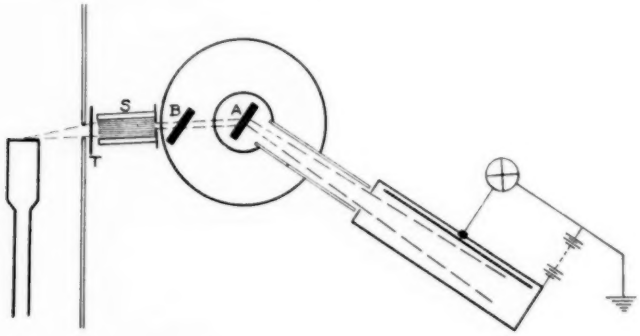

Fig. 1. Arrangement of apparatus.

The author has observed the scattered intensities from powdered crystals of KCl, NaF, and MgO, using an ionization chamber whose window subtended approximately 5 degrees of angle at the scattering plates. The observed intensities from KCl are in close agreement with the values obtained by Wollan[6] for argon and the intensities from NaF and MgO agree with Wollan's values for neon.[6] Wollan's values are in agreement with values calculated from Eq. (1), using structure factors calculated from the Hartree charge distribution.

II. Apparatus and Procedure

Fig. 1 shows the arrangement of the apparatus. A molybdenum target x-ray tube was immersed in oil in a lead box placed close to the axis of an ionization spectrometer. The scatterers were mounted directly over the axis on the spectrometer table. The x-ray tube was operated at a potential of approximately 40 k.v. and a current of 35 m.a. A Compton electrometer indicated the ionization currents. A Soller slit, S, collimated the primary beam. The use of this slit limited the divergence of the primary rays to less than a

[6] E. O. Wollan, Phys. Rev. **37**, 862 (1931).

half-degree of angle. The scattered rays passed through a bronze tube 2.7 cm in diameter, 14 cm long, with 1.5 mm walls. This tube prevented stray radiation from entering the ionization chamber with the scattered rays. The window of the chamber was 1.67 cm high and 1.64 cm wide. The distance from the window to the axis of the spectrometer was 18.05 cm. The chamber contained methyl bromide vapor at atmospheric pressure.

Balanced filters of ZrO_2 and SrO were placed at T in the primary beam. These separated the $K\alpha$ lines from the general radiation as shown in Fig. 2, where the difference in the transmission by the ZrO_2 and the SrO is re-

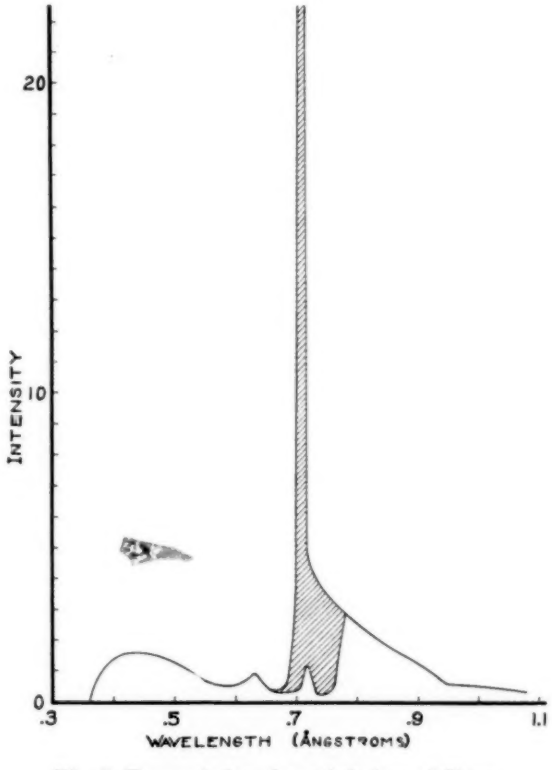

Fig. 2. Transmission through balanced filters.

presented by the shaded portion. This is the portion that was used as the primary radiation in all of the measurements of scattered intensities.

The scattering from the crystalline powders and from paraffin was observed throughout an angular range of from 20° to 100°. The scattering from each of the powdered crystal plates was compared with the scattering from a similar plate of paraffin. Since the scattering from paraffin can be calculated to a close approximation, the values of the scattered intensities for each of the other materials could be put on an absolute scale. For the $K\alpha$ radiation of molybdenum Woo[7] has found that the ratio of the incoherent to coherent radiation scattered from paraffin at 90° is 4.69. If it is assumed that for

[7] Y. H. Woo, Phys. Rev. **27**, 119 (1926).

paraffin at 90° the effect of constructive interference is negligible, the total scattering can be obtained from classical theory, if the incoherent portion is corrected by the Breit-Dirac factor. Thus, at 90°, the scattering from paraffin is given by

$$S_t = 0.825(R^{-3}) + 0.175 = 0.93.$$

From this value and the experimental measurements of relative intensities at various angles, S_t for paraffin was found to be equal to unity in the range from 30° to 70°. The comparisons of the powdered crystal intensities with the paraffin intensity were all made at 60°.

The pure, finely ground, powdered crystals were pressed into brass rings which fitted into holders that could be conveniently mounted on the spectrometer table. The paraffin was melted into a similar ring so that it could be quickly substituted for any one of the powdered crystal plates.

Potassium chloride

The scattering from a thin plate of the KCl powder 2.5 cm in diameter and having a mass per unit area of 0.141 g/cm² was compared with the scattering from the paraffin which was also 2.5 cm in diameter and had a mass per unit area of 0.275 g/cm². The arrangement of the two was as shown in Fig. 1, where one scatterer is in the primary beam at A and the other in the primary beam at B, each plate being set so that the normal to its surface made an angle of 30° with the primary beam. The ionization chamber was set at the scattering angle of 60°. The intensity with the KCl at A and the paraffin at B was first observed. Then the intensity with the paraffin at A and the KCl at B was observed. The ratio of the first intensity to the second multiplied into the ratio of the masses per unit area and the ratio of the values of Z/W for the samples then gave the value of S_t for KCl at 60°. Z is atomic number and W is atomic weight. The paraffin was assumed to be equivalent to a molecule of $C_{24}H_{50}$, for which Z/W has a value of 0.5. No correction for absorption of the x-rays in the samples was necessary since by this method of comparison the portion of the primary rays transmitted by the scatterer at A does not change when the scatterers are interchanged in their positions at A and B. The intensity of the scattered rays entering the ionization chamber from each substance was of the same order of magnitude by this method, even though the absorption in the KCl was much greater than that in the paraffin.

Relative values of the scattering from KCl were observed by reflections from a plate of the powdered crystals 4.5 cm in diameter and thick enough to absorb completely the $K\alpha$-rays of molybdenum. The scatterer was always set so that the face of the crystal plate was at an angle equal to half the scattering angle. Thus the absorption of the primary and scattered rays was approximately the same in the thickness of the plate penetrated, and proportional to the reciprocal of the absorption coefficient. For the relative values, therefore, no absorption correction was necessary. The relative values of S_t were given by the relative intensities multiplied into the ratios of the values of the polarization factor, $1+\cos^2\phi$.

Sodium fluoride

The intensities from paraffin and the NaF plate, which had a mass per unit area of 0.470 g/cm², were of the same order of magnitude and the comparison between them at 60° was made without resorting to the method used for KCl of placing both samples in the primary beam. When a scatterer is at A and none at B (Fig. 1), S_t is proportional to $(W/mZ)(I_\phi/i_\phi)(1+\cos^2\phi)^{-1}$, where Z is atomic number, W is atomic weight, m is mass per unit area, I_ϕ is the scattered intensity, and i_ϕ is the portion of the primary rays penetrating the scatterer. i_ϕ is equal to $Ie^{-m\mu/\rho\cos(\phi/2)}$ where I is the incident ray intensity and μ/ρ is the mass absorption coefficient of the incident rays in the scatterer. The absorption of the Mo $K\alpha$ rays in the paraffin and in the NaF plate was measured with the Compton double crystal x-ray spectrometer.[8] μ/ρ for paraffin was found to have a value of 0.52 and for NaF 2.63. Relative intensities for NaF at various scattering angles were measured from the same scatterer that was compared with paraffin.

Magnesium oxide

The MgO plate that was compared with paraffin at 60° had a mass per unit area of 0.331 g/cm.² The intensity comparison was made exactly as it was for NaF and paraffin. μ/ρ for MgO was calculated to be 3.18 from the values of the atomic absorption coefficients for Mg and O given on page 182 of Compton's *X-Rays and Electrons*. The relative intensities were measured from reflections from a thick plate of the powdered MgO crystals as was done for KCl.

III. Experimental Results

Froman[9] and Harvey[10] have respectively measured the intensities of the lines from powdered KCl and the diffuse scattering from a single crystal of KCl. Froman's values of F for KCl have been used to calculate values of S_d for values of ϕ between 15° and 90°, each value extending over a range of 5° and differing from adjacent values by 5°. Thus for each value of ϕ the energy in all the diffraction lines included in the 5° range made up the value of S_d. The sum of the S_d values would represent the sum of the energy in the diffraction lines between the minimum and maximum values of ϕ, 15° and 90°. At each value of ϕ the value of S_d was added to the value of S_c as shown in Fig. 3. S_y is the theoretical curve for argon as calculated by Hartree by his method of self-consistent fields. The data for the curve were taken from a paper by Herzog.[11] His values for the incoherent radiation have been reduced by the Breit-Dirac factor before being added to the values of the coherent radiation to get the values of S_y from which the curve was drawn. The F^2/Z curve was drawn from Froman's data. The circles are values of S_d and the crosses are the values of S_r+S_d. The author's experimental values of S_t, as given in column 3 of Table I, are plotted as dots.

[8] A. H. Compton, Rev. Sci. Inst. **2,** 365 (1931).
[9] D. K. Froman, Phys. Rev. **36,** 1330 (1930).
[10] G. G. Harvey, Phys. Rev. **38,** 593 (1931).
[11] G. Herzog, Zeits. f. Physik **70,** 583 (1931).

Jauncey and Williams[12] have recently measured the diffuse scattering from a single crystal of NaF. Their values were kindly sent to the author by Professor G. E. M. Jauncey and have been used together with the F values

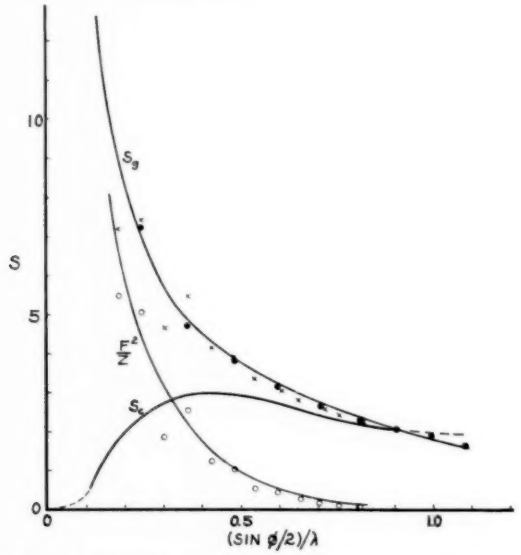

Fig. 3. Scattering from KCl. Dots S_t experimental, circles S_d, crosses S_c+S_d, S_g from argon.

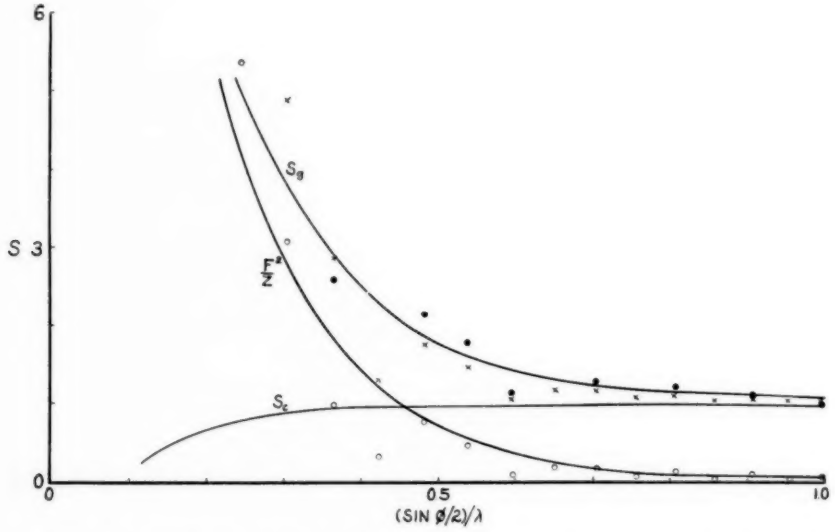

Fig. 4. Scattering from NaF. Dots S_t experimental, circles S_d, crosses S_c+S_d, S_g from neon.

of Havighurst[13] to calculate values of S_c+S_d as shown by the crosses in Fig. 4. The F^2/Z curve is also from the data of Havighurst. The S_g curve for neon is again from Herzog's values.[11] The author's experimental values of S_t for

[12] G. E. M. Jauncey and P. S. Williams, Phys. Rev. **41**, 127 (1932).
[13] R. J. Havighurst, Phys. Rev. **29**, 1 (1927).

NaF are shown by the dots. These values appear in column 4 of Table I. Values of S_d are shown by the circles.

Fig. 5 shows the results for MgO. The author is grateful to Dr. Wollan for the values of diffuse scattering from a single crystal of MgO which he has recently measured but not yet published. These have been used to draw the S_c curve. Values of S_d as shown by the circles were calculated from Wollan's[14] values of F for powdered MgO crystals. The F^2/Z curve is also drawn from Wollan's values. Values of S_c+S_d are shown by the crosses and the author's experimental values of S_t by the dots. These are the values appearing in column 5 of Table I. The S_g curve for neon is the same as the one in Fig. 4.

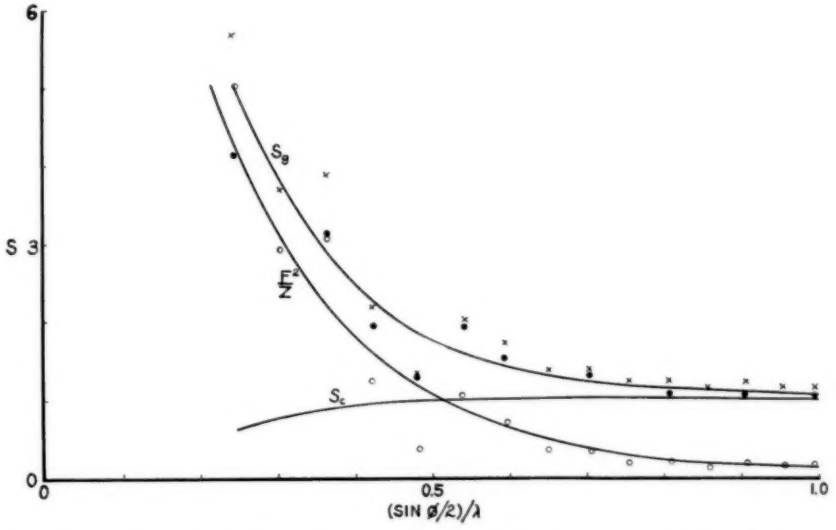

Fig. 5. Scattering from MgO. Dots S_t experimental, circles S_d, crosses S_c+S_d, S_g from neon.

The values of the total scattering, S_t, observed by the author for powdered crystals of KCl, NaF, and MgO and for paraffin are all shown in Fig. 6 together with the theoretical curves for neon and argon. The crosses indicate the values for KCl, the circles are the NaF values, the large dots are for MgO, and the small dots for paraffin.

TABLE I. *Values of S_t for paraffin and powdered crystals.*

Angle	(sin ϕ/2)/λ	KCl	NaF	MgO	Paraffin
20°	0.245	7.25		4.16	1.22
30	0.365	4.77	2.59	3.13	1.00
35	0.423			1.96	
40	0.482	3.83	2.15	1.30	1.00
45	0.539		1.78	1.95	
50	0.596	3.14	1.13	1.55	1.00
60	0.705	2.65	1.28	1.31	1.00
70	0.808	2.28	1.20	1.10	1.00
80	0.906	2.01	1.10	1.09	0.93
90	0.996	1.85	1.00	1.06	0.93
100	1.082	1.80			0.89

[14] E. O. Wollan, Phys. Rev. **35**, 1019 (1930).

IV. Discussion

Fig. 6 shows that the measured values of the total scattering from KCl are in excellent agreement with the theoretical argon curve. Wollan's experimental values of the scattering from argon are slightly higher than the theoretical curve at values of $(\sin \phi/2)/\lambda$ below 0.7 and above 0.9. Hence the agreement between the author's values of the scattering from KCl and the scattering from argon is better for the theoretical values than for the experimental values. The experimental values of the total scattering from NaF and MgO are in good agreement with the theoretical neon curve for the higher values of $(\sin \phi/2)/\lambda$. At the lower values of $(\sin \phi/2)/\lambda$ the points do not lie

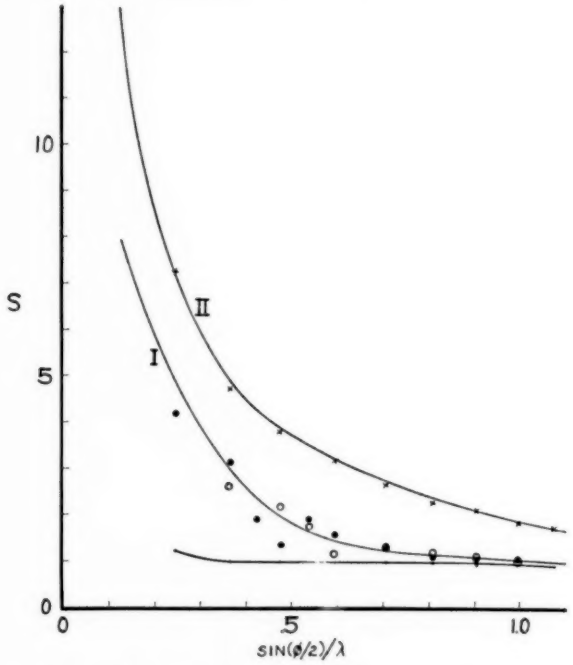

Fig. 6. Values of S_t. Crosses KCl, circles NaF, large dots MgO, small dots paraffin. Curve I neon (theoretical), curve II argon (theoretical).

on a smooth curve. This is to be expected, because crystals of NaF and MgO have a small grating constant. The diffraction lines are consequently widely separated and a good average of the diffracted energy is not obtained. However, the average distribution of the points appears to lie along the gas scattering curve. The larger grating constant of KCl insures a good average of the diffracted portion of the energy throughout the whole range of scattering angles at which observations were made. This explains the excellent agreement of the KCl values with the gas curve at all points.

Jauncey and Williams[12] have found that the values of S_c+F^2/Z for NaF are lower than the values of the scattered intensities from neon. The author's calculated values of S_c+S_d, as shown by the crosses in Fig. 4, are also lower than the gas scattering curve. The author's experimental values of the total

scattering from NaF are on the average higher than the values of S_c+S_d, but slightly less than Wollan's neon values. The values of S_c+S_d are probably more reliable than the experimental values of the total scattering because of the difficulty of averaging the diffracted energy in the ionization chamber. The values of S_c+S_d for MgO lie slightly above the theoretical curve for neon and are in good agreement with Wollan's experimental measurements of the neon intensities. The S_c+S_d values for KCl are slightly lower than the argon theoretical curve, and the author's values of the total scattering lie between the S_c+S_d values and the argon curve. The difference between the values is, however, less than the probable uncertainty in the determination of the absolute value of the total scattering by comparison with paraffin. Using the F values of Froman[9] for powdered KCl, the values of S_c+F^2/Z fall exactly on the theoretical argon curve. James and Brindley[15] have measured the F values for a single crystal of KCl and have found them to be slightly greater than Froman's values. Using these F values of James and Brindley, the S_c+F^2/Z values for KCl agree better with Wollan's values of the argon intensities than with the theoretical curve. Jauncey and Harvey[16] have used. Wollan's and James and Brindley's values in testing the S_c+F^2/Z relation.

In a former paper[17] the author has published the results of measurements of the total scattering from aluminum, copper, and lead sheets. Since a sheet of metal consists of a collection of small crystals, we may consider it to be a plate of powdered crystals of the metal. The total scattering from a metal sheet measured with a wide-window ionization chamber should thus be approximately the same as the scattering from the same metal in the vapor state, for values of $(\sin\phi/2)/\lambda$ greater than 0.5. This method of measurement yields values of the atomic structure factor for the atom at rest, since from Eq. (1) we have

$$f^2 = \frac{(S - R^{-3})}{(Z - R^{-3})} Z^2.$$

The author wishes to thank Professor A. H. Compton for suggesting measurements of the total scattering from powdered crystals and Dr. E. O. Wollan for his generous and helpful advice during the course of the experiment.

[15] R. W. James and G. W. Brindley, Proc. Roy. Soc. **A121,** 155 (1928).
[16] G. E. M. Jauncey and G. G. Harvey, Phys. Rev. **38,** 1071 (1931).
[17] A. W. Coven, Phys. Rev. **38,** 1424 (1931).

Sum Rules for Atomic Transition Probabilities

By J. P. VINTI
Massachusetts Institute of Technology

(Received June 27, 1932)

Some new sum rules for atomic transition probabilities are developed; they are similar to the well-known rule of Kuhn, Reiche, and Thomas. They give, if unpolarized light is incident on any gaseous element in any given discrete energy level, the total absorption, excitation plus ionization, with various types of frequency weighting. The results are similar to those of Dirac and Harding, but are more general in that they apply to any discrete state of any atom, rather than to the ground state of hydrogen only. The method differs from that of Dirac and Harding.

INTRODUCTION

THERE are well-known relations connecting the coefficients of spontaneous and induced transitions in atomic systems (the Einstein A's and B's) with the matrix components of electric moment between the initial and final states and the corresponding frequency differences. A_{0n}, the spontaneous transition probability from a state n to a lower state 0 is equal (in the dipole approximation) to a universal constant multiplied by the cube of the frequency difference and the square of the absolute value of the matrix component of electric moment, $e^2(|x_{0n}|^2+|y_{0n}|^2+|z_{0n}|^2)$, where ex, ey, ez, are the rectangular components of electric moment, so that e.g., x is equal to the sum of the x coordinates of all the electrons. B_{0n}, the induced transition probability, is proportional directly to $e^2(|x_{0n}|^2+|y_{0n}|^2+|z_{0n}|^2)$, where in this case, either 0 or n may be the lower state.

x_{0n} is given by an integral of the form $\int\bar{\psi}_0(\Sigma_{\mu=1}{}^N x_\mu)\psi_0 d\tau$, where ψ_0 and ψ_n are the wave functions of the atom for the states 0 and n, N is the number of extranuclear electrons in the atom, and the integration is extended over the coordinates of all the electrons. We see, then, that in general one must know the wave functions of the atom for the states concerned in order to calculate A_{0n} and B_{0n}. One, can, however, give some general relations satisfied by the A's or B's without knowing any wave functions, or knowing at the most the wave function of one discrete state only.

The sum rule of Kuhn, Reiche, and Thomas[1] is an example of the type of thing one can say about the matrix components, and thus about the A's and B's, without knowing any wave functions. Using atomic units, and letting x denote $\Sigma_1{}^N x_\mu$, the sum of the N cartesian coordinates, W_n the energy of the state n with reversed sign, this rule can be expressed in the form $\Sigma_n(W_0-W_n)|x_{0n}|^2=N$, where the state 0 denotes an arbitrary state of the discrete spectrum, and the summation is understood to include a summation over all the discrete states that have dipole combinations with the state 0, and an integral

[1] W. Kuhn, Zeits. f. Physik **33**, 408 (1925). F. Reiche and W. Thomas, Zeits. f. Physik **34**, 510 (1925).

over the continuous spectrum. (Similar relations hold for the y and z components of electric moment.) This rule is directly deducible from the commutation rules and the relation connecting the matrix components of momentum and coordinate. In terms of the A's it enables us to evaluate at once $\Sigma_n A_{0n}/\nu_{0n}^2$, where ν_{0n} is the frequency of the spectral line associated with the transition from a *running* state n to the *base* state 0. Furthermore, Wigner[2] has shown that this rule may be *sharpened* by dividing transitions into three classes: $+$, $-$, and 0, $+$ transitions being those in which the total azimuthal quantum number L increases by 1—those in which it diminishes by 1, and 0 those in which it does not change. Wigner's rule then gives the sum $g_+(L)\Sigma^+ + g_0(L)\Sigma^0$ in terms of the L-value of the state 0, where g_+ and g_0 are simple functions of L, and the summands are the f values A_{0n}/ν_{0n}^2. We wish to mention at this point that all the sum rules developed in this paper can be sharpened in a similar way.

Matrix multiplication of the simple type $xx = x^2$ furnishes another general relation connecting the matrix components:

$$\sum_n |x_{0n}|^2 = (x^2)_{00}.$$

Here, as above, 0 means a discrete state and the summation is to be extended by means of integration over the continuous spectrum. This relation can also be looked on as a sum rule, although of a less general type, since the evaluation of the sum depends on a knowledge of the wave function of the state 0. It gives directly $\Sigma_n B_{0n}$, if one knows ψ_0.

The above rules tell us how to evaluate $\Sigma_n(W_0 - W_n)^j |x_{0n}|^2$ when j has the value 1 or 0. We develop in this paper other rules of the same general type, letting j take on the values 2, 3 and 4. They constitute rules for the summation of the A's and B's (of a given base state) over all the states of the atom, with various kinds of frequency weighting.

SECTION I

We begin with the case $j=2$, and attempt to evaluate $\sum_n(W_0 - W_n)^2 (|x_{0n}|^2 + |y_{0n}|^2 + |z_{0n}|^2)$. (We abbreviate expressions of this type hereafter to $\sum_{n,xyz}(W_0 - W_n)^2 |x_{0n}|^2$). Let x_μ, y_μ, z_μ denote the coordinates of the μth electron, N the total number of extranuclear electrons in the atom, $p_{x\mu}$, $p_{y\mu}$, $p_{z\mu}$ the components of momentum of the μth electron, and $p_{x\mu}(0n)$ the matrix component of $p_{x\mu}$ between the stationary states 0 and n. Also, we shall use the contractions:

$$\sum_{\mu=1}^{N} x_\mu = x, \quad \sum_{\mu=1}^{N} p_{x\mu} = p_x, \text{ and } W_0 - W_n = W_{0n}.$$

Now

$$p_{x\mu}(0n) = (h/2\pi i) \int \bar{\psi}_0 \frac{\partial}{\partial x_\mu} \psi_n d\tau,$$

[2] E. Wigner, Phys. Zeits. **11**, 450 (1931).

and it is well known that when at least one of the states 0 and n is a discrete state (to insure the vanishing of surface integrals at infinity which occur in the derivation), this can be thrown into the form $m(2\pi i/h)W_{0n}x_\mu(0n)$, where $x_\mu(0n)$ is the matrix component of x_μ between the states 0 and n, and m is the rest mass of the electron. On summing over the index μ from 1 to N, we obtain the relation:

$$p_x(0n) = m(2\pi i/h)W_{0n}x_{0n}. \tag{1}$$

Similarly

$$p_x(n0) = \bar{p}_x(0n) = m(2\pi i/h)W_{n0}x_{n0}, \tag{2}$$

(since p_x is hermitian, and $W_{n0} = -W_{0n}$). On multiplying (1) by (2) we obtain:

$$p_x(0n)p_x(n0) = m^2(2\pi/h)^2W_{0n}^2\,|\,x_{0n}\,|^2. \tag{3}$$

Summing (3) over all states n (complete set), and making use of the simple rule for a matrix product, *viz*:

$$\sum_n p_x(0n)p_x(n0) = (p_x^2)_{00},$$

we obtain the relation:

$$m^2(2\pi/h)^2\sum_n W_{0n}^2\,|\,x_{0n}\,|^2 = (p_x^2)_{00}. \tag{4}$$

Similar relations hold on replacing x by y or z. Adding,

$$m^2(2\pi/h)^2\sum_{n,\,xyz} W_{0n}^2\,|\,x_{0n}\,|^2 = (p_x^2 + p_y^2 + p_z^2)_{00}. \tag{5}$$

We next attempt to give the right hand side of (5) a physical meaning. Since

$$p_x^2 = \sum_\mu \sum_\nu p_{x_\mu}p_{x_\nu} = \sum_{\mu=1}^{N} p_{x_\mu}^2 + \sum_{\mu\neq\nu}\sum p_{x_\mu}p_{x_\nu},$$

$$(p_x^2)_{00} = \sum_{\mu=1}^{N}(p_{x_\mu}^2)_{00} + \sum_{\mu\neq\nu}\sum(p_{x\mu}p_{x\nu})_{00}.$$

The right side of (5) thus decomposes into two parts:

$$\sum_{\mu=1}^{N}(p_{x\mu}^2 + p_{y\mu}^2 + p_{z\mu}^2)_{00} \text{ and } \sum_{\mu\neq\nu}\sum(p_{x\mu}p_{x\nu} + p_{y\mu}p_{y\nu} + p_{z\mu}p_{z\nu})_{00}.$$

The former term is recognizable as $2mT_{00}$, where T_{00} is the diagonal component of kinetic energy in the state 0. By the virial theorem, making use of the fact that the interaction potentials in the atom are all Coulombian, we can equate T_{00} to $-W_0$. The cross-product term is expressible as

$$-(h/2\pi)^2\int \bar{\psi}_0 \nabla_\mu \cdot \nabla_\nu \psi_0 d\tau,$$

or

$$\sum_{\mu\neq\nu}\sum(\vec{p}_\mu \cdot \vec{p}_\nu)_{00}, \text{ where } \vec{p}_\mu = (p_{x\mu}, p_{y\mu}, p_{z\mu}).$$

Then

$$m^2(2\pi/h)^2 \sum_{n,xyz} W_{0n}{}^2 \left| x_{0n} \right|^2 = -2mW_0 + \sum_{\mu \neq \nu} \sum (\vec{p}_\mu \cdot \vec{p}_\nu)_{00} \tag{6}$$

where $|W_0|$ is the energy necessary to strip the atom of all its electrons when in the state 0.

Eq. (6), then, is the general sum rule for the case $j=2$. If the wave function of the state 0 is simple enough so that $\sum\sum_{\mu \neq \nu}(\vec{p}_\mu \cdot \vec{p}_\nu)_{00}$ can be evaluated, it is of use. For states like the ground state of helium, where one can assume separability to a good approximation,

$$(p_{x\mu} p_{x\nu})_{00} = \tilde{p}_{x\mu} \tilde{p}_{x\nu}$$

where the tilde indicates an average with respect to the wave function of that electron alone. But

$$\tilde{p}_{x\mu} = \tilde{p}_{x\nu} = 0.$$

In such a case, and for one-electron atoms, the rule becomes

$$\sum_{n,xyz} W_{0n}{}^2 \left| x_{0n} \right|^2 = -(h^2/2\pi^2 m) W_0. \tag{7}$$

For those cases above mentioned in which the cross term vanishes, it is of interest to express the rule in terms of the A and B coefficients:

$$\sum_n \frac{A_{0n}}{\nu_{0n}} = \frac{32\pi^2 e^2}{3mc^3 h^2} |W_0| \tag{8}$$

or

$$\sum_n \nu_{0n}{}^2 B_{0n} = \frac{4\pi e^2}{3mh^2} |W_0| \tag{9}$$

the Kuhn-Reiche rule ($j=1$) being expressible as

$$\sum_n \frac{A_{0n}}{\nu_{0n}{}^2} = \frac{8\pi^2 e^2}{mc^3} N$$

or

$$\sum_n \nu_{0n} B_{0n} = -\frac{\pi e^2}{3m} N.$$

Alternative method

The sum $\sum_n W_{0n}{}^2 |x_{0n}|^2$ can be expressed alternatively as $\sum_n \sum_\mu W_{0n}{}^2 x_\mu(0n) \sum_\nu x_\nu(n0)$. (In the rest of the paper matrix components of coordinates and momenta are understood to have time factors of the form $\exp[(2\pi i/h) W_{0n} t]$.) As before, $p_{x\mu}(0n) = m(2\pi i/h) W_{0n} x_\mu(0n)$, and making use of the above convention as to the time factor of a matrix component, we have, letting the dot denote differentiation with respect to time:

$$\dot{p}_{x\mu}(0n) = m(2\pi i/h)^2 W_{0n}{}^2 x_\mu(0n)$$

so that

$$W_{0n}{}^2 x_\mu(0n) = (1/m)(h/2\pi i)^2 \dot{p}_{x\mu}(0n).$$

The sum then becomes $(1/m)(h/2\pi i)^2 \sum_n \sum_\mu \sum_\nu \dot{p}_{x\mu}(0n)x_\nu(n0)$. We now make use of the fact that $\dot{p}_{x\mu}(0n) = -(\partial V/\partial x_\mu)_{0n}$, where V is the potential energy of the atom,[3] and of the rule for a matrix product, obtaining for the sum the expression

$$\frac{1}{m}\left(\frac{h}{2\pi}\right)^2 \sum_\mu \sum_\nu \left(\frac{\partial V}{\partial x_\mu} x_\nu\right)_{00}.$$

Summing on x, y, z, we get

$$\sum_{n,xyz} W_{0n}{}^2 \left| x_{0n} \right|^2 = \frac{1}{m}\left(\frac{h}{2\pi}\right)^2 \sum_\mu \sum_\nu (\nabla_\mu V \cdot R_\nu)_{00}$$

where ∇_μ is the gradient operator in the coordinates of the μth electron, and R_ν is the radius vector to the νth electron. This expression can be split into the parts

$$\frac{1}{m}\left(\frac{h}{2\pi}\right)^2 \sum_{\mu=1}^{N} (\nabla_\mu V \cdot R_\mu)_{00} \text{ and } \frac{1}{m}\left(\frac{h}{2\pi}\right)^2 \sum_{\mu \neq \nu} \sum (\nabla_\mu V \cdot R_\nu)_{00}.$$

The first part can be transformed by Euler's theorem (since V is a homogeneous function of the electron coordinates of degree -1), and becomes $(-1/m)\ (h/2\pi)^2 V_{00}$. Application of the virial theorem, according to which $V_{00} = 2W_0$, gives finally for the first part $-(h^2/2\pi^2 m)W_0$, agreeing with the non-cross term of the first method. The cross term $(1/m)(h/2\pi)^2 \sum \sum_{\mu \neq \nu} (\nabla_\mu V \cdot R_\nu)_{00}$ must thus be equal to that obtained by the first method, $(1/m^2)(h/2\pi)^2 \sum \sum_{\mu \neq \nu} (\vec{p}_\mu \cdot \vec{p}_\nu)_{00}$. It does not appear that this equivalence could be shown in any other way. The new form for the cross term is more useful for calculation, since it does not require us to differentiate a wave function which may be unwieldy. For an atom of atomic number Z with N electrons it becomes:

$$\frac{e^2}{2m}\left(\frac{h}{2\pi}\right)^2 \int \bar{\psi}_0 \Bigg[Z \sum_{\mu \neq \nu}^{N} \sum \frac{1}{r_\mu{}^3}(r_\mu{}^2 + r_\nu{}^2 - r_{\mu\nu}{}^2) + \sum_{\mu \neq \nu}^{N} \sum \sum_{j \neq \mu} \frac{1}{r_{j\mu}{}^3}(r_j{}^2 - r_\mu{}^2 + r_{\mu\nu}{}^2 - r_{j\nu}{}^2) \Bigg] \psi_0 d\tau .$$

For the special case of a two-electron atom the cross term becomes

$$\frac{1}{m}\left(\frac{h}{2\pi}\right)^2 \int \bar{\psi}_0 \left[Ze^2 r_1 r_2 \cos \Theta_{12} \left(\frac{1}{r_1{}^3} + \frac{1}{r_2{}^3}\right) + \frac{e^2}{r_{12}} \right] \psi_0 d\tau$$

where Θ_{12} is the angle between the radius vectors. If this is calculated out with a separated wave function, the term e^2/r_{12} leads to a nonvanishing result, in contrast to the first method, which gave zero. This discrepancy is undoubtedly due to the inaccuracy of the assumption of separability.

[3] The proof is like that given by Sommerfeld, Wellenmechanischer Ergänzungsband, pp. 288, 289 for a diagonal component of momentum. The operators div, grad, and Δ, however, are now operators in 3 N-space, rather than 3-space, and with us the time component of a wave function of a stationary state k is $\exp\left[-(2\pi i/h)W_k t\right]$ rather than $\exp\left[+(2\pi i/h)W_k t\right]$, so that $z_{0n} = \int \bar{\psi}_0 z \psi_n d\tau$, rather than $\int \psi_0 z \bar{\psi}_n d\tau$, as with Sommerfeld.

Section II

We continue with the case $j=3$. The problem is to evaluate $\sum_n W_{0n}{}^3 |x_{0n}|^2$. First, $W_{0n}{}^3 |x_{0n}|^2$, because of the hermitian character of our matrices, can be expressed as $-(W_{0n}{}^2 x_{0n})(W_{n0}x_{n0})$. The factor $W_{n0}x_{n0}$ can be then placed equal, as before, to $(h/2\pi im)p_x(n0)$. Also, as before,

$$\dot{p}_x(0n) = m\left(\frac{2\pi i}{h}\right)^3 W_{0n}{}^2 x_{0n}$$

Thus

$$W_{0n}{}^2 x_{0n} = \left(\frac{h}{2\pi i}\right)^2 \frac{1}{m}\,\dot{p}_x(0n)$$

and

$$W_{0n}{}^3 |x_{0n}|^2 = \frac{h}{2\pi i}\,\frac{h^2}{4\pi^2 m^2}\,\dot{p}_x(0n)\,p_x(n0).$$

Now

$$\dot{p}_x(0n) = \sum_{\mu=1}^{N} \dot{p}_{x\mu}(0n)$$

and

$$\dot{p}_{x\mu}(0n) = -\left(\frac{\partial V}{\partial x_\mu}\right)_{0n}$$

Thus $\dot{p}_x(0n) = -\sum_\mu (\partial V/\partial x_\mu)_{0n}$, so that

$$W_{0n}{}^3 |x_{0n}|^2 = -\frac{h}{2\pi i}\,\frac{h^2}{4\pi^2 m^2} \sum_\mu \sum_\nu \left(\frac{\partial V}{\partial x_\mu}\right)_{0n} p_{x\nu}(n0).$$

Upon summing on n, making use of the rule for a matrix product, we obtain

$$\sum_n W_{0n}{}^3 |x_{0n}|^2 = -\frac{h}{2\pi i}\,\frac{h^2}{4\pi^2 m^2} \sum_\mu \sum_\nu \left(\frac{\partial V}{\partial x_\mu} p_{x\nu}\right)_{00}. \tag{10}$$

Eq. (10), then, is the rule for $j=3$ in the general case of an N-electron atom. (The i, of course, is cancelled on performing the indicated operations.) We next consider the special cases $N=1$ and $N=2$.

Case 1: $N=1$

Letting 0 denote any discrete state of an H-like atom

$$\sum_k W_{0k}{}^3 |x_{0k}|^2 = \frac{1}{m^2}\left(\frac{h}{2\pi}\right)^4 \left(\frac{\partial V}{\partial x}\,\frac{\partial}{\partial x}\right)_{00}$$

and

$$\sum_{k,\,xyz} W_{0k}{}^3 |x_{0k}|^2 = \frac{1}{m^2}\left(\frac{h}{2\pi}\right)^4 J, \text{ where } J = \int \bar{\psi}_0 \nabla V \cdot \nabla \psi_0 d\tau.$$

But $V = V$ (r only). So that

$$\nabla V \cdot \nabla \psi_0 = \frac{dV}{dr}\,\frac{\partial \psi_0}{\partial r} = \frac{Ze^2}{r}\,\frac{\partial \psi_0}{\partial r},$$

(since $V = -Ze^2/r$). Thus

$$J = Ze^2 \int \bar{\psi}_0 \frac{1}{r^2} \frac{\partial \psi_0}{\partial r} d\tau$$

and since $\psi_0 = R(r)\Theta(\theta)\Phi(\phi)$,

$$J = Ze^2 \int_0^\infty R \frac{dR}{dr} dr \int_0^\pi \Theta^2 \sin\theta d\theta \int_0^{2\pi} \bar{\Phi}\Phi d\phi.$$

Letting R, Θ, and Φ be separately normalized,

$$J = Ze^2 \int_0^\infty R \frac{dR}{dr} dr = \frac{Ze^2}{2}\left[R^2(\infty) - R^2(0)\right] = -\frac{Ze^2}{2} R^2(0),$$

since the radial wave function always vanishes at infinity. Then, making use of the properties of the Laguerre polynomials involved in the radial wave function, we find:

$$J = 0, \; l \neq 0$$
$$= -(2e^2/a_0^3)Z^4/n^3, \; l = 0$$

where a_0 is the Bohr radius, n the principal quantum number, and l the azimuthal quantum number of the state 0. Thus the cube sum vanishes for $l \neq 0$, and equals

$$-\frac{1}{m^2}\left(\frac{h}{2\pi}\right)^4 \frac{2e^2}{a_0^3} \frac{Z^4}{n^3} \text{ for } l = 0.$$

It is interesting to express these relations in terms of the A's. Since

$$A_{0k} = \frac{64\pi^4 e^2}{3c^3 h^4} W_{0k}^3 (|x_{0k}|^2 + |y_{0k}|^2 + |z_{0k}|^2),$$

$$\sum_k A_{0k} = 0, \; l \neq 0$$
$$= -\frac{8e^4}{3m^2c^3a_0^3} \frac{Z^4}{n^3}, \; l = 0.$$

Expressed in words, in any hydrogen-like atom, the sum of the spontaneous transition probabilities from any state not an S-state to all lower states is equal to the sum of the spontaneous transition probabilities from all higher states down to the given state. For an S-state they are unequal, the difference varying inversely with the cube of the principal quantum number and directly with the fourth power of atomic number; for S-states near the ionization limit they approach equality. (By a *state* is here meant a level with given l and m; if one wishes to treat state as meaning a given l only, that is, to average over different *orbital orientations*, one must take into account such orbital degeneracy in writing down the formulas for the A's or the B's in terms of matrix components. The necessary quantum weight factors can be found most explicitly in a paper by Y. Sugiura.[4])

[4] Y. Sugiura, Phil. Mag. [7] **4**, 495 (1927).

For example, the sum of the spontaneous transition probabilities from all higher states, continuous included, to the state $2P$ (with given m) in hydrogen-like atoms is equal to the spontaneous transition probability from that state to the groundstate $1S$. (m here means magnetic quantum number.)

Applied to the case in which 0 denotes the ground state of an H-like atom, this cube rule furnishes an independent proof of a theorem familiar from direct examination of the hydrogenic functions. We have shown that this sum is of the order Z^4/n^3 for S-states of H-like atoms, and zero for other states. Since for the ground state all the A_{0k}'s have the same sign, it follows that their sum cannot vanish, so that we have: the ground state of an H-like atom must be an S-state.

Case 2: $N=2$, helium-like atoms

On writing out the double sum, we obtain:

$$\sum_n W_{0n}{}^3 \left| x_{0n} \right|^2 = -\frac{h}{2\pi i}\frac{h^2}{4\pi^2 m^2}\left(\frac{\partial V}{\partial x_1}p_{x1}+\frac{\partial V}{\partial x_2}p_{x2}+\frac{\partial V}{\partial x_1}p_{x2}+\frac{\partial V}{\partial x_2}p_{x1}\right)_{00}.$$

Using $V=-Ze^2/r_1-Ze^2/r_2+e^2/r_{12}$, and carrying through the indicated operations in a straightforward way, we obtain:

$$\sum_{n,xyz} W_{0n}{}^3 \left| x_{0n} \right|^2 = \left(\frac{h}{2\pi}\right)^4 \frac{Ze^2}{m^2}\left[\frac{1}{r_1{}^3}\sum_{xyz}x_1\frac{\partial}{\partial x_1}+\frac{1}{r_2{}^3}\sum_{xyz}x_2\frac{\partial}{\partial x_2}\right.$$
$$\left.+\frac{1}{r_1{}^3}\sum_{xyz}x_1\frac{\partial}{\partial x_2}+\frac{1}{r_2{}^3}\sum_{xyz}x_2\frac{\partial}{\partial x_1}\right]_{00}.$$

Letting 1_{r_μ}, $1_{\theta\mu}$, $1_{\phi\mu}$ be unit vectors along the radius, meridian, and parallel of latitude through the μth electron,

$$\sum_{xyz}x_\mu\frac{\partial}{\partial x_\mu}=r_\mu\frac{\partial}{\partial r_\mu}$$

Also

$$\sum_{xyz}x_\mu\frac{\partial}{\partial x_\nu}=r_\mu 1_{r\mu}\cdot\nabla_\nu,$$

where ∇_ν is the gradient in the coordinates of the νth electron. Using these abbreviations, we can write the cube sum for $N=2$ in the form:

$$\left(\frac{h}{2\pi}\right)^4\frac{Ze^2}{m^2}\int\bar{\psi}_0\left[\frac{1}{r_1{}^2}\frac{\partial}{\partial r_1}+\frac{1}{r_2{}^2}\frac{\partial}{\partial r_2}+\frac{1}{r_1{}^2}1_{r1}\cdot\nabla_2+\frac{1}{r_2{}^2}1_{r2}\cdot\nabla_1\right]\psi_0 d\tau.$$

Knowing the wave function of any discrete state of a helium-like atom, we have here a rule for the evaluation of $\sum_n A_{0n}$ for the atom. We might mention that for S-states (e.g., $(1s)^2$ or $(1s)(2s)$), an approximate function of the form $\psi_0=\psi_0(r_1, r_2)$ (no angular dependence) is often used. In such a case

$$1_{r1} \cdot \nabla_2 \psi_0 = \cos \Theta_{12} \frac{\partial}{\partial r_2} \psi_0$$

$$1_{r2} \cdot \nabla_1 \psi_0 = \cos \Theta_{12} \frac{\partial}{\partial r_1} \psi_0,$$

where Θ_{12} is the angle between the radius vectors $\vec{r}_1$ and $\vec{r}_2$. But $\int \cos \Theta_{12} \sin \theta_1 d\theta_1 d\phi_1 \sin \theta_2 d\theta_2 d\phi_2 = 0$. Thus if $\psi_0 = \psi_0(r_1, r_2)$, the terms involving both electrons drop out of the integrand and the cube sum reduces to the integral

$$\left(\frac{h}{2\pi}\right)^4 \frac{Ze^2}{m^2} \int \bar{\psi}_0 \left(\frac{1}{r_1^2} \frac{\partial}{\partial r_1} + \frac{1}{r_2^2} \frac{\partial}{\partial r_2}\right) \psi_0 d\tau.$$

In applying this to the ground state of helium, it is convenient to express the cube sum in atomic units, in which case the factor in front of the integral becomes $8Z$. Using a simple screening constant wave function $\psi_0 = -(\alpha^3/\pi)^{1/2} e^{-\alpha(r_1+r_2)}$ where $\alpha = Z - 5/16$, the cube sum becomes $-32Z(Z-5/16)^3$.

Section III $j = 4$

To evaluate $\sum_{n,xyz} W_{0n}{}^4 |x_{0n}|^2$. Taking the general case of an N-electron atom, we begin as before:

$$\left(\frac{\partial V}{\partial x_\mu}\right)_{0n} = -\dot{p}_{x\mu}(0n)$$

$$= m(2\pi/h)^2 W_{0n}{}^2 x_\mu(0n).$$

Thus

$$\sum_\mu \left(\frac{\partial V}{\partial x_\mu}\right)_{0n} = m(2\pi/h)^2 W_{0n}{}^2 x_{0n}$$

and

$$m^2(2\pi/h)^4 W_{0n}{}^4 |x_{0n}|^2 = \sum_\mu \sum_\nu \left(\frac{\partial V}{\partial x_\mu}\right)_{0n} \left(\frac{\partial V}{\partial x_\nu}\right)_{n0}.$$

Summing over all the states n,

$$\sum_n (2\pi/h)^4 m^2 W_{0n}{}^4 |x_{0n}|^2 = \sum_\mu \sum_\nu \left(\frac{\partial V}{\partial x_\mu} \frac{\partial V}{\partial x_\nu}\right)_{00}$$

$$= \left\{\left(\sum_{\mu=1}^N \frac{\partial V}{\partial x_\mu}\right)^2\right\}_{00}$$

$$= \int \bar{\psi}_0 \left(\sum_{\mu=1}^N \frac{\partial V}{\partial x_\mu}\right)^2 \psi_0 d\tau.$$

For a hydrogen-like atom, $N=1$, we obtain for the fourth-power sum:

$$\left(\frac{h}{2\pi}\right)^4 Z^2 e^4 \left(\frac{1}{r^4}\right)_{00}$$

where

$$\left(\frac{1}{r^4}\right)_{00} = \frac{\frac{3}{2}Z^3\left[1 - \frac{l(l+1)}{3n^2}\right]}{a_0{}^4 n^3 (l+3/2)(l+1)(l+\frac{1}{2})l(l-\frac{1}{2})}.$$

This fourth-power rule gives a rule for summing $\sum_k \nu_{0k} A_{0k}$. The presence of l in the denominator of the above expression leads to the result that a sum of transition probabilities with this sort of frequency weighting diverges for S-states of hydrogen-like atoms.

For a helium-like atom, this rule takes a simple form. Using

$$V = -\frac{Ze^2}{r_1} - \frac{Ze^2}{r_2} + \frac{e^2}{r_{12}},$$

we find

$$\left(\sum_\mu \frac{\partial V}{\partial x_\mu}\right)^2 = Z^2 e^4 \left(\frac{x_1{}^2}{r_1{}^6} + \frac{x_2{}^2}{r_2{}^6} + 2\frac{x_1 x_2}{r_1{}^3 r_2{}^3}\right).$$

Summing over x, y, z,

$$\sum_{xyz}\left(\sum_\mu \frac{\partial V}{\partial x_\mu}\right)^2 = Z^2 e^4 \left(\frac{1}{r_1{}^4} + \frac{1}{r_2{}^4} + \frac{2}{r_1{}^2 r_2{}^2}\cos\Theta_{12}\right)$$

where Θ_{12} is the angle between the radius vectors $\vec{r}_1$, $\vec{r}_2$, from which is obtained the fourth-power sum:

$$\left(\frac{h}{2\pi}\right)^4 Z^2 e^4 \int \bar{\psi}_0 \left(\frac{1}{r_1{}^4} + \frac{1}{r_2{}^4} + \frac{2}{r_1{}^2 r_2{}^2}\cos\Theta_{12}\right)\psi_0 d\tau.$$

Going back to H-like atoms, we can use the cube and fourth-power rules to deduce the asymptotic behavior of the A's between the ground state and the continuous spectrum. $\sum_k \nu_{0k} A_{0k}$ diverges for S-states, and therefore for the ground state. For this state the $\nu_{0k} A_{0k}$ all have the same sign. For the discrete spectrum (Lyman series), $\nu_{0k} A_{0k}$ is asymptotically of the order $1/n_k{}^3$, and since $\sum_1{}^\infty 1/n_k{}^3$ is known to converge, it follows that the sum $\sum_k \nu_{0k} A_{0k}$ over the discrete spectrum only must converge. Thus $\int \nu (dA_{0\nu}/d\nu) d\nu$ over the continuous spectrum must diverge. In a similar manner, using the cube rule, it follows that $\int (dA_{0\nu}/d\nu) d\nu$ over the continuous spectrum must converge. Writing $dA_{0\nu}/d\nu$ asymptotically (large ν) as const./$\nu^{1+\epsilon}$ we see that $\int_{\nu_0}{}^\infty d\nu/\nu^{1+\epsilon}$ must converge and $\int_{\nu_0}{}^\infty d\nu/\nu^\epsilon$ must diverge, (where ν_0 = frequency of Lyman series limit). The first requirement gives $\epsilon > 0$, the second $\epsilon \leqq 1$, so that $0 < \epsilon \leqq 1$. Thus the f-value $df_{0\nu}/d\nu (= \nu^{-2}\, dA_{0\nu}/d\nu)$ is of the order $1/\nu^i$, where

$3 < j \leqq 4$. This example serves to illustrate how the sum rules can be used to obtain information about the intensity distribution in the continuous spectrum without knowing anything about the continuous wave functions.

It should be mentioned that Dirac and Harding[5] have already obtained the sum rules of this paper for the special case when the state 0 is the ground state of hydrogen. Besides this restriction, their method encounters an ambiguity of a peculiar sort, in that part of an operator may operate backwards and part forwards; this ambiguity has to be removed by a special investigation.

The author is indebted to Professors J. C. Slater and M. S. Vallarta,who have read the manuscript and offered suggestions, and especially to Professor P. M. Morse, who has taken a very helpful interest in the paper and offered many valuable suggestions.

[5] Dirac and Harding, Proc. Camb. Phil. Soc. **28,** 209 (1932).

Multiplet Splitting and Intensities of Intercombination Lines Part I

By HUGH C. WOLFE*
Utrecht University

(Received June 13, 1932)

Kramers' symbolic representation method for the treatment of those properties of free atoms which can be derived on the basis of irreducible representations of rotations in R_3 is outlined. Wave functions and operators are represented by functions of spinor quantities (ξ, η) whose properties are known from the theory of invariants. Integrations yielding matrix elements are only symbolic and the results, being determined by the rotation invariance properties, contain therefore undetermined constant factors of the nature of radial integrals. The method is particularly adapted to the problem of multiplets (interaction between two or more "vectors"—e.g., orbital angular momenta, spins—treated as a perturbation). The method is applied to configurations involving two valence electrons of which one is in an s state. Such a configuration gives rise to a singlet and a triplet with the l value of the second electron. The deviations from the normal l to $l+1$ interval ratio in the triplet are due to a repulsion between the singlet level and the center triplet level, their j values being the same. The mixing up of the wave functions of these two levels gives rise to singlet-triplet intercombinations. The constants which represent the interaction energies (1) interchange, (2) spin-orbit, (3) spin of one electron—orbit of the other (assuming that other types of interaction may be neglected) are found in terms of the three intervals of the multiplet. Corrections to the Kronig-Hönl intensity formulas are found in terms of the intervals of the two multiplets between which the transitions occur. These formulas then give the relative intensities of combination and intercombination lines. The sum rules for intensity hold for the complete multiplet and not for the singlet and triplet separately. Part II will contain application of the theory to observed spectra.

IN HIS book, *Quantenmechanik und Gruppentheorie*, Weyl has shown that many of the properties of free atoms can be derived on the basis of irreducible representations of the rotations in three dimensional space. Kramers[1] has obtained a very elegant formulation of Weyl's methods through the use of symbolic representations of wave functions and operators with properties well known from the theory of invariants. We propose here to outline this method and to show its application to a problem in complex spectra.

THE SYMBOLIC METHOD

1.

Let ξ and η be the components of a *spinor* or *half-vector*, i.e., a two-dimensional complex vector. The transformations of the monomials $\xi^{l+m}\eta^{l-m}$ $(m=-l,\ -l+1,\ \cdots\ l)$, when ξ and η suffer a unitary transformation, constitute an irreducible representation of degree $2l+1 (l=1/2,\ 1,\ 3/2,\ \cdots)$ of the space rotation group. Except the identity, there are no other irreducible

* Fellow of the Lorentz Foundation.

[1] H. A. Kramers, Proc. Amst. Acad. **33,** 953 (1930) and **34,** 965 (1931).

representations. Then a series of $2\tau+1$ quantities G_f, which transform into each other in an irreducible way under space-rotation, may be gathered up in the one formula

$$\sum_f \binom{2\tau}{\tau-f} a^{\tau-f}(-b)^{\tau+f} G^f = (a\eta - b\xi)^{2\tau}, \tag{1}$$

where a and b are the components of an arbitrary constant spinor. The G_f can always be so chosen that they transform like $\xi^{\tau+f}\eta^{\tau-f}$. $(a\eta - b\xi)$ is invariant.

2.

In the study of multiplets, a free atom may be treated as if it consisted of two or more *vector-frames* (Vektorgerüste), to each of which belongs a quantum number of the total angular momentum and whose mutual orientation has, in first approximation, no influence on the energy of the stationary states. In the complete energy expression there appear small interaction terms which depend, in a not purely additive fashion, on the elements (Bestimmungsstücke) of a pair of vectors and which denote an energetic coupling of these vectors.[2] As a consequence of this coupling every *state*, defined by the quantum numbers of the vectors, splits up into a multiplet.

Consider the coupling of just two vectors. In analogy with the notation for Russell-Saunders coupling but without assuming anything about the physical nature of the vectors, we may designate their quantum numbers of angular momentum by l and s.

The interaction terms in the complete energy expression may be written down in the form

$$\Omega = \sum_n a_n \lambda_n \sigma_n . \tag{2}$$

Here λ_n and σ_n are functions, respectively, only of the elements of the l-frame and only of the elements of the s-frame in such fashion that λ_n and σ_n are not invariant under an arbitrary space-rotation but transform according to some linear law. The coefficients a_n may contain any combination of rotation-invariant functions of the elements of either frame. In practice, Ω is usually given immediately in this form or else, when the l-frame and the s-frame are associated with different particles, Ω contains terms involving $1/r_{12}$. The expansion

$$\frac{1}{r_{12}} = \frac{1}{r_b} \sum_m \left(\frac{r_a}{r_b}\right)^m P_m\left(\frac{(\boldsymbol{r}_1 \cdot \boldsymbol{r}_2)}{r_1 r_2}\right), \tag{3}$$

where r_a and r_b are, respectively, the smaller and the larger of the distances r_1 and r_2 (the distances of the two particles from the center of gravity), brings these terms into the required form.

In an arbitrarily rotated coordinate system K' a selected λ_n, call it $\lambda^{(1)}$, assumes the form

$$\lambda^{(1)} = \sum_{\mu=1}^{g} \gamma_\mu{}^{(1)} \lambda'^{(\mu)},$$

[2] There may also be energy terms involving more than two vectors. To avoid complication, we shall not discuss these for the present. They are treated by an extension of the method.

where $\lambda'^{(1)}$ is the same quantity with respect to K' as $\lambda^{(1)}$ with respect to the original coordinate system K. Thus there are $g-1$ other l-frame functions $\lambda^{(p)}$ $(p=2, \cdots, g)$ associated with $\lambda^{(1)}$ and these quantities transform in a way which gives a representation of the space-rotation group of degree g. If this representation is irreducible we shall say, for brevity: $\lambda^{(1)}$ transforms irreducibly. If it is not, one can always reduce the transformation with the result that each $\lambda^{(p)}$ is expressed by the finite sum $\sum_f \lambda_f{}^{(p)}$ where the $\lambda_f{}^{(p)}$ transform irreducibly. Thus it is always possible to express Ω in the form (2) in such a way that every λ_n and also every σ_n transforms irreducibly.

Since we are dealing with a free atomic system, the series (2) is rotation-invariant and therefore can be divided up into parts such that the λ and σ in each part transform irreducibly with the same degree g.[3] Thus we may write

$$\Omega = \sum_{g=1}^{\infty} T_g, \tag{4}$$

$$T_g = \sum a\lambda_{(g)}\sigma_{(g)}, \tag{5}$$

where the summation indices have been omitted in the last sum.

In the quantum theory, the elements which determine an atomic system are uniquely defined according to their significance; the elements of the electron spin (its angular momentum components) as well as the ordinary coordinates and momenta have this property. That we consider them as operators makes no difference. But, for even values of g, the transforming quantities are only defined up to a factor ± 1. Actually, in the series (4), only odd values of g occur and, if we set $g=2\tau+1$ and $T_g=\Omega_\tau$, (4) assumes the form

$$\Omega = \sum_{\tau=0}^{\infty} \Omega_\tau. \tag{6}$$

We are now ready to consider the symbolic representation of the energy operators. We have already remarked that $2\tau+1$ quantities which transform irreducibly under space-rotation may be represented by $\xi^{\tau+f}\eta^{\tau-f}$. If we represent the $\lambda_{(g)}$ by $x_1{}^{\tau+f_1}\, y_1{}^{\tau-f_1}$ and the $\sigma_{(g)}$ by $x_2{}^{\tau+f_2}\, y_2{}^{\tau-f_2}$, then Ω_τ must contain these quantities in the form

$$\omega_\tau = (x_2y_1 - y_2x_1)^{2\tau}. \tag{7}$$

For Ω_τ is invariant under rotation and the only simultaneous invariant that can be formed of two spinors is $(x_2y_1-y_2x_1)^n$, where n is a positive integer. In general, Ω_τ may be a sum of expressions like (7).[4]

3.

Let us now consider the symbolic representation of the wave functions. Each state of a multiplet is uniquely defined by the quantum number j of the

[3] It is well known that $\Sigma a\lambda_{(g)}\lambda_{(g')}$ is never invariant for $g \neq g'$.

[4] In case of an energy term involving three vector-frames, we shall have symbolic terms of the type

$$(x_2y_1-y_2x_1)^\alpha(x_3y_1-y_3x_1)^\beta(x_3y_2-y_3x_2)^\gamma,$$

where α, β, and γ must be all even or all odd integers.

resultant angular momentum, where

$$|l - s| \leqq j \leqq l + s.$$

Wave functions satisfying the unperturbed (i.e., interaction terms neglected) wave equation may be composed of products of two functions, one of coordinates associated only with the l-frame and one of coordinates associated only with the s-frame. There are $2l+1$ functions of the first type which transform irreducibly under space-rotation and may be represented symbolically by ${\xi_1}^{l+m_1}\ {\eta_1}^{l-m_1}$ and $2s+1$ functions of the second type, which may be represented by ${\xi_2}^{s+m_2}\ {\eta_2}^{s-m_2}$. For the state with quantum number j of the multiplet there must be $2j+1$ functions which transform irreducibly under rotation and are composed linearly of terms ${\xi_1}^{l+m_1}\ {\eta_1}^{l-m_1}\ {\xi_2}^{s+m_2}\ {\eta_2}^{s-m_2}$. We introduce a constant spinor (a, b) and form the invariants

$$P = (\xi_2\eta_1 - \eta_2\xi_1);\ Q = (a\eta_1 - b\xi_1);\ R = (a\eta_2 - b\xi_2). \tag{8}$$

Then the state with quantum number j is represented by the invariant

$$\psi_{lsj} = P^\alpha Q^\beta R^\gamma, \tag{9}$$

where

$$\alpha + \beta = 2l;\ \alpha + \gamma = 2s;\ \beta + \gamma = 2j. \tag{10}$$

The $2j+1$ functions, which would be required for the study of the Zeeman effect, are the coefficients in ψ_{lsj} of $a^{j-m'}\ b^{j+m'}$ $(m' = -j,\ -j+1,\ \cdots,\ j)$.[5]

4.

We now proceed to show that every term of (6) makes a contribution to the energetic splitting of the multiplet which is, up to a numerical constant C_τ which does not depend on j, a completely determined function of l, s, j, and τ.

According to the principles of the quantum mechanics, the energy splitting E_τ, due to the interaction term (7), is given by

$$E_\tau \int \psi_{lsj}{}^* \psi_{lsj} = \int \psi_{lsj}{}^* \omega_\tau \psi_{lsj}, \tag{11}$$

where $\int$ means integration and summation over all space and spin coordinates. Both integrals are invariant under rotation and every term must contain (a, b) and (a^*, b^*) each to the power $2j$. The only invariant of (a, b) and (a^*, b^*) is (a^*a+b^*b) to some integral power. Therefore, these quantities appear in both integrals only in the form of a factor $(a^*a+b^*b)^{2j}$ and E_τ does not depend on (a, b).

[5] In case there were more than two vector frames composing our atomic system, we should form our wave functions of products of all the invariants $(\xi_i\eta_k - \eta_i\xi_k)$ and $(a\eta_k - b\xi_k)$ in such a way that in every term the sum of the powers of ξ_i and η_i is $2l_i$ and the sum of the powers of a and b is $2j$. In general, it will be possible to do this in a number of linearly independent ways, say f, which means that there will be f states of the multiplet with the same j value. To find the *stabilized* linear combinations of these f functions is a perturbation problem involving the solution of an f order secular determinant.

In (11), ω_τ is an operator which works on $\psi_{ls}{}_j$. ω_τ is built up by multiplication and addition of operators which involve only the coordinates of the l-frame or only those of the s-frame. Accordingly, when we have written out all the terms in (11), every term may be put in the form

$$CI_1I_2$$

where I_1 and I_2 involve, respectively, the coordinates of the l-frame and of the s-frame and are integrals of the type:

$$I_1 = \int \xi_1{}^{*l+m_1'}\eta_1{}^{*l-m_1'}x_1{}^{\tau+\mu_1}y_1{}^{\tau-\mu_1}\xi_1{}^{l+m_1}\eta_1{}^{l-m_1}, \tag{12a}$$

$$I_2 = \int \xi_2{}^{*s+m_2'}\eta_2{}^{*s-m_2'}x_2{}^{\tau+\mu_2}y_2{}^{\tau-\mu_2}\xi_2{}^{s+m_2}\eta_2{}^{s-m_2}. \tag{12b}$$

The j value appears only in the factor C which contains, in a known manner, the expansion coefficients of the various factors in (11). We will show that, on account of the irreducibility of the transformations which the factors in I_1 and in I_2 suffer under space-rotation, both integrals are completely determined in their dependence on the various m's. There remains over only a common constant C_τ, in principle undeterminable by the symbolic method, which depends in general on l, s, τ, and the particular atomic system with which we have to do and which is of the nature of a radial integral.

All integrals of the type (12a) are obtained by comparing coefficients of like powers of the components of the constant spinors on the two sides of

$$\int (a^*\eta_1{}^* - b^*\xi_1{}^*)^{2l}(A\,y_1 - Bx_1)^{2\tau}(a\eta_1 - b\xi_1)^{2l}$$

$$= \text{const}\ (a^*a + b^*b)^{2l-\tau}(a^*A + b^*B)^{\tau}(aB - bA)^{\tau}. \tag{13}$$

The evaluation of this integral follows directly from the invariance under rotation of all the factors in the integrand and of the domain of integration. The result must be built up of the three invariants of (a^*, b^*), (a, b) and (A, B) and these quantities appear to the proper powers only in the form given in (13).

5.

Having seen that the results of the integrations in (11) are determined by the transformation properties of the factors and therefore do not depend on the special form of the operators which occur in ω_τ, we may simplify the integration in (11) by choosing special expressions for the operators $x_k{}^{\tau+\mu}$ $y_k{}^{\tau-\mu}$ which transform in the same way. We have only to take care that in so doing we do not make the integral vanish identically.

Replacing $x_k{}^{\tau+\mu}$ $y_k{}^{\tau-\mu}$ by operators acting on functions of the symbols ξ_k and η_k, we shall obtain, in place of (12a) and (12b), integrals of the type

$$\int \xi_k{}^{*\rho'+\nu'}\eta_k{}^{*\rho'-\nu'}\xi_k{}^{\rho+\nu}\eta_k{}^{\rho-\nu}. \tag{14}$$

All integrals of this type are found by comparing coefficients on the two sides of

$$\int (a^*\eta^* - b^*\xi^*)^{2\rho'}(a\eta - b\xi)^{2\rho} = \text{const. } (a^*a + b^*b)^{2\rho}\delta_{\rho'\rho}, \tag{15}$$

where the results of integration are again determined immediately by the invariance. We find for (14) the result

$$\text{const.}\begin{pmatrix} 2\rho \\ \rho + \nu \end{pmatrix}^{-1} \delta_{\rho'\rho\nu'\nu}. \tag{16}$$

Thus we find that our choice of operators to replace $x_k^{\tau+\mu}$, $y_k^{\tau-\mu}$ is limited to such as make $\psi_{ls_i}^*\, \omega_\tau\, \psi_{ls_j}$ homogeneous in (ξ_k^*, η_k^*) to the same degree as in (ξ_k, η_k). The most satisfactory operators fulfilling this requirement are obtained from the formula

$$(Ay_k - Bx_k)^{2\tau} = (A\eta_k - B\xi_k)^\tau \left(A\frac{\partial}{\partial \xi_k} + B\frac{\partial}{\partial \eta_k}\right)^\tau. \tag{17}$$

Both sides are rotation-invariant and the $x_k^{\tau+\mu}\, y_k^{\tau-\mu}$ are uniquely defined by comparison of terms with the same powers of A and B. We may remark that the order of the factors on the right hand side of (17) is arbitrary since we have the same thing still after exchanging them. (17) is the special case $\rho = 0$ of the more general formula

$$(Ay_k - Bx_k)^{2\tau} = (A\eta_k - Bx_k)^{\tau+\rho} \left(A\frac{\partial}{\partial \xi_n} + B\frac{\partial}{\partial \eta_k}\right)^{\tau-\rho}. \tag{18}$$

The Configuration: Two Electrons, One in an *s*-State

6.

We shall now see how this symbolic method works as applied to spectra involving two valence electrons, of which one is in an *s*-state.[6]

The two electrons have angular momentum quantum numbers respectively l for the orbit, $1/2$ for the spin and 0 for the orbit, $1/2$ for the spin. The $2l+1$ wave functions of the orbital coordinates of the first particle, which transform irreducibly under rotation, may be represented symbolically by the $2l+1$ monomials $\xi^{l+m}\, \eta^{l-m}$. Likewise we have two monomials S_+ and S_- (the two components of a *spinor*; hence the name) to represent the spin functions of the first particle and two monomials $\overline{S}_+$ and $\overline{S}_-$ to represent the spin functions of the second. From the spinors (ξ, η), (S_+, S_-), $(\overline{S}_+, \overline{S}_-)$, and (a, b) we form the six invariants:

$$(a\eta - b\xi), (aS_- - bS_+), (a\overline{S}_- - b\overline{S}_+), (S_+\eta - S_-\xi), (\overline{S}_+\eta - \overline{S}_-\xi), (S_+\overline{S}_- - S_-\overline{S}_+).$$

[6] Houston (Phys. Rev. **33**, 297 (1929)) has treated this case, using the explicit wave functions and energy operators. The present treatment takes account of the interaction of the spin of each electron with the orbit of the other, which Houston did not consider. As we shall see in Part II, this interaction is not negligible.

These must be multiplied together to form polynomials homogeneous in (ξ, η) to the power $2l$, in (S_+, S_-) and in $(\bar{S}_+, \bar{S}_-)$ to the power one, and in (a, b) to the power $2j$.

We find (as we should expect from the vector model) that the only possible values of j are $l+1$, l, $l-1$. The symbolic functions for $j=l+1$ and $j=l-1$ are uniquely determined but there are three functions for $j=l$, of which two are independent. Thus our multiplet will consist of four levels (a triplet and a singlet in case of pure Russell-Saunders coupling). We form the symbolic functions:

$$\begin{aligned}
j &= l+1 \quad I = A\{(a\eta - b\xi)^{2l}(S_+b - S_-a)(\bar{S}_+b - \bar{S}_-a)\} \\
j &= l \begin{cases} II_\alpha = A\{(a\eta - b\xi)^{2l-1}(\bar{S}_+\eta - \bar{S}_-\xi)(S_+b - S_-a)\} \\ II_\beta = A\{(a\eta - b\xi)^{2l-1}(S_+\eta - S_-\xi)(\bar{S}_+b - \bar{S}_-a)\} \\ II_\gamma = A\{(a\eta - b\xi)^{2l}(S_+\bar{S}_- - S_-\bar{S}_+)\} \end{cases} \qquad (19) \\
j &= l-1 \quad III = A\{(a\eta - b\xi)^{2l-2}(S_+\eta - S_-\xi)(\bar{S}_+\eta - \bar{S}_-\xi)\}.
\end{aligned}$$

The symbol A in front of a bracket means to subtract from the expression in the bracket the same expression with (S_+, S_-) and $(\bar{S}_+, \bar{S}_-)$ interchanged and (ξ, η) replaced by $(\bar{\xi}, \bar{\eta})$. Expressions in $(\bar{\xi}, \bar{\eta})$ refer to functions of the coordinates of the second particle. Thus our wave functions are made to satisfy the Pauli principle requirement of antisymmetry.

7.

Of all the terms in the interaction energy of two electrons,[7] we shall neglect, to begin with, all except Ω_1, the electrostatic interaction,[8] e^2/r_{12}; Ω_2, the leading terms,

$$\frac{Ze^2}{2m_0c^2}\left\{\frac{([\boldsymbol{r}_1, \boldsymbol{v}_1]\cdot \mathbf{s}_1)}{r_1^3} + \frac{([\boldsymbol{r}_2, \boldsymbol{v}_2]\cdot \mathbf{s}_2)}{r_2^3}\right\},$$

in the interaction of the spin of each electron with its own orbital motion; Ω_3, the leading terms,

$$\frac{e^2}{m_0c^2}\left\{\frac{([\boldsymbol{r}_1, \boldsymbol{v}_1]\cdot \mathbf{s}_2)}{r_b^3} + \frac{([\boldsymbol{r}_2, \boldsymbol{v}_2]\cdot \mathbf{s}_1)}{r_b^3}\right\},$$

in the interaction of each spin with the orbit of the other electron. In Ω_2 and Ω_3 we have neglected all terms but the first in the expansion (3) of $1/r_{12}^3$.

To find the symbolic representation of Ω_1, we must use the expansion (3). Ω_1 then assumes the form $\sum_n a_n(\boldsymbol{r}_1\cdot\boldsymbol{r}_2)^n$, where the a_n are functions of the invariants, r_1 and r_2. Then the symbolic representation is

$$\sum_n a_n(x\bar{y} - y\bar{x})^{2n}. \qquad (20)$$

[7] See, for example, Heisenberg, Zeits. f. Physik **39**, 499 (1926).

[8] Of course, the term e^2/r_{12} does not properly constitute a small perturbation, since it is of considerable importance in fixing what one should like to consider as the *unperturbed* orbit. However, the true perturbation may be considered to be the difference between some well-chosen *central field* Hamiltonian and the true Hamiltonian in which e^2/r_{12} appears. The symbolic representation of this perturbation is the same as that of e^2/r_{12}.

In the matrix integrals which we wish to calculate, the factors coming from the wave functions will give us either (ξ^*, η^*) and (ξ, η) [or $(\bar{\xi}^*, \bar{\eta}^*)$ and $(\bar{\xi}, \bar{\eta})$] to the same power $2l$ or (ξ^*, η^*) and $(\bar{\xi}, \bar{\eta})$ [or $(\bar{\xi}^*, \bar{\eta}^*)$ and (ξ, η)] to the same power $2l$. Consequently, only the terms $n=0$ and $n=l$ in (20) will yield integrals different from zero. The term from $n=l$ is the so-called resonance term. Thus, for our purpose, the operator may be represented by[9]

$$\Omega_1 = A_0 + \frac{C_1}{(2l)!}\left\{\left(\xi\frac{\partial}{\partial\bar{\xi}} + \eta\frac{\partial}{\partial\bar{\eta}}\right)^{2l} + \left(\bar{\xi}\frac{\partial}{\partial\xi} + \bar{\eta}\frac{\partial}{\partial\eta}\right)^{2l}\right\}. \tag{21}$$

The operator Ω_2 is in the form to be represented symbolically by

$$C_2\{(Xy - Yx)^2 + (\bar{X}\bar{y} - \bar{Y}\bar{x})^2\}$$

where (x, y) is associated with the orbital coordinates and (X, Y) with the spin coordinates. We find the representation of Ω_2 in terms of the spinors which occur in the wave functions by a double use of (17):

$$\begin{cases} (Xy - Yx)^2 = (X\eta - Y\xi)\left(X\dfrac{\partial}{\partial\xi} + Y\dfrac{\partial}{\partial\eta}\right) \\ x^2 = -\xi\dfrac{\partial}{\partial\eta};\quad xy = \dfrac{1}{2}\left(\xi\dfrac{\partial}{\partial\xi} - \eta\dfrac{\partial}{\partial\eta}\right);\quad y^2 = \eta\dfrac{\partial}{\partial\xi} \end{cases}$$

$$\begin{cases} (Xy - Yx)^2 = (xS_- - yS_+)\left(x\dfrac{\partial}{\partial S_+} + y\dfrac{\partial}{\partial S_-}\right) \\ X^2 = -S_+\dfrac{\partial}{\partial S_-};\quad XY = \tfrac{1}{2}\left(S_+\dfrac{\partial}{\partial S_+} - S_-\dfrac{\partial}{\partial S_-}\right);\quad Y^2 = S_-\dfrac{\partial}{\partial S_+}. \end{cases}$$

Substituting these expressions, we obtain

$$\begin{aligned}\Omega_2 = C_2 S\Big\{&(S_+\eta - S_-\xi)\left(\frac{\partial^2}{\partial S_+\partial\eta} - \frac{\partial^2}{\partial S_-\partial\xi}\right) \\ &- \tfrac{1}{2}\left(\xi\frac{\partial}{\partial\xi} + \eta\frac{\partial}{\partial\eta}\right)\left(S_+\frac{\partial}{\partial S_+} + S_-\frac{\partial}{\partial S_-}\right)\Big\}\end{aligned} \tag{22}$$

where the symbol S in front of the bracket means to add to the expression in the bracket the same expression with barred and unbarred symbols interchanged.

The operator Ω_3 differs from Ω_2 only in the interchange of (S_+, S_-) and $(\bar{S}_+, \bar{S}_-)$.

$$\begin{aligned}\Omega_3 = C_3 S\Big\{&(\bar{S}_+\eta - \bar{S}_-\xi)\left(\frac{\partial^2}{\partial\bar{S}_+\partial\eta} - \frac{\partial^2}{\partial\bar{S}_-\partial\xi}\right) \\ &- \tfrac{1}{2}\left(\xi\frac{\partial}{\partial\xi} + \eta\frac{\partial}{\partial\eta}\right)\left(\bar{S}_+\frac{\partial}{\partial\bar{S}} + \bar{S}_-\frac{\partial}{\partial\bar{S}_-}\right)\Big\}.\end{aligned} \tag{23}$$

[9] The term for $n=l$ comes from (18) with $\tau=l$ and $\rho=-\tau$.

Applying the operator

$$\Omega = \Omega_1 + \Omega_2 + \Omega_3 \tag{24}$$

to the wave functions (19), we find

$$\begin{aligned}
\Omega \mathrm{I} &= \{A_0 + C_1 - l(C_2 + C_3)\}\mathrm{I} \\
\Omega \mathrm{II}_\alpha &= \{A_0 - lC_2 + (l+1)C_3\}\mathrm{II}_\alpha + \{C_1 + C_2\}\mathrm{II}_\beta \\
\Omega \mathrm{II}_\beta &= \{A_0 + (l+1)C_2 - lC_3\}\mathrm{II}_\beta + \{C_1 + C_3\}\mathrm{II}_\alpha \\
\Omega \mathrm{III} &= \{A_0 + C_1 + (l+1)(C_2 + C_3)\}\mathrm{III} \ .
\end{aligned} \tag{25}$$

The multiplet energy levels ϵ_1 and ϵ_3, defined by

$$\epsilon_1 \int \mathrm{I}^*\mathrm{I} = \int \mathrm{I}^*\Omega\mathrm{I}; \ \epsilon_3 \int \mathrm{III}^*\mathrm{III} = \int \mathrm{III}^*\Omega\mathrm{III}, \tag{26}$$

are given immediately by (25) without integration:

$$\begin{aligned}
\epsilon_1 &= A_0 + C_1 - l(C_2 + C_3) \\
\epsilon_3 &= A_0 + C_1 + (l+1)(C_2 + C_3).
\end{aligned} \tag{27}$$

To find the other two energy levels and to find the linear combinations of II_α and II_β to represent the stabilized zero-approximation wave functions, we must solve the second order secular perturbation problem. The stabilized functions may be written in the form

$$\begin{aligned}
\phi_2 &= \gamma_2\mathrm{II}_\alpha + \delta_2\mathrm{II}_\beta \\
\phi_4 &= \gamma_4\mathrm{II}_\alpha + \delta_4\mathrm{II}_\beta \ .
\end{aligned} \tag{28}$$

Then our γ_2, δ_2 and γ_4, δ_4 are the two solutions of

$$\begin{aligned}
\gamma(\Omega_{\alpha\alpha} - \epsilon\Delta_{\alpha\alpha}) + \delta(\Omega_{\alpha\beta} - \epsilon\Delta_{\alpha\beta}) &= 0 \\
\gamma(\Omega_{\beta\alpha} - \epsilon\Delta_{\beta\alpha}) + \delta(\Omega_{\beta\beta} - \epsilon\Delta_{\beta\beta}) &= 0
\end{aligned} \tag{29}$$

corresponding to the two roots ϵ_2, ϵ_4 of the determinant of the coefficients in (29). Here we have defined

$$\Omega_{\alpha\beta} = \int \mathrm{II}_\alpha^*\Omega\mathrm{II}_\beta; \ \Delta_{\alpha\beta} = \int \mathrm{II}_\alpha^*\mathrm{II}_\beta; \ \text{etc.} \tag{30}$$

Making use of (15) and of the integration formula

$$\begin{aligned}
\int (a^*\eta^* - b^*\xi^*)^{q+t}(a\xi^* + b\eta^*)^{q-t}(a\eta - b\xi)^{q+t'}(a^*\xi + b^*\eta)^{q-t'} \\
= \text{const.}\ \delta_{tt'}\binom{2q}{q-t}^{-1}(a^*a + b^*b)^{2q},
\end{aligned} \tag{31}$$

which is obtained by replacing a by $a+fb^*$ and b by $b-fa^*$ in (15) and equating the coefficients of like powers of ff^* in the result, we proceed to carry out

the integrations (30). It is convenient to integrate first over the spin variables and then to make use of the relation

$$(a^*a + b^*b)(\xi^*\xi + \eta^*\eta) = (a^*\eta^* - b^*\xi^*)(a\eta - b\xi) + (a\xi^* + b\eta^*)(a^*\xi + b^*\eta), \quad (32)$$

which leaves us integrals of the type (31). We find

$$\begin{aligned} \Delta_{\alpha\alpha} &= \Delta_{\beta\beta} = \text{const.}\ (2l+1)(a^*a + b^*b)^{2l}\cdot(1/l) \\ \Delta_{\alpha\beta} &= \Delta_{\beta\alpha} = \text{const.}\ (a^*a + b^*b)^{2l}\cdot(1/l). \end{aligned} \quad (33)$$

The integrals $\Omega_{\alpha\alpha}$, etc. are given in terms of these by (25).

For the secular determinant, we find

$$\begin{vmatrix} C_1+C_2+(2l+1)\{A_0-lC_2+(l+1)C_3-\epsilon\} & & \\ & (2l+1)C_1+(l+1)(C_2+C_3)+A_0-\epsilon & \\ (2l+1)C_1+(l+1)(C_2+C_3)+A_0-\epsilon & & \\ & & C_1+C_3+(2l+1)\{A_0+(l+1)C_2-lC_3-\epsilon\} \end{vmatrix} = 0. \quad (34)$$

The solution is

$$\epsilon = A_0 + (\tfrac{1}{2})(C_2 + C_3) \pm (l(l+1)(C_2 - C_3)^2 + [C_1 + (\tfrac{1}{2})(C_2 + C_3)]^2)^{1/2}.$$

If we define the quantities ρ and θ by

$$\begin{aligned} C_1 + (\tfrac{1}{2})(C_2 + C_3) &= \rho\cos 2\theta \\ [l(l+1)]^{1/2}(C_2 - C_3) &= \rho\sin 2\theta, \end{aligned} \quad (35)$$

we have, as the roots of (33),

$$\begin{aligned} \epsilon_2 &= A_0 + (\tfrac{1}{2})(C_2 + C_3) + \rho \\ \epsilon_4 &= A_0 + (\tfrac{1}{2})(C_2 + C_3) - \rho. \end{aligned} \quad (36)$$

The complete multiplet, given by (27) and (36), is

$$\begin{aligned} \epsilon_1 &= A_0 + C_1 - l(C_2 + C_3) \\ \epsilon_2 &= A_0 + C_1 + (C_2 + C_3) + 2\rho\sin^2\theta \\ \epsilon_3 &= A_0 + C_1 + (l+1)(C_2 + C_3) \\ \epsilon_4 &= A_0 - C_1 - 2\rho\sin^2\theta. \end{aligned} \quad (37)$$

We observe that, in the limit $\theta = 0$, ϵ_1, ϵ_2, ϵ_3 form a Russell-Saunders triplet with the intervals in the ratio $l+1$ to l, while ϵ_4 appears as a singlet at a distance proportional to the resonance energy, C_1. Using these limit values of ϵ_2 and ϵ_4 in (29) and substituting in (28), we find for the *pure triplet* and *pure singlet* linear combinations of Π_α and Π_β

$$\begin{aligned} \phi_t &= N_t(\Pi_\alpha + \Pi_\beta) \\ \phi_s &= N_s(\Pi_\alpha - \Pi_\beta) = N_s\Pi_\gamma. \end{aligned} \quad (38)$$

From (33), we find for the normalizing constants

$$N_t = \text{const.}\ l^{1/2}; N_s = \text{const.}\ (l+1)^{1/2}. \tag{39}$$

ϕ_t, like I and III, is antisymmetric in the coordinates, symmetric in the spins; ϕ_s is symmetric in the coordinates, antisymmetric in the spins.

Now, substituting for II_α and II_β in terms of ϕ_s and ϕ_t in (28) and using the values of γ and δ obtained by putting (36) in (29), we find for our stabilized wave functions

$$\begin{aligned} \phi_2 &= -\sin\theta\,\phi_s + \cos\theta\,\phi_t \\ \phi_4 &= \cos\theta\,\phi_s + \sin\theta\,\phi_t. \end{aligned} \tag{40}$$

Here the normalizing factors have already been introduced.

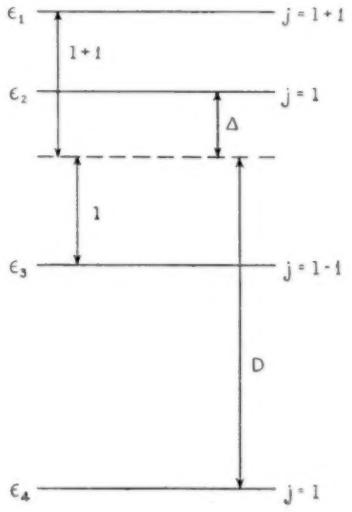

Fig. 1.

Introducing the notation $d_{12} = \epsilon_1 - \epsilon_2$, etc. and using the symbols Δ and D to represent the distances from the *normal* position of the center triplet level to ϵ_2 and ϵ_4 respectively (see Fig. 1) we find from (37)

$$\begin{aligned} \Delta &= \left| \left[(l+1)d_{23} - l d_{12}\right]/(2l+1) \right| \\ \Delta &= \left| d_{24} \right| - \Delta \\ \sin^2\theta &= \left[(l+1)d_{23} - l d_{12}\right]/\left[(2l+1)d_{24}\right] \\ C_1 &= (\tfrac{1}{2})(d_{24} + d_{12} - d_{23}) \\ C_2 + C_3 &= -(d_{12} + d_{23})/(2l+1) \\ C_2 - C_3 &= (\Delta D/l(l+1))^{1/2}. \end{aligned} \tag{41}$$

Since $\sin^2\theta$ must be positive, the sign of $(l+1)d_{23} - l d_{12}$ must be the same as the sign of d_{24}. This means that, if the singlet, ϵ_4, lies below the triplet, the

center triplet level, ϵ_2, must lie above its normal position and vice versa. A convenient way of stating this rule is that: *the center triplet level is repelled by the singlet level.*[10]

In (41), the quantities C_2 and C_3 are not completely determined since we do not know the sign of $C_2 - C_3$. They become determined when we make the physical assumption that the interaction of the spin of each electron with its own orbital motion is larger than with that of the other electron, i.e., $|C_2| > |C_3|$. This is equivalent to making the sign of $C_2 - C_3$ the same as the sign of $C_2 + C_3$. This determines also the sign in (40) of the angle, θ, which was defined by (35). The sign of $C_2 + C_3$ (and so likewise the sign of $C_2 - C_3$) is always the same. Since we can express $C_2 - C_3$ in the form

$$C_2 - C_3 = d_{24} \sin\theta \cos\theta / [l(l+1)]^{1/2},$$

we must change the sign of θ according as d_{24} is positive or negative, i.e., according as the singlet lies above or below the triplet.

8.

While ϵ_2 is regarded as a triplet level in spectral classification and ϵ_4 as a singlet, we observe in (40) that the wave functions for these states are partly singlet and partly triplet in character so that we may expect transitions between both of these levels and other singlet and triplet levels—i.e., we shall expect *forbidden* intercombinations between singlet and triplet systems as well as combinations within these systems—with relative intensities determined by θ.

The intensities of transitions between levels are proportional to the squared absolute values of the corresponding matrix elements of the polarization. Kramers has shown[1] how the symbolic method is adapted to calculating the matrix elements. The operators for the components of the polarization must have the transformation properties of the components of a space-vector. These operators may all be represented symbolically by the spinor invariant

$$\Omega = (AY - BX)^2, \tag{42}$$

where we make the association, according to the transformation properties,

$$P_x + iP_y \rightarrow X^2; \quad -P_x + iP_y \rightarrow Y^2; \quad P_z \rightarrow XY.$$

Brinkman[11] has shown in detail that calculation with the wave functions corresponding to Russell-Saunders multiplets leads to the well-known intensity rules as given by Kronig and by Hönl.[12] Hence, for our purpose, we may regard the matrix elements associated with the functions I, ϕ_t, III, ϕ_s as

[10] We must not expect this rule to hold in case of very small displacements of the center triplet from its normal position, since this may arise from cancellation of the opposite effects of the perturbations Ω_2 and Ω_3, in which case the effect of the other perturbation terms we have left out may not be negligible in comparison.

[11] Brinkman, Dissertation Utrecht 1932.

[12] Kronig, Zeits. f. Physik **31,** 885 (1925); **33,** 261 (1925). Hönl, Ann. d. Physik **79,** 273 (1926).

known. We may indicate the matrix elements for the group of transitions $l+1 \to l$ by

$$\int I \Omega \phi_l' = \Omega_{1l}, \text{ etc.} \tag{43}$$

where quantities referring to the final state are distinguished by a dash. We shall make explicit use of the fact that all matrix elements Ω_{1s}, Ω_{st}, etc., and all matrix elements for $|\Delta j| > 1$ vanish and that[13]

$$\Omega_{ss} = \frac{l+1}{[l(l+2)]^{1/2}} \Omega_{tt}. \tag{44}$$

Then we obtain, for the actual multiplet, the matrix elements

$$\begin{aligned}
&\int \mathrm{I}\Omega\mathrm{I}' = \Omega_{11} \\
&\int \phi_2 \Omega I' = \cos\theta\, \Omega_{l1} \\
&\int \mathrm{III}\Omega\mathrm{I}' = \Omega_{31} \\
&\int \phi_4 \Omega \mathrm{I}' = \sin\theta\, \Omega_{l1} \\
&\int \phi_2 \Omega \phi_2' = \left\{ \frac{l+1}{[l(l+2)]^{1/2}} \sin\theta \sin\theta' + \cos\theta \cos\theta' \right\} \Omega_{ll} \\
&\int \mathrm{III}\Omega\phi_2' = \cos\theta'\, \Omega_{3l} \\
&\int \phi_4 \Omega \phi_2' = \left\{ -\frac{l+1}{[l(l+2)]^{1/2}} \cos\theta \sin\theta' + \sin\theta \cos\theta' \right\} \Omega_{ll} \\
&\int \phi_2 \Omega \phi_4' = \left\{ -\frac{l+1}{[l(l+2)]^{1/2}} \sin\theta \cos\theta' + \cos\theta \sin\theta' \right\} \Omega_{ll} \\
&\int \mathrm{III}\Omega\phi_4' = \sin\theta'\, \Omega_{3l} \\
&\int \phi_4 \Omega \phi_4' = \left\{ \frac{l+1}{[l(l+2)]^{1/2}} \cos\theta \cos\theta' + \sin\theta \sin\theta' \right\} \Omega_{ll} \\
&\int \mathrm{III}\Omega\mathrm{III}' = \Omega_{33}.
\end{aligned} \tag{45}$$

The sum rules for intensity hold for the complete multiplet and not for the singlet and the triplet separately.[14] In applying the formulas (45), we must use the rule at the end of section 7 for determining the signs of θ and θ'.

[13] This relation is given by carrying out the symbolic integrations. Apart from the sign, it follows from the sum rules.

[14] Compare with Ornstein and Burger, Zeits. f. Physik **40**, 403 (1926).

9.

The formulas for the relative intensities of spectral lines, which are obtained by squaring the expressions in (45) and substituting in the Kronig-Hönl values for $|\Omega_{11}|^2$, $|\Omega_{t1}|^2$, etc., hold only in a sort of first approximation, i.e., with neglect of quantities of the order of magnitude $\Delta\nu/\nu$, where $\Delta\nu$ is the interval between the frequencies of the lines compared. In many cases this ratio is not small and the ambiguity may be correspondingly large. Thus we should not attempt to compare our results with experimental intensity ratios except for groups of lines of about the same frequency. The origin of this ambiguity lies in the fact that the matrix elements calculated, while assumed to be those of the polarization, might equally well be those of, say, the second time derivative of the polarization; for this quantity has the same rotation properties. But the squared matrix elements for these two quantities differ by a factor ν^4.

As remarked at the beginning of section 7, we have taken account only of certain selected terms in the interaction energy of two electrons as given by Heisenberg (reference 7). With the exception of the leading term in the spin-spin interaction, all of the neglected terms involve more than two vector-frames. To show how the method is applied in such cases, we treat now the leading term (i.e., we take only the first term in the expansion (3)) in the interaction

$$\frac{e^2}{m_0c^2}\left\{\frac{([\boldsymbol{r}_1, \boldsymbol{v}_2]\cdot\mathbf{s}_1) + ([\boldsymbol{r}_2, \boldsymbol{v}_1]\cdot\mathbf{s}_2)}{r_{12}^3}\right\}. \tag{46}$$

The expression $([\boldsymbol{r}_1, \boldsymbol{v}_2]\cdot\mathbf{s}_1)$ involves the orbital motions of both particles and the spin of one of them. To obtain a symbolic representation, we associate each of the vectors with a spinor:

$$\boldsymbol{r}_1 \rightarrow (x, y);\ \boldsymbol{v}_2 \rightarrow (X, Y);\ \mathbf{s}_1 \rightarrow (r, s).$$

We may make the association in this way. If (a, b, c) are the components of a vector and (ξ, η) are the components of a spinor, we may set[15]

$$a = \tfrac{1}{2}(\xi^2 - \eta^2);\quad b = -\frac{i}{2}(\xi^2 + \eta^2);\quad C = -\xi\eta.$$

This gives us, as the symbolic representation of $([\boldsymbol{r}_2, \boldsymbol{v}_2]\cdot\mathbf{s}_2)$,

$$(rY - sX)(ry - sx)(Xy - Yx). \tag{47}$$

We proceed to replace each of these spinors by operators involving the spinor representing the corresponding vector-frame in the wave functions. Thus we substitute

for (x, y) expressions involving $\xi, \eta, \partial/\partial\xi, \partial/\partial\eta$;
for (X, Y) expressions involving $\bar{\xi}, \eta, \partial/\partial\bar{\xi}, \partial/\partial\bar{\eta}$;
for (r, s) expressions involving $S_+, S_-, \partial\overline{S}_+, \partial/\partial\overline{S}_-$.

We observe that, in general, it will not be possible to find an operator representing this interaction term whose matrix elements do not vanish identically. Only in case $l = 1$ do we get integrals different from zero. The operator may be

[15] ξ, η are the coordinates by stereographic projection of a point a, b, c on the zero sphere.

put into a form where it contains first derivatives with respect to S_+ and S_- and either second derivatives with respect to ξ and η and no derivatives with respect to $\bar{\xi}$ and $\bar{\eta}$ or second derivatives with respect to $\bar{\xi}$ and $\bar{\eta}$ and no derivatives with respect to ξ and η. We then obtain nonvanishing resonance integrals when $l=1$.

To get (47) into a form where we can use (18), we introduce a symbol T_f which means to pick out the coefficient of f in the expression following.

$$(ry - sx)(Xy - Yx) = \tfrac{1}{2}T_f\{(X + fr)y - (Y + fs)x\}^2$$

$$\rightarrow \tfrac{1}{2}T_f\left\{(X + fr)\frac{\partial}{\partial\xi} + (Y + fs)\frac{\partial}{\partial\eta}\right\}^2 = \left(r\frac{\partial}{\partial\xi} + s\frac{\partial}{\partial\eta}\right)\left(X\frac{\partial}{\partial\xi} + Y\frac{\partial}{\partial\eta}\right).$$

Applying (18) a second time[16]

$$(rY - sX)\left(r\frac{\partial}{\partial\xi} + s\frac{\partial}{\partial\eta}\right) = \tfrac{1}{2}T_f\left\{\left(Y + f\frac{\partial}{\partial\xi}\right)r - \left(X - f\frac{\partial}{\partial\eta}\right)s\right\}^2$$

$$\rightarrow \tfrac{1}{2}T_f\left\{\left(Y + f\frac{\partial}{\partial\xi}\right)S_+ - \left(X - f\frac{\partial}{\partial\eta}\right)S_-\right\}\left\{\left(X - f\frac{\partial}{\partial\eta}\right)\frac{\partial}{\partial S_+} + \left(Y + f\frac{\partial}{\partial\xi}\right)\frac{\partial}{\partial S_-}\right\}$$

$$= \tfrac{1}{2}\left\{(S_+Y - S_-X)\left(\frac{\partial^2}{\partial\xi\partial S_-} - \frac{\partial^2}{\partial\eta\partial S_+}\right) + \left(S_+\frac{\partial}{\partial\xi} + S_-\frac{\partial}{\partial\eta}\right)\left(X\frac{\partial}{\partial S_+} + Y\frac{\partial}{\partial S_-}\right)\right\}.$$

In the final step, we have simply $X\rightarrow\bar{\xi}$, $Y\rightarrow\bar{\eta}$. This gives us the symbolic operator for (47) in the form

$$\left\{(S_+\bar{\eta} - S_-\bar{\xi})\left(\frac{\partial^2}{\partial\xi\partial S_-} - \frac{\partial^2}{\partial\eta\partial S_+}\right) + \left(S_+\frac{\partial}{\partial\xi} + S_-\frac{\partial}{\partial\eta}\right)\left(\bar{\xi}\frac{\partial}{\partial S_+} + \bar{\eta}\frac{\partial}{\partial S_-}\right)\right\}\left(\bar{\xi}\frac{\partial}{\partial\xi} + \bar{\eta}\frac{\partial}{\partial\eta}\right).$$

The other usable form of the operator differs from this only in the interchange of $(\bar{\xi}, \bar{\eta})$ and (ξ, η). The term $([\boldsymbol{r}_2, \boldsymbol{v}_1]\cdot\mathbf{s}_2)$ yields operators which differ from these two by a complete interchange of barred and unbarred quantities. Obtaining symmetrical operators by lumping together those operators that differ from each other by a complete interchange and putting them in a somewhat different form, we find as the operator representing the leading term in (46),

$$\begin{aligned}\omega = {} & C_4\cdot S\left\{\left(\bar{\xi}\frac{\partial}{\partial\xi} + \bar{\eta}\frac{\partial}{\partial\eta}\right)\left[(S_+\bar{\eta} - S_-\bar{\xi})\left(\frac{\partial^2}{\partial S_+\partial\eta} - \frac{\partial^2}{\partial S_-\partial\xi}\right)\right.\right. \\ & \left.\left. - \tfrac{1}{2}\left(\bar{\xi}\frac{\partial}{\partial\xi} + \bar{\eta}\frac{\partial}{\partial\eta}\right)\left(S_+\frac{\partial}{\partial S_+} + S_-\frac{\partial}{\partial S_-}\right)\right]\right\} \\ & + C_5\cdot S\left\{\left(\xi\frac{\partial}{\partial\bar{\xi}} + \eta\frac{\partial}{\partial\bar{\eta}}\right)\left[(S_+\eta + S_-\xi)\left(\frac{\partial^2}{\partial S_+\partial\bar{\eta}} - \frac{\partial^2}{\partial S_-\partial\bar{\xi}}\right)\right.\right. \\ & \left.\left. - \tfrac{1}{2}\left(\xi\frac{\partial}{\partial\bar{\xi}} + \eta\frac{\partial}{\partial\bar{\eta}}\right)\left(S_+\frac{\partial}{\partial S_+} + S_-\frac{\partial}{\partial S_-}\right)\right]\right\}.\end{aligned} \tag{48}$$

[16] $\partial/\partial\xi$ transforms like η and $\partial/\partial\eta$ like $-\xi$.

In the special case $l = 1$, we apply the operator (48) to the wave functions (19) and find

$$\begin{aligned}
\omega \mathrm{I} &= (C_4 + C_5)\mathrm{I} \\
\omega \mathrm{II}_\alpha &= -C_4 \mathrm{II}_\alpha + (C_4 - 2C_5)\mathrm{II}_\beta \\
\omega \mathrm{II}_\beta &= -C_5 \mathrm{II}_\beta + (C_5 - 2C_4)\mathrm{II}_\alpha \\
\omega \mathrm{III} &= (C_4 + C_5)\mathrm{III}.
\end{aligned}$$

In addition to neglecting what we believe to be the unimportant terms in the interaction energy, we have made another omission which may in some cases completely invalidate our results. We have assumed in our treatment of the interaction of two electrons as a perturbation that each electron configuration (defined by the n and l values for the two electrons) may be treated quite by itself. This treatment is valid only so long as there are not similar terms of nearly equal energy arising from different configurations.[17] As we follow through a series of terms from configurations differing in the n value of one of the electrons, irregularities in the values of n^* reveal the presence of perturbing terms arising from other types of configuration. Shenstone and Russell[18] have shown that perturbations of this sort are common. We cannot expect our formulas (41) for the energies of the different interaction terms as functions of the multiplet intervals to have much meaning for a configuration which is much perturbed by a neighboring one.

Part II of this paper, containing the application of the theory developed in Part I to observed spectra, will appear later. The relative energy values of the different types of interaction will be calculated for many spectra. The calculated intensities of certain multiplet lines in the spectrum of mercury will be compared with the experimental values.

The writer wishes to express his thanks to the Lorentz Foundation for the grant of a fellowship and to Professor Kramers for suggesting this problem and for many discussions while the work was in progress.

[17] This was first emphasized by Condon, Phys. Rev. **36,** 1121 (1930).
[18] Shenstone and Russell, Phys. Rev. **39,** 415 (1932).

The Isotope Shift in Hyperfine Structure

By JENNY E. ROSENTHAL AND G. BREIT
New York University, University Heights

(Received July 8, 1932)

The effect of deviations of the nuclear field from the inverse square law such as are suggested by the theory of radioactive disintegration is calculated. The isotope shift due to a change of the nuclear radius by 1 percent is found to be larger than those observed. The spectrum of Tl appears not to fit any simple modification of the theory. The isotope shifts in Pb I and Pb II can be explained roughly on the supposition that the deviations of the nuclear field from the inverse square law are local but that for the valence electrons these deviations should be taken to be smaller than is usually supposed in the theory of radioactive disintegration.

§1. INTRODUCTION

IN THE analysis of the *hfs* of Tl,[1,2] Pb[3,4,5] and Hg[6,7] there have been observed isotope shifts of the order of magnitude of 0.05 cm^{-1} in the arc spectra to 0.5 cm^{-1} in the spark spectra. It has been pointed out[1] that this displacement is greater than that to be expected on account of the mass correction to the Rydberg constant and that it might possibly be due to deviations of the nuclear electric field from the Coulomb law. The effect of such deviations has been investigated by Bartlett[8] with the apparent result that they may easily account for the observed isotope displacement. In view of the fact that Bartlett's estimate does not take into account the relativisitic nature of the electron and the screening of the nucleus by the other electrons it has been thought of interest to make a more detailed calculation. Since this work was completed there appeared a letter of Racah[9] in which the same effect is estimated for S terms of Hg with the result that it is hard to explain why the isotope shifts are as small as they are. This is in agreement with our calculations. In the course of the work the effect has been estimated for other terms as well with the same result for some and quite different results for others. Also the effect of the deviations of the nuclear field from the Coulomb law on the interaction of the electron with the nuclear spin has been estimated.

[1] H. Schuler and J. E. Keyston, Zeits. f. Physik **70,** 1 (1931).
[2] D. A. Jackson, Zeits. f. Physik **75,** 233 (1932).
[3] H. Kopfermann, Zeits. f. Physik **75,** 363 (1932); Naturwiss. **19,** 400 (1931); **19,** 675 (1931).
[4] J. L. Rose and L. P. Granath, Phys. Rev. **40,** 760 (1932).
[5] H. Schuler and E. G. Jones, Zeits. f. Physik **75,** 563 (1932).
[6] H. Schuler and J. E. Keyston, Zeits. f. Physik **72,** 423 (1931).
[7] H. Schuler and E. G. Jones, Zeits. f. Physik **74,** 631 (1932).
[8] J. H. Bartlett, Nature **128,** 408 (1931).
[9] G. Racah, Nature **129,** 723 (1932). In this letter the potential inside the nucleus is supposed to be constant and at the boundary of the nucelus it is taken to be continuous. Below the potential is taken to be discontinuous at the nuclear boundary so as to represent the potential wall of nuclear models for α-particle emission. In comparing the formulas in this paper with those of Racah one should start with (11) since in (11a) Δv is supposed to be zero. The resultant isotope shift becomes then $1/(2\rho+1)$ of (11a) with $v=0$ in the latter formula.

§2. Solutions of the Wave Equation

The central field equations for the Darwin-Gordon radial functions ϕ_1 and ϕ_2 for Dirac's equation are:

$$\begin{aligned}(d\phi_1/dy) - j'\phi_1/y &= (\tfrac{1}{2}a)[1 - (E - V)/mc^2]\phi_2 \\ (d\phi_2/dy) + j'\phi_2/y &= (\tfrac{1}{2}a)[1 + (E - V)/mc^2]\phi_1 \\ y = 8\pi^2 mZe^2 r/h^2 &= 2Zr/a_H;\ a = Z\alpha = 2\pi Ze^2/hc\end{aligned} \tag{1}$$

Z is the atomic number, a_H the radius of the first Bohr orbit for hydrogen, E is the energy and V the potential energy and j' is the quantum number (analogous to Sommerfeld's k) taking the values $-1, +1, -2, +2, -3, \cdots$ for $S_{1/2}, P_{1/2}, P_{3/2}, D_{3/2}, D_{5/2} \cdots$ terms respectively.

We consider first the solutions of Eqs. (1) for $y < y_0$, where y_0 is the value of y corresponding to the nuclear radius r_0. If we assume a Gamow field inside the nucleus, V is constant for $y < y_0$. A satisfactory approximation is obtained by letting $E/mc^2 = 1$ which means that the term value energy is negligible in comparison with mc^2. The solutions can then be written:

$$\begin{aligned}\phi_1 &= s y^{1/2} J_{|j'-1/2|}(v^{1/2}(v-2)^{1/2}y/(2a)) \\ \phi_2 &= \mp s v^{-1/2}(v-2)^{1/2} y^{1/2} J_{|j'+1/2|}(v^{1/2}(v-2)^{1/2}y/(2a))\ \ (j' \gtrless 0).\end{aligned} \tag{2}$$

The positive index of the Bessel functions is required by the condition of integrability; $v = V/mc^2$ and s are constants, $y < y_0$ is small and if $|v|$ is not very large the Bessel functions are sufficiently accurately represented by their first term. The values of v for which this is valid may be taken to be given by $-20 < v < 20$. In this approximation:

$$\phi_1 = k^{(1)} y';\ \phi_2 = k^{(2)}(2 - v) y^{j'+1}/[2a(2j' + 1)]\ \ (j' > 0) \tag{3'}$$

$$\phi_1 = k^{(2)} y^{1+|j'|} v/[2a(1 + 2|j'|)];\ \phi_2 = k^{(2)} y^{|j'|}\ \ (j' < 0) \tag{3''}$$

and

$$\begin{aligned}\phi_1/\phi_2 &= 2a(2j' + 1)/[(2 - v)y]\ \ (j' > 0) \\ \phi_1/\phi_2 &= vy/[2a(1 + 2|j'|)]\ \ (j' < 0)\end{aligned}$$

$k^{(1)}$ and $k^{(2)}$ are constants which will be determined later.

In the region $y > y_0$, V is the Coulomb potential and the equations for ϕ_1 and ϕ_2 are:

$$\begin{aligned}(d\phi_1/dy) - j'\phi_1/y &= (1/2a)[1 - (E/mc^2) - 2a^2/y]\phi_2 \\ (d\phi_2/dy) + j'\phi_2/y &= (1/2a)[1 + (E/mc^2) + 2a^2/y]\phi_1.\end{aligned} \tag{5}$$

Letting as before $E/mc^2 = 1$, we have as the solution of Eqs. (5)

$$\begin{aligned}\phi_1/a &= CJ_{2\rho}(2y^{1/2}) + C_- J_{-2\rho}(2y^{1/2}) \\ \phi_2 &= CA_{2\rho}(2y^{1/2}) + C_- A_{-2\rho}(2y^{1/2})\end{aligned} \tag{6}$$

with the abbreviations:

$$A_{2\rho} = (j' - \rho)J_{2\rho} + y^{1/2}J_{2\rho+1}$$
$$A_{-2\rho} = (j' - \rho)J_{-2\rho} - y^{1/2}J_{-2\rho-1} \tag{7}$$

where C and C_- are constants.

The condition of continuity across the boundary is:

$$\phi_1(y_0 - \epsilon) = \phi_1(y_0 + \epsilon), \quad \phi_2(y_0 - \epsilon) = \phi_2(y_0 + \epsilon); \quad \epsilon \to 0. \tag{8}$$

Substitution of the actual solutions for ϕ_1 and ϕ_2 into (8) gives:

$$C[(\phi_1/a\phi_2)A_{2\rho} - J_{2\rho}] = C_-[J_{-2\rho} - (\phi_1/a\phi_2)A_{-2\rho}]. \tag{9}$$

The argument of the functions $J_{2\rho}$, etc. is $2y_0^{1/2}$; $\phi_1/a\phi_2$ is given by (4′) or (4″) depending on whether $j'>0$ or $j'<0$. Condition (8) also gives $k^{(1)}$ (respectively $k^{(2)}$) in terms of C and C_-.

If the field were Coulomb at the nucleus, C_- would be zero since the condition of integrability for ϕ_1 and ϕ_2 must be satisfied. The presence of the Gamow field results therefore in a modification of the eigenfunctions represented by the term in C_-. These modified or perturbed eigenfunctions will be denoted by ϕ_1 and ϕ_2; the unperturbed functions (i.e., functions with $C_-=0$) will be written as ϕ_1^0 and ϕ_2^0.

The ratio C_-/C as given by (9) was computed for a wide range of values of v in order to see to what extent the wave function is affected by deviations of the potential from the inverse square law. The results of this calculation for $j'=\pm 1$ are tabulated below. They are accurate within 5 percent for $-20<v<20$. The formulas also may be used to compute C_-/C for values of v lying outside these limits but the results will be less accurate due to the fact that for large values of $|v|$ (3′) respectively (3″) are no longer satisfactory approximations to (2). For $j'=-2$, C_-/C was estimated to be quite negligible in comparison with those for $j'=\pm 1$.

TABLE I. $Z=81$

$r_0 = 10^{-12}$ cm; $y_0 = 0.03$, $a = 0.590$, $\rho = 0.807$

$J_{2\rho} = 0.0403$, $J_{2\rho+1} = 0.0027$, $J_{-2\rho} = -4.736$, $J_{-2\rho-1} = 43.0$

$j' = 1$, $A_{2\rho} = 0.0082$, $A_{-2\rho} = -8.356$, $\phi_1/a\phi_2 = 200/(2 - v)$

$C(1.58 + 0.0403v) = C_-(4.736v + 1662)$

$j' = -1$, $A_{2\rho} = -0.0724$, $A_{-2\rho} = 1.116$, $\phi_1/a\phi_2 = v/69.6$

$C(0.0724v + 2.81) = C_-(1.116v + 330.0)$

v:	-20	-4	0	4	20
$C_-/C(j'=1)$;	0.0005	0.0009	0.0009	0.0010	0.0014
$C_-/C(j'=-1)$;	0.0044	0.0077	0.0085	0.0093	0.0120

$$Z = 91$$

$$r_0 = 10^{-12}\text{ cm};\quad y_0 = 0.035,\qquad a = 7^{1/2}/4,\qquad \rho = \tfrac{3}{4}$$

$$J_{2\rho} = 0.0600,\ J_{2\rho+1} = 0.0044,\ J_{-2\rho} = -3.722,\ J_{-2\rho-1} = 28.62$$

$$j' = 1,\qquad A_{2\rho} = 0.0158,\ A_{-2\rho} = -6.286$$

$$C_-(5.440 + 0.1259v) = C(2245 + 7.806v)$$

$$j' = -1\qquad A_{2\rho} = -0.1042\ A_{-2\rho} = 1.158$$

$$C_-(7.806 + 0.0324v) = C(0.1259 + 0.0029)$$

v:	-20	-4	0	4	20
$C_-/C(j' = 1)$;	0.0014	0.0022	0.0024	0.0026	0.0033
$C_-/C(j' = -1)$;	0.0095	0.0149	0.0161	0.0173	0.0218

§3. The Isotope Displacement

Corresponding to a change δV of the potential inside the nucleus there is a change δW in the energy. The usual way of evaluating it is by means of the perturbation method using the unperturbed functions ϕ_1^0 and ϕ_2^0 corresponding to $C_- = 0$

$$\delta W = \int_0^{r_0} [V + (Ze^2/r)](\phi_1^{(0)2} + \phi_2^{(0)2})dr \tag{10}$$

where the normalization is such that

$$\int_0^{\infty} (\phi_1^{(0)2} + \phi_2^{(0)2})dr = 1.$$

To evaluate (10) $\phi_1^{(0)}$ and $\phi_2^{(0)}$ are expanded in terms of y. For small values of y such as $0 < y < y_0$ these expansions converge very rapidly, and for a first approximation it is sufficient to use only the first term of each expansion.

$$\phi_1^{(0)2} + \phi_2^{(0)2} = 2C^2 j'(j' - \rho)y^{2\rho}/\Gamma^2(2\rho + 1).$$

Performing the integration we get:

$$\delta W = 2Ze^2C^2 j'(j' - \rho)[(y_0^{2\rho}/2\rho) + (v/2a^2)y_0^{2\rho+1}/(2\rho + 1)]/\Gamma^2(2\rho + 1). \tag{11}$$

Supposing that y_0 changes by Δy_0 and that v remains unchanged δW changes by:

$$\Delta\delta W = 2Ze^2C^2 j'(j' - \rho)[y_0^{2\rho} + (v/2a^2)y_0^{2\rho+1}](\Delta y_0/y_0)/\Gamma^2(2\rho + 1). \tag{11a}$$

For S terms the magnitude of the isotope shift can be conveniently expressed in terms of the value of $\psi^2(0)$ which the square of the nonrelativistic Schroedinger function $\bar{\psi}$ would have at $r = 0$. The normalization of the function ψ is for S terms such that

$$4\pi \int_0^{\infty} \psi^2 \cdot r^2 dr = 1.$$

The function ϕ_2 for all but very small values of r satisfies the same differential equation as $r\psi$. It may be equated to the latter provided ϕ_1 and ϕ_2 are normalized so as to have

$$4\pi \int_0^\infty (\phi_1^2 + \phi_2^2) dr = 1.$$

The expression for $\Delta\delta W$ given by (11) must then be also multiplied by 4π.

The leading term in the expression for ϕ_2 at not too small y is $Cy^{1/2} J_{2\rho+1}(2y^{1/2})$. Nonrelativistically the function $r\psi$ must have the form $-C'y^{1/2}J_1(2y^{1/2})$. The constants C and C' should be the same because the asymptotic expansions of the Bessel functions differ only by a constant phase in the trigonometric term. We have thus

$$\psi(0) = -C(y/r) = -C(2Z/a_H).$$

Substituting into (11) and noting that

$$2Zc^2C^2 = (e^2/2a_HZ)a_H^3\psi^2(0) = (R_\infty/Z)a_H^3\psi^2(0)$$

where R_∞ is the energy corresponding to the Rydberg constant we have

$$\Delta\delta W = \frac{4\pi R_\infty}{Z} a_H^3\psi^2(0) \frac{1+\rho}{[\Gamma(2\rho+1)]^2}\left[y_0^{2\rho} + \frac{v}{2a^2} y_0^{2\rho+1}\right]\frac{\Delta y_0}{y_0} \qquad (12)$$

which is in agreement with Racah's[9] formula.

Supposing $v=0$ and using Racah's[10] value $\psi^2(0)=0.49\times10^{26}$ cm^{-3} for the $7s$ term of Tl I we obtain for it

$$\Delta\delta W \leqq 360(\Delta y_0/y_0) \text{ cm}^{-1}.$$

If $\Delta y_0/y_0 \leqq 0.01$ the isotope shift for this term should be 3.6 cm^{-1} which is much too large according to Schüler and Keyston[1] and to Jackson.[2] This value may conceivably have to be multiplied by a factor of about 1/2 (see §4 below) in order to take into account the change in the wave functions due to the finite size of the nucleus and it may have to be multiplied by 1/3 to take into account the fact that the nuclear radius would be expected to vary with the cube root of the atomic number rather than with the first power. But even 0.6 cm^{-1} appears much too large for this term particularly when it is considered that according to Schüler and Keyston the isotope shift for it is considerably less than that for 7 $^2P_{1/2}$ which itself is about 0.05 cm^{-1}. It should be noted that the magnetic moment of the Tl nucleus as calculated[10,11] using the splitting of the 6^2S term and the value of $\psi^2(0)$ used above is smaller than that calculated using the splitting of 7 $^2P_{1/2}$ by a factor of about 4. It appears that the interaction of the $6s$ electron of Tl I with the nuclear spin as well as with the Gamow trough is smaller in reality than would be expected by comparison with other terms of the same spectrum.

[10] Racah, Il Nuovo Cimento **8,** 178 (1931); Zeits f. Physik **71,** 431 (1931).
[11] G. Breit, Phys. Rev. **38,** 463 (1931), see p. 471.

For P, D, $\cdots$ terms of single electron spectra the magnitude of C can be obtained from the doublet splitting of these terms as has been already done in the discussion of the hyperfine structure by Racah.[10] Using Sommerfeld's doublet splitting formula one obtains for the energy difference between two parts of the doublet

$$\delta = 2l(l+1)(2l+1)Z\mu_0^2\{[(l+1)^2 - a^2]^{1/2} - 1 - (l^2 - a^2)^{1/2}\}a^{-2}\overline{(r^{-3})}_{\text{Schr}}$$
$$(\mu_0 = eh/(4\pi mc))$$

where the suffix "Schr" indicates that the average of r^{-3} is to be taken using Schroedinger's nonrelativistic wave functions. If the relativistic effects were absent we would have

$$\phi_2 = r\psi = C\lim_{a\to 0} A_{2\rho} = \pm Cy^{1/2}J_{2l+1}(2y^{1/2}) \quad (j' \gtrless 0). \tag{13}$$

For sufficiently large values of y there is no difference between the Dirac and the Schroedinger wave equations. The amplitude of the oscillations of the wave function as given by (7) is the same as that given by the nonrelativistic Eq. (13) provided the same values are given to C in the two expressions. The value of C is thus determined in terms of $\overline{(r^{-3})}$ by

$$\overline{(r^{-3})}_{\text{Schr}} = C^2(32Z^2a_H^{-2})\int_0^\infty J_{2l+1}^2(z)z^{-3}dz = 2C^2Z^2a_H^{-2}/[l(l+1)(2l+1)]$$

where a_H is the Bohr radius. Using now the relation between $(r^{-3})_{\text{Schr}}$ and δ and the expression (11) we have

$$\delta W = 2j'(j'-\rho)[\Gamma(2\rho+1)]^{-2}\{[(l+1)^2 - a^2]^{1/2} - 1$$
$$- (l^2 - a^2)^{1/2}\}^{-1}[(y_0^{2\rho}/2\rho) + (v/2a^2)y_0^{2\rho+1}/(2\rho+1)]\delta.$$

Keeping v constant the change in δW due to a change in the nuclear radius corresponding to a change Δy_0 in y_0 is

$$\Delta\delta W = 2j'(j'-\rho)[\Gamma(2\rho+1)]^{-2}\{[(l+1)^2 - a^2]^{1/2} - 1$$
$$- (l^2 - a^2)^{1/2}\}^{-1}[y_0^{2\rho} + (v/2a^2)y_0^{2\rho+1}](\Delta y_0/y_0)\delta. \tag{14}$$

For the $P_{1/2}$ normal level of Tl I substitution of $j'=1$, $\rho=0.807$, $y_0=0.03$, $\delta=7792$ cm^{-1} gives

$$\Delta\delta W \leqq 49(\Delta y_0/y_0)\ \text{cm}^{-1}.$$

The difference in the term values of $P_{1/2}$ for the isotopes 203 and 205 would be estimated therefore to be of the order of 0.5 cm^{-1} if it is supposed that the nuclear radius differs for these two isotopes by 1 percent. The isotope shift for $P_{3/2}$ should be negligible in comparison. According to Schüler and Keyston[1] the difference in $\Delta(\delta W)$ for $P_{1/2}$ and $P_{3/2}$ is not greater than about 0.05 cm^{-1} and according to Jackson[2] it is probably of the order of 0.01 cm^{-1}. The calculated value is, therefore, considerably greater than that observed.

Essentially the same result is obtained using direct numerical calculations[11] for the wave functions ϕ_1, ϕ_2. One finds that at the nucleus $\phi_1^2+\phi_2^2 = 9.82\times10^{-4}\, y^{2\rho}/a_H$ which leads to

$$\Delta\delta W \leqq 60(\Delta y_0/y_0)\ \text{cm}^{-1}.$$

§4. Validity of the Perturbation Method

Although δW is small the fields responsible for it are large so that it is not clear without an additional calculation to what extent the first order of the perturbation method is a valid approximation. It will be seen that a correction factor of the order of $1/2$ must in fact be applied for the calculation of $\Delta(\delta W)$. This correction is clearly not large enough to bring about agreement with experiment for the S term of Tl.

As long as one is interested in changes of the nuclear radius the only thing which matters for $\Delta(\delta W)$ is the value of $\phi_1^2+\phi_2^2$ at $y=y_0$ because $\Delta(\delta W)$ may be considered as the change in the energy due to the perturbing potential $(Ze^2/r)+V$ applied in the region $r_0<r<r_0+\Delta r_0$. It is, furthermore, clear from the numerical calculations given above that the wave functions are practically unaffected by this perturbation. It is, therefore, sufficient to multiply the values so far obtained for $\Delta(\delta W)$ by the ratio of the (*perturbed*) value of $\phi_1^2+\phi_2^2$ at $y=y_0$ to the approximate (*unperturbed*) value which has been used so far. This ratio is found by observing that the constant C in (6) must be practically independent of y_0 and v for the range of values considered. In fact for large y the asymptotic expansions of the Bessell functions make (6) equivalent to

$$\phi_2 = y^{1/4}\pi^{-1/2}\left[C^2 + C_-^2 - 2CC_- \cos(2\rho+1)\pi\right]^{1/2} \cos(2y^{1/2} - \epsilon)$$

where ϵ is a constant phase (independent of y) which is immaterial for the present purpose. The function ϕ_2 is therefore essentially an oscillating function the amplitude of which depends on C, C_-. The dependence on C_- is seen however to be very slight in view of the small values of C_-/C. The amplitude of the oscillations for large y must be the same whether the nucleus has a finite size or not because it is determined by the continuation of the wave function from still larger values in towards the nucleus. We will thus suppose that C has the same value whether the nucleus gives a purely Coulomb field or whether it has a finite size. The factor by which the previously calculated values should be multiplied is then by (6)

$$\left[a^2J_{2\rho}^2 + A_{2\rho}^2 + 2(C_-/C)(a^2J_{2\rho}J_{-2\rho} + A_{2\rho}A_{-2\rho}) + (C_-/C)^2(a^2J_{-2\rho}^2 + A_{-2\rho}^2)\right]/(a^2J_{2\rho}^2 + A_{2\rho}^2).$$

For Tl $P_{1/2}$, $S_{1/2}$ terms this factor has the values:

$$P_{1/2}\ (j'=1): \quad 1 - 422.8(C_-/C) + 1.22\times 10^5(C_-/C)^2$$

$$S_{1/2}\ (j'=-1): 1 - 50.76(C_-/C) + 1561(C_-/C)^2.$$

Using the values of C_-/C tabulated above it is seen that the correction factor is generally greater than $1/2$ and lies between $1/2$ and 1. For any given v it is readily computed by the above formulas.

§5. Effect of Nuclear Field on Hyperfine Structure

The coupling of the electron to the nuclear spin axis is known to depend on the radial integrals[10,11]

$$I = \int_0^\infty \phi_1\phi_2 y^{-2} dy.$$

It has been seen in §4 that $\phi_1^2+\phi_2^2$ in the neighborhood of the nucleus is smaller than its unperturbed value $\phi_1^{(0)2}+\phi_2^{(0)2}$ corresponding to an inverse square field of force. It may be expected that $\phi_1\phi_2$ is also smaller numerically on account of the changes brought about in the functions ϕ_1, ϕ_2 by deviations of the field from the Coulomb law. The dependence of the integrand of I on y has been examined graphically for $Z=91$, 81, $v=-4$. The main modification due to the finiteness of the size of the nucleus consists in reducing $\phi_1\phi_2 y^{-2}$ to a relatively negligible amount for $y \leqq y_0$. For $y > y_0$ the integrand approaches rapidly the value which it would have if the nucleus had negligible dimensions. An inspection of the figures indicates that the area under the perturbed $\phi_1\phi_2 y^{-2}$ curve is approximately the same as the area under the unperturbed $\phi_1^{(0)}\phi_2^{(0)} y^{-2}$ curve from $y=2y_0$ to $y=\infty$. We have for the unperturbed functions

$$\int_0^\infty \phi_1^{(0)}\phi_2^{(0)} y^{-2} dy = \int_0^\infty 8aC^2[(j'-\rho)J_{2\rho}(z) + (z/2)J_{2\rho+1}(z)]J_{2\rho}(z) z^{-3} dz$$
$$= aC^2(2j'-1)/[2\rho(4\rho^2-1)]$$
$$\int_0^{py_0} \phi_1^{(0)}\phi_2^{(0)} y^{-2} dy \leqq aC^2(j'-\rho)(py_0)^{2\rho-1}/[(2\rho-1)(\Gamma(2\rho+1))^2].$$

Thus the integral over the perturbed functions is

$$I = \int_0^\infty \phi_1\phi_2 y^{-2} dy = \left\{1 - \frac{2(j'-\rho)\rho(2\rho+1)}{(2j'-1)[\Gamma(2\rho+1)]^2}(py_0)^{2\rho-1}\right\} \times$$
$$\int_0^\infty \phi_1^{(0)}\phi_2^{(0)} y^{-2} dy$$

where $p \geqq 2$. The quantity in $\{\ \}$ is a correction factor which must be applied to I as evaluated on the hypothesis of the inverse square law. It is seen that the correction factor depends in addition to y_0 also on j' and ρ. It is largest for S terms and is appreciable for $P_{1/2}$ but is negligible for $P_{3/2}$ terms. Taking $p=2$ for $Z=91$ the correction factor is 0.67 for $S_{1/2}$ and 0.86 for $P_{3/2}$ terms. Schüler and Keyston[6] and Schüler and Jones[7] find apparently that the hyperfine structure splittings of the two odd isotopes of Hg are not always proportional to each other as one would expect on a simple theory, the splitting of 199 being sometimes greater and sometimes less than that of 201. One might suppose that this is due to the difference between $\phi_1\phi_2$ and $\phi_1^{(0)}\phi_2^{(0)}$. The above estimates show however that the effect is not accounted for by the theory because the nuclear radii of the two isotopes must differ from each other by much less than 1 percent as shown by the smallness of the isotopes displacements. The resultant difference in I is then expected to be surely not greater than 0.33 percent. Nevertheless for the absolute calculation of magnetic moments the above correction factors may have to be considered.

§6. Summary and Discussion

1. The observed isotope displacements in the spectra of Hg, Tl, Pb are smaller than those calculated on the supposition that the nuclear radius changes by about 1 percent for isotopes differing from each other by 2 in their atomic number.

2. The validity of the perturbation method has been examined and it has been found that it introduces at the most a decrease in the theoretically expected value by a factor of 1/2.

3. The change in the radial functions due to deviations from the inverse square law is found to cause an appreciable effect on the coupling of the valence electron to the nuclear spin for $S_{1/2}$ and $P_{1/2}$ terms of single electron spectra. This change is not large enough however to account for the difference between the ratio of the splittings of the isotopes 199, 201 of Hg observed for different terms by Schüler and Keyston and by Schüler and Jones.

The disagreement between theory and experiment presented in §3 appears to be universal. Thus in the spectrum of Pb II Schüler and Jones[5] have found a displacement between the 206, 208 isotopes of 0.052 cm^{-1} for the lines 6660, 5609 ($7\ ^2S_{1/2}-7\ ^2P_{1/2}$, $7\ ^2S_{1/2}-7\ ^2P_{3/2}$). By formulas (13), (14) it is estimated that if this shift should be due to a change in the nuclear radius it would have to be attributed to the $7\ ^2S_{1/2}$ term. The value of $\psi^2(0)$ to be used for $7S$ Hg II should be approximately the same as that for $7S$ Tl II. The latter is given by Racah[10] as 0.44×10^{26} cm^{-3}. The expected displacement is thus approximately the same as for $6S$ of Tl I and is obviously too large. All of the shifts could of course be decreased by supposing that y_0 and v change just in the correct proportion. Such an explanation appears to be a forced one at present, however.

The situation is quite different with the $6s^26d$ configuration of Pb II. The ^2D term is inverted. The *hfs* of lines terminating on it has been observed by Kopfermann,[3] Schüler and Jones,[5] and in especial detail by Rose and Granath[4] who subsequently to the publication of their results have measured the structure of the higher series members of 4245 *viz.*, λλ2948, 2526 ($6\ ^2D_{5/2}-5$, 6, $7\ ^2F_{7/2}$) also λλ5372, 3451, 2887 ($6s6p^2\ ^2D_{5/2}-5$, 6, $7\ ^2F_{7/2}$) as well as λλ3786, 2719 ($6s6p^2\ ^2D_{3/2}-5$, 6, $^2F_{5/2}$), λ5367 ($6s6p^2\ ^2D_{5/2}-5\ ^2F_{5/2}$) and λ4242 ($6^2D_{5/2}-5\ ^2F_{5/2}$). According to their data as well as that of Kopfermann and Schüler and Jones the shift between Pb^{206} and Pb^{208} is practically the same for all lines ending on the same D term so that the shifts must be attributed to the D rather than the F terms. The displacement for

$6s^26d\ ^2D_{5/2}$	is 0.20 cm^{-1}	$6s6p^2\ ^2D_{5/2}$	0.28 cm^{-1}
$6s^26d\ ^2D_{3/2}$	0.09 cm^{-1} or (0.08)	$6s6p^2\ ^2D_{3/2}$	0.43 cm^{-1}.

An application of Eq. (14) shows that for the $6s^26d\ ^2D_{3/2}$ terms one expects an entirely negligible shift ($10^{-4}cm^{-1}$) as a result of a 1 percent change in the nuclear radius. Still smaller displacements are expected for $^2D_{5/2}$. The opposite is true experimentally. It is also remarkable that $6s6p^2$ gives larger isotope shifts than $6s^26d$. It may be however that the $6s^26d$ terms are per-

turbed[12] by $6s6p^2$. If this is the case the isotope displacements of all four terms could be attributed to the *lack* of one 6*s* electron in the $6s6p^2$ configuration. This view is in agreement with the fact that for the 6660, 5609 lines the Pb^{206} component is displaced towards shorter wave-lengths with respect to Pb^{208} while for 4245 and the other lines ending on the ^2D terms the Pb^{206} component lies towards longer wave-lengths. The direction of the displacement is correctly explained by an increase in the radius for the heavier isotope since the heavier isotope has the looser binding to the nucleus for the 6*s* as well as the 7*s* electron. Furthermore the sum of the isotope displacements of $6s^26d^2D_{5/2}$ and $6s6p^2\ ^2D_{5/2}$ is $0.20+0.28=0.48$ cm^{-1} while for the two $^2D_{3/2}$ the sum is 0.52 cm^{-1}. This sum may be taken to be the isotope shift of a single 6*s* electron. It is approximately 10 times as great as the shift for the 7*s* electron (0.052 cm^{-1}). It appears reasonable to suppose that the ratio of $\psi^2(0)$ for these two electrons is also approximately 10 since Racah's numerical calculations gave a ratio 6.4 for of the 6*s* and 7*s* electrons of Tl II.

Thus even though the absolute value of the isotope shift is smaller than would be expected on the hypothesis that it is due to a change of the nuclear radius by (2/3) percent (for 206 and 208) the comparison of the 6*s* and 7*s* displacements indicates that the shift is roughly proportional to the value of $\psi^2(0)$ at the nucleus that the shifts for *p*, *d*, electrons are small and that therefore the shift may be due to deviations of the field from the inverse square law.

In the *hfs* of the spectrum of Tl I as it has been analyzed by Schüler and Keyston[1] and by Jackson,[2] even this appears untrue. The main argument against such an explanation lies in the fact that according to Schüler and Keyston[1] λλ6550, 5528, 5110 ($7\ ^2S_{1/2}-8, 9, 10\ ^2P_{3/2}$) and λλ6714, 5584 ($7\ ^2S_{1/2}-8, 9\ ^2P_{1/2}$) show no isotope shift. For this reason the $7\ ^2S_{1/2}$ term is supposed to have no shift and therefore the shift of 0.05 cm^{-1} present in the 5351 line is attributed to a displacement of $^2P_{3/2}$. It should be noted, however, that while Schüler and Keyston[1] have found no isotope shift for 3776 ($6^2P_{1/2}-7\ ^2S_{1/2}$) Jackson[2] reports a displacement of roughly the same amount as for 5351. If, therefore, the experimental difficulties present in the observation of 6550, 5528, 5110, 6714, 5584 have masked the shift in these lines one could suppose that the 6 ^2P terms have a negligible isotope displacement while 7 ^2S of Tl^{205} has an energy higher than that of 7 ^2S of Tl^{203} by 0.05 cm^{-1}. This assignment would not fit in however with the sense of the displacement in Tl II as observed by Schüler and Keyston[1] because the energy difference between the $6s7p$ and $6s7s$ configurations is higher for 205 than 203. In the Tl II spectrum the 7*s* electron appears to be more tightly bound to the nucleus in the 205 than in the 203 isotope while in Tl I even forcing the *P* terms to have no displacements the opposite is the case. Thus this spectrum appears not to fit in with a theory of isotopic shifts due to deviations of the nuclear field from the inverse square law even in a roughly qualitative manner.

There is another possibility for accounting for the isotope displacement

[12] Shenstone and Russell, Phys. Rev. **39**, 415 (1932). Note remark on influence of perturbations on isotope shifts in Hg.

as a direct effect of the mass.[13] It is a striking feature of the observed isotope displacements, however, that the odd isotopes of Hg and Pb fall not exactly between the even isotopes of closest atomic weight but somewhat closer to the even isotope of smaller atomic weight. This displacement cannot have anything to do with the mass and it is not due to observational error inasmuch as in the case of Pb it has been found by three independent sets of observers.[3,4,5]

The fact that the observed shifts for S terms are much smaller than those expected on the supposition of a progressive change in the nuclear radius shows that either the field used in the theory of radioactive disintegration cannot be applied in the discussion of the interaction of extranuclear electrons with the nucleus or that the change in the radius of nucleii of the same element is smaller than has been supposed. However, even with such modifications the shifts in Tl remain quite unexplained.

Note in Proof: Since the paper was written we learned of a new nuclear theory of Heisenberg according to which the nucleus is supposed to consist of protons and neutrons. The Gamow mountain may then be understood as the result of exchange forces. We have also learned of the new considerations of Bohr according to which the collision between neutrons and electrons is very improbable. According to these views the electron may be regarded as subject only to the influence of protons within the nucleus. The density of protons may be imagined either to be approximately uniform or else to vary as a simple function of the distance from the center. It is clear that the term displacement is smaller on this view than according to the model used above. A calculation for the isotope shift was made using a potential energy $V=[-(n+1)/n+(1/n)(r/r_0)^n](Ze^2/r_0)$ inside the nuclear radius r_0. The displacement of the energy for s terms is

$$\delta W = \frac{4\pi R_\infty}{Z} a_H{}^3\psi^2(0)\frac{1+\rho}{\Gamma^2(2\rho+1)}\ \frac{(n+1)y_0{}^{2\rho}}{2\rho(2\rho+n+1)(2\rho+1)}$$

and for $l>0$

$$\delta W=\frac{2j'(j'-\rho)}{\Gamma^2(2\rho+1)}\ \frac{(n+1)y_0{}^{2\rho}}{2\rho(2\rho+n+1)(2\rho+1)}\left\{[(l+1)^2-a^2]^{\frac{1}{2}}-1-(l^2-a^2)^{\frac{1}{2}}\right\}^{-1}\delta.$$

The expected differences in term displacements for isotopes are given therefore by the same expressions as before except for the factor

$$A(n) = (n+1)/(2\rho+1)(2\rho+n+1).$$

For $n=2$ (uniform charge density in the nucleus) and $\rho=0.81$, $A=0.25$ and for $n=1/2$, $A=0.18$. Using $A=1/5$ the isotope shift of Pb^{206} and Pb^{208} would be estimated to be 0.46 cm^{-1} for the $7s$ and 2.9 cm^{-1} for the $6s$ electrons while the observed values are 0.052 cm^{-1} and 0.50 cm^{-1} respectively. In order to bring about agreement between theory and experiment one would have to use $n \leqq -0.84$, i.e., the nuclear charge would have to be concentrated practi-

[13] D. S. Hughes and C. Eckart, Phys. Rev. **36**, 694 (1930).

cally entirely at the center. It is probably incorrect however to give such a literal interpretation to the nuclear charge because forces between neutrons and electrons may not be entirely negligible and because α-particles may form groups having a volume which is affected only slightly by increasing the atomic weight. It must be recalled that in the cases considered here one isotope can be obtained from another one simply by the addition of neutrons. The small magnitude of the isotope shift suggests that the volume occupied by the positive charges is not affected greatly by the addition of neutrons to the nucleus as though the repulsive forces between the positive charges were balanced by the cementing influence of neutrons in their immediate neighborhood.

Our thanks are due to Professor W. Heisenberg for informing us of the new developments before publication and for a helpful discussion of the interaction of electrons with the nucleus.

Isotope Separations in the Infrared Absorption Spectrum of HCl and the Possible Existence of a Chlorine Isotope of Mass 39

By J. D. HARDY* AND G. B. B. M. SUTHERLAND**
Physics Department, University of Michigan

(Received June 30, 1932)

The absorption band of HCl at 1.7μ has been reëxamined under high dispersion in an attempt to verify the work of Hettner and Böhme on the existence of a third chlorine isotope, Cl^{39}. No trace of the isotope was observed although a path length of three meters, some ten times the path used by Hettner and Böhme, was used. The isotope separations due to Cl^{35} and Cl^{37} have been measured very accurately and do not agree with the separations calculated by the simple theory. When the anharmonic terms in the energy are taken into account the agreement between the calculated and observed isotope separations is within the experimental error. The isotope separation for HCl^{39} molecule has been calculated and found to be slightly different from that observed by Hettner and Böhme. Our results indicate that the relative abundance of Cl^{39} to Cl^{39} cannot be greater than 1 to 500.

RECENTLY Becker[1] has predicted the existence of a chlorine isotope, Cl^{39}, from a consideration of the form of the infrared absorption curves of HCl. This prediction was made from the curves published by Meyer and Levin[2] and by Becker[1] himself. The absorption maxima in these curves which Becker attributes to HCl^{39} are so small as to be probably within the error of the experiment. In fact, Meyer and Levin state specifically that the unevenness of their base line was due to errors in galvanometer readings, and if one examines the original curves of Meyer and Levin it is seen that the maxima mentioned by Becker do not fall at equal distances from the maxima due to Cl^{35} and in many cases do not show up at all. However, the existence of Cl^{39} was later apparently confirmed by Hettner and Böhme[3] working on the *R* branch of the HCl harmonic. In this work the maxima due to HCl^{39} stand out in all clearness with the expected constant frequency difference between these maxima and those due to Cl^{35}. The present work was undertaken with two objects in view, to verify the work of Hettner and Böhme and to measure more accurately, under high dispersion, the separation of the maxima due to HCl^{35} and HCl^{37}. The interest in the third isotope arose naturally from the apparent disagreement of observers about its existence. Aston[4] at one time considered the possibility of a Cl^{39} isotope but finally decided against its existence. Ashley and Jenkins[5] studied the absorption of AgCl in a region

* National Research Fellow.
** Commonwealth Fund Fellow.
[1] H. Becker, Zeits. f. Physik **59**, 583 and 601 (1930).
[2] C. F. Meyer and A. Levin, Phys. Rev. **34**, 44 (1929).
[3] G. Hettner and J. Böhme, Zeits. f. Physik **72**, 95 (1931).
[4] F. W. Aston, Isotopes, p. 68, 2nd ed., 1924.
[5] M. Ashley and J. A. Jenkins, Phys. Rev. **37**, 1712 (1931).

favorable for showing the isotope but found no trace of an $AgCl^{39}$ molecule. E. K. Plyler (private communication) made an attempt to find the absorption lines due to the third isotope by a close examination of the fundamental band at 3.4μ. He used the same instrument that Meyer and Levin used in their work and his results were negative within the error of his observations. The interest in the isotope separation arose from a discrepancy in the observed values and those calculated on the simple theory.

With a new type spectrometer[6] whose resolution and sensitivity are greater than any of those yet applied to the problem, the work of Hettner and Böhme, Becker, and Meyer and Levin has been repeated. That is, the short wave-length side of the harmonic band at 1.7μ has been carefully examined. A description of the spectrometer has already appeared and it need only be mentioned here that by altering the dimensions of the thermocouple a 50 percent gain in sensitivity has been realized over previous arrangements.

The region to be investigated, between 1.71μ and 1.75μ, is a particularly favorable one in which to work. It is practically free from water vapor absorption and in it lies the energy peak of the Nernst heater. Further, the impurity of the spectrum due to overlapping orders is very slight even without the use of any filtering device. The first order energy of 0.85μ is small and in the second order the energy will be only 10 percent of that in the first order. The difference between curves taken with a filter and without a filter is negligible. The filter used was opaque to visible light, transmitted 9 percent from 0.8μ to 0.9μ, and had 70 percent transmission at 1.73μ.

The grating used in this experiment was ruled by Wood with 15,000 lines to the inch and had a ruled surface of 6×3.5 inches. Previously the emission lines of helium had been examined with this grating and the definition was found to be good enough to resolve lines at 10829.1A and 10830.3A in the second order. The spectrometer was calibrated by means of the helium lines at 10830.3A and 20582.1A. The width of the slits for the most detailed examination was 0.075 mm and for the rougher curve 0.15 mm. The wave-length range across the slit in the first instance was 0.97A or 0.32 cm^{-1}, and in the rougher curve 0.64 cm^{-1}. Readings were taken one slit-width apart, and each point represents usually a single observation. The steadiness of the instrument was such that an observation could be repeated to within 2 percent in the detailed curves, where the deflections were about 30 cm between lines, and to within about 1 percent in the rougher curve where the deflections were about 60 cm. The deflections at places of maximum absorption were practically zero for the strong lines, the residual deflection probably being due to a slight impurity of the spectrum coming from overlapping orders. No radical departures from the base line were observed anywhere except in regions of the absorption lines of HCl^{35} and HCl^{37}.

The present work was done with two cell lengths. The first work, with very narrow slits, was done with a cell 31 cm long. This is the length of cell used by previous workers and it was found that the strong lines due to

[6] J. D. Hardy, Phys. Rev. **38**, 2162 (1931).

HCl^{35} gave nearly 100 percent absorption with this cell length. When this length of cell failed to show the lines due to HCl^{39} a cell of three meters length was used, and it was felt that had the isotope been present in the HCl gas which was examined, it would not have escaped detection, assuming that its relative abundance to Cl^{35} is about that shown by Hettner and Böhme's curves.

The 31 cm cell was a brass tube provided with strong windows of plate glass. The cell was evacuated and filled with HCl gas from a liquid air trap so as to ensure dryness of the gas. The HCl was prepared in the usual manner by allowing sulfuric acid to combine with pure NaCl in an evacuated Kipps apparatus. The HCl was frozen out by liquid air and then introduced into the

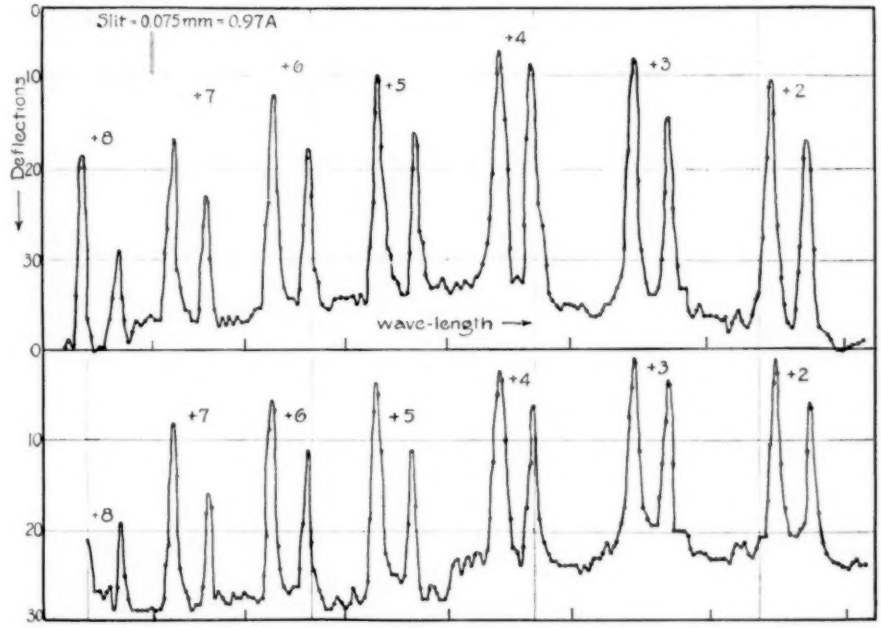

Fig. 1. Two sets of observations: *R* branch of HCl harmonic with 30 cm cell.

evacuated cell to a pressure of 90 cm of mercury. The trap from which the HCl was evaporated was never allowed to come up to the temperature of 0°C during this process. The three meter cell was of galvanized iron thickly coated inside with paraffin. The cell was eight inches in diameter and provided with stout mica windows. The HCl was introduced into the cell from a liquid air trap and the air gradually displaced by continuous flowing of the gas for several hours. Tests at the end of the filling showed that the gas inside was about 92 percent HCl.

Readings were made by taking a complete curve with the empty cell and then a run with the cell full. The background with the empty cell was found to be very smooth and since lines and line positions were desired, percentage absorption was plotted for only one curve, and deflections with the cell full for the detailed curves.

The results of observations with the 31 cm cell are shown in Fig. 1. Lines are drawn to indicate the places where the third isotope might be expected from theory, account being taken of the anharmonic terms in the energy. In Table I are given the wave-lengths and frequency separations measured in this experiment as compared with the values obtained by Meyer and Levin.

TABLE I. *Wave-length and frequency separations in absorption spectrum of HCl.*

Line	Wave-length (A)		Isotope separation Hardy and Sutherland	
	Hardy and Sutherland	Meyer and Levin	(A)	(cm^{-1})
2	17519.8	17520.2	12.3	4.04 ± 0.08
3	17467.7	17467.9	12.2	4.03
4	17418.3	17419.2	12.2	4.03
5	17373.8	17374.9	12.7	4.21
6	17334.6	17334.0	12.7	4.21
7	17298.3	17298.1	12.4	4.14
8	17266.3	17265.2	12.7	4.24
9	17238.1		12.6	4.23 ± 0.09
10	17213.3		13.0	4.34
11	17193.2		12.8	4.29
12	17176.4			
13	17163.4			

The lines 9, 10, 11, 12, and 13 were observed with the three meter cell. The isotope separation for the last two lines is not given since the convergence of the band is so strong that the HCl^{37} component of one line overlaps the HCl^{35} component of its neighbor. In Fig. 2 are shown the results obtained with the three meter cell. Again no trace of the third isotope is visible. The strong lines toward the center of the band are very wide because of the very intense absorption in this region.

Hettner and Böhme state that the theoretical separation between the lines due to HCl^{35} and HCl^{37} is $\Delta\lambda = 13.54$A, whereas the value found by Meyer and Levin is $\Delta\lambda = 12.0 \pm 1$A. Hettner and Böhme attribute the discrepancy to the lack of good separation in the curves of Meyer and Levin, and thus to a resulting "attraction" of the stronger line for the weaker. In the present experiment the lines are well resolved, not overlapping at all, and the resulting separation is in good agreement with the value found by Meyer and Levin. Upon closer examination it is found that the separation expressed in wave numbers is not constant but steadily decreases as one goes toward longer wave-lengths. This variation in isotope separation from line to line illustrates the well-known rotational isotope effect. The agreement between the accurate theory and the most precise measurements is worth examining in some detail.

We start from the Fues[7] expression for the energy of a rotating vibrating dipole.

$$E = A + h\nu_0(n + \tfrac{1}{2})[1 + B(j + \tfrac{1}{2})^2] + (h^2/8\pi^2 J)(j + \tfrac{1}{2})^2[1 - K^2(j + \tfrac{1}{2})^2] - (h^2/8\pi^2 J)(n + \tfrac{1}{2})^2 C. \quad (1)$$

[7] E. Fues, Ann. d. Physik **80**, 367 (1926).

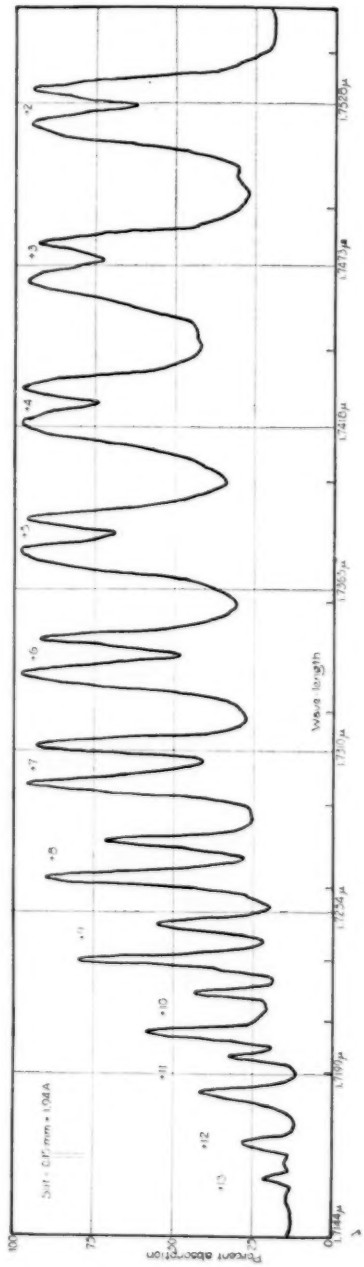
Slit : 0.1 mm = 1.04 A
Wave length
Percent absorption
100
75
50
25
0
1.744μ
1.769μ
1.794μ
1.819μ
1.844μ
1.869μ
1.894μ
1.919μ
1.944μ
1.969μ
1.994μ
2.019μ
2.044μ
2.069μ
2.094μ
2.119μ
2.144μ
2.169μ
2.194μ
2.219μ
2.244μ
2.269μ
2.294μ
2.319μ
2.344μ
2.369μ
2.394μ
2.419μ
2.444μ
2.469μ
2.494μ
2.519μ
2.544μ
2.569μ
2.594μ
2.619μ
2.644μ
2.669μ
2.694μ
2.719μ

Where n is the vibrational quantum number; j is the rotational quantum number;

$$K = h/4\pi^2\nu_0 I;\ B = (3/2)K^2(1 + 2C_3);\ C = 3 + 15C_3 + (15/2)C_3^2 + 3C_4$$

and C_3 and C_4 are constants in the potential energy expression which measure the degree of anharmonicity of the motion. From this we can immediately write down the expression for the frequencies in a vibration-rotation band corresponding to the jump of n from 0 to Δn.

$$\begin{aligned} \nu = {} & \nu_0\Delta n - \tfrac{1}{4}\nu_0 B\Delta n - (h/8\pi^2 I)C(\Delta n^2 + \Delta n) \\ & + j(-\nu_0 B - \nu_0 B\Delta n + h/4\pi^2 I - hK^2/8\pi^2 I) \\ & - j^2\nu_0 B\Delta n - j^3(h/8\pi^2 I)4K^2. \end{aligned} \tag{2}$$

Here we have arranged that j is the number of the line from the center of the band, positive for the positive branch, and negative for the negative branch. Colby[8] has shown that this formula is in excellent agreement with the experimental work of Meyer and Levin on the fundamental and overtone bands of HCl.

As usual let us take ρ as the ratio of the square roots of the reduced masses of the two molecules, then

$$\begin{aligned} \nu_1 - \nu_2 = {} & \nu_0\Delta n(1-\rho) - \tfrac{1}{4}\nu_0 B\Delta n(1-\rho^3) - (h/8\pi^2 I)C(\Delta n^2 + \Delta n)(1-\rho^2) \\ & + j\{-\nu_0 B(1+\Delta n)(1-\rho^3) + h/4\pi^2 I(1-\rho^2) - (h/8\pi^2 I)K^2(1-\rho^4)\} \\ & - j^2\nu_0 B\Delta n(1-\rho^3) - j^3(h/2\pi^2 I)K^2(1-\rho^4) \end{aligned} \tag{3}$$

Where ν_1 corresponds to the HCl^{35} molecule, ν_2 corresponds to the HCl^{37} molecule,

$$\rho = [\mu(HCl^{35})/\mu(HCl^{37})]^{1/2}$$

and the dependence of the various factors on ρ can easily be verified. The values of the constants taken from Colby's analysis of the bands show that the terms with the coefficient $h^2/\pi^2 I$ are quite negligible.

Taking out $(1-\rho)$ as a factor this may be written

$$\begin{aligned} \nu_1 - \nu_2 = {} & (1-\rho)\{\nu_0\Delta n - \tfrac{1}{4}\nu_0 B\Delta n(1+\rho+\rho^2) - (h/8\pi^2 I)C(\Delta n^2+\Delta n)(1+\rho) \\ & + j[-\nu_0 B(1+\Delta n)(1+\rho+\rho^2) + (h/4\pi^2 I)(1+\rho)] \\ & - j^2\nu_0 B\Delta n(1+\rho+\rho^2)\}. \end{aligned} \tag{4}$$

We may simplify this further by putting $\rho = 1$ everywhere except in the first factor. So the frequency separation for the general band when n changes from 0 to Δn is

$$\begin{aligned} \nu_1 - \nu_2 = {} & (1-\rho)\{\nu_e - (h/8\pi^2 I)C(\Delta n^2 + \Delta n) - \tfrac{1}{2}\nu_0 B\Delta n \\ & + j[h/2\pi^2 I - 3B\nu_0(1+\Delta n)] - 3j^2 B\nu_0\Delta n\}. \end{aligned} \tag{5}$$

[8] W. F. Colby, Phys. Rev. **34**, 53 (1929).

Where $\nu_c = \nu_0 \Delta n - \frac{1}{4}\nu_0 B \Delta n - (h/8\pi^2 J)\ C(\Delta n^2 + \Delta n)$ denotes the center of the band. The values of the constants deduced in Colby's[8] paper for the fundamental band of HCl^{35} are $C = 4.885$, $B\nu_0 = 0.303$, $h/4\pi^2 J = K\nu_0 = 21.17$. Substituting those we obtain for the separations:

Fundamental

$$\nu_1 - \nu_2 = 0.000751\{2885.88 - 103.3 + 40.5j - 0.91j^2\}. \qquad (6)$$

Harmonic

$$\nu_1 - \nu_2 = 0.000751\{5667.96 - 309.9 + 39.6j - 1.82j^2\}. \qquad (7)$$

Tables II and III show the agreement between the values of the separations as determined experimentally and as calculated from these expressions.

TABLE II. *Isotope separations in the fundamental band in cm⁻¹.*

j	Positive branch		Negative branch	
	Calculated value	Meyer and Levin's value	Calculated value	Meyer and Levin's value
1	2.12	2.09	2.06	2.10
2	2.14	2.09	2.03	1.97
3	2.17	2.10	1.99	1.98
4	2.20	2.16	1.96	1.90
5	2.23	2.22	1.92	2.02
6	2.25	2.12	1.88	1.72
7	2.27	2.13	1.84	1.74
8	2.29	2.27	1.80	1.77
9	2.31	2.26	1.76	1.83
10	2.33	2.23	1.72	1.61
11	2.34	2.25	1.67	1.71
12	2.36	2.34	1.63	1.57

TABLE III. *Isotope separations in the harmonic band—positive branch.*

j	Calculated		Observed				
			Hardy and Sutherland		Hettner and Böhme		Meyer and Levin
	(cm^{-1})	(A)	(cm^{-1})	(A)	(A)	(A)	(cm^{-1})
2	4.08	12.5	4.04	12.3	12.5	12.5	4.20
3	4.10	12.5	4.03	12.2	12.0	12.5	3.87
4	4.12	12.5	4.03	12.2	12.5	12.5	4.03
5	4.14	12.5	4.21	12.7	12.0	12.0	4.19
6	4.15	12.5	4.21	12.7	12.0		4.22
7	4.16	12.45	4.14	12.4	12.0		4.14
8	4.17	12.4	4.24	12.7			4.26
Mean	4.13	12.5	4.12	12.5	12.3		4.13

The discrepancies between individual line separations as computed and as observed lie in each case within the experimental error. The agreement of the various values for the mean separation in the harmonic band is very satisfactory. The variation in the separation from one end of the fundamental band to the other illustrates particularly well the rotational isotope effect. The result of considering the anharmonic terms is to reduce the value

of the separation from that calculated on the simple theory which would be given by Eq. (5) with $B=C=0$. The anharmonic term involving C is the most effective in reducing the separation. The interaction terms involving B begin to contribute appreciably only when j is very large.

If now we use the above formulae (with an appropriate value of ρ) to compute the isotope separations for an HCl^{39} molecule we obtain a set of values which disagree slightly with those found experimentally by Hettner and Böhme. The comparison is shown in Table IV.

TABLE IV. *Isotope separations in the harmonic band of HCl^{39}.*

j	Calculated value (A)	Hettner and Böhme's value (A)	
2	23.8	24.5	24.5
3	23.8	24.5	25.5
4	23.8	24.5	24.5
5	23.8	23.5	23.5
6	23.8		25.5
7	23.7		23.5
Mean	23.8	24.5	

The difference is small but the close agreement of calculated and observed separations in the case of the Cl^{37} isotope make it doubtful whether these lines are due to HCl^{39}.

To obtain an estimate of the smallest relative abundance of HCl^{39} to HCl^{35} which we could detect, we may compare the absorption coefficient of the weakest line of HCl^{35} which we could detect with that of the strongest, *viz.*, line 3. This can be done theoretically with formulae due to Dunham.[9] Now when α is the absorption coefficient so computed for a certain line it is well known that[10]

$$\alpha = KN$$

where N is the number of molecules in the initial energy level and K is an abbreviation for a number of factors which would not change appreciably for an HCl^{35} or an HCl^{39} molecule. If then we know the least ratio of α's which we can detect, we know the least ratio of N's which we can detect. We employ an equation of Dunham's, modified for use in the positive branch.

$$\frac{\alpha_3}{\alpha_m} = \frac{\bar{p}_3}{\bar{p}_m}\,\frac{\nu_3}{\nu_m}\left\{1 + 2a(\nu_m - \nu_3)\right\} e^{(E_{m-1}-E_2)/kT}$$

where m denotes the number of the line in the positive branch; $\bar{p}$ is the mean of the statistical weights of the initial and final states of the molecule; $2a$ is a small correction factor which we can calculate from Dunham's paper to be very close to 0.0154; E denotes the energy of the molecule in the mth rotational level of the zero vibrational level. When we apply this equation to calculate α_3/α_{13} using energy and frequency values from Colby's paper[8] we ob-

[9] J. L. Dunham, Phys. Rev. **34**, 438 (1929).
[10] D. M. Dennison, Phys. Rev. **31**, 503 (1928).

tain a ratio of 460 to 1. The calculated ratio of α_3/α_{14} was 1600 to 1. Using the three meter cell we could easily detect line 13 and there is an indication on the curve of what may be line 14. The latter is, however, uncertain, but we can safely state that had the Cl^{39} isotope been present in a ratio to Cl^{35} of 1 to 500 we could not have failed to detect it.[11]

There is still another viewpoint from which our inability to substantiate the work of Hettner and Böhme seems remarkable. The instrument we used was of considerably higher resolving power than that employed by them. Our lines are consequently deeper and have higher maxima than theirs and so our instrument is better adapted for the detection of faint companion lines. When we remember that the path length used in the present work was ten times that employed by Hettner and Böhme our failure to detect any sensible change in absorption at the expected places is quite irreconcilable with their conclusions.

It is a pleasure to express our thanks to Professor D. M. Dennison for the suggestion that the anharmonic terms might be important in the calculation of isotope separations and for his interest in the problem.

[11] *Note added in proof:* Since the above article was written the experiment has been repeated using an absorption cell seven meters long. There were still no indications of lines which might be interpreted as coming from an HCl^{39} molecule. Line 14 of the positive branch was easily detected giving quite a distinct absorption peak on the curve. This enables us to place the abundance ratio of Cl^{39} to Cl^{39} lower than 1 to 1600.

The Spectra of Na II, III, and IV in the Extreme Ultraviolet

By BRUCE B. VANCE
Ryerson Physical Laboratory, University of Chicago

(Received July 7, 1932)

New lines of Na II, III and IV have been found and classified in the region between 434,000 and 242,000 cm^{-1}.

INTRODUCTION

THE spectrum of Na II in the near ultraviolet has been classified by Frisch[1] in a recent article, who also gives a list of references to previous work on this spectrum. In the extreme ultraviolet region Bowen[2] and Edlen and Ericson[3] have observed the resonance lines 372.065A and 376.350A.[3] The spectrum of Na III (fluorine-like) has been studied by Edlen and Ericson[4] and Mack and Sawyer.[5] The lines corresponding to the $2s-2p$ transitions are the only lines recorded by these investigators for this ion. Both Edlen and Ericson[4] and Mack and Sawyer[5] predict a PP° group of Na IV in the region of 244,000 cm^{-1}. This group had been found and identified previously by Gale and Hoag of this laboratory, but had not been published. The observation of this group and of other lines in this region, which might be attributed to sodium, caused Professor Gale to suggest the present problem to the author.

GENERAL PROCEDURE

The source was a high potential vacuum spark, (*hot spark*).[6] This took place between hollow aluminum electrodes stuffed with metallic sodium which had first been rolled in nickel gauze. It was found that when the pressure in the discharge chamber was below 10^{-4} cm of Hg and the electrodes were separated about 1.5 mm, the vacuum gap (source) would not break down below 40,000 volts. The maximum voltage of the high potential source was above 100,000 volts. The primary circuit of the transformer was automatically made and broken by a very quick acting switch twenty-two times each minute, the duration of the sparks being from one-twentieth to one-tenth seconds each. The total time required for an exposure was from two to four hours.

The vacuum spectrograph used in this investigation was the one designed by Hoag,[7] with a few changes. The grating was glass, instead of speculum, with 1500 lines to the inch. The plate holder accommodated 2×18 inch plates

[1] R. Frisch, Zeits. f. Physik **70,** 498 (1931).
[2] I. S. Bowen, Phys. Rev. **23,** 1 (1924).
[3] B. Edlen and A. Ericson, Comptes Rendus **190,** 116 (1930).
[4] B. Edlen and A. Ericson, Comptes Rendus **190,** 173 (1930).
[5] J. E. Mack and R. A. Sawyer, Phys. Rev. **35,** 299 (1930).
[6] I. S. Bowen, J.O.S.A. **13,** 89 (1927).
[7] B. Hoag, Astrophys. J. **66,** 225 (1927).

and was so arranged that it could be raised to allow three exposures on one plate without removing it from the vacuum. Very thin glass Schumann plates, made by Hilger and Company, were used.

In reducing the plates a linear dispersion was assumed between the Al IV line of 160.073A[8] and the O III line at 599.598A,[9] error curves were then plotted by the aid of intermediate standards (O III 266.992,[10] Na II 372.065,[3] Na III 380.091[4] and O III 525.795A).[9] These error curves were found to be extremely smooth for all plates.

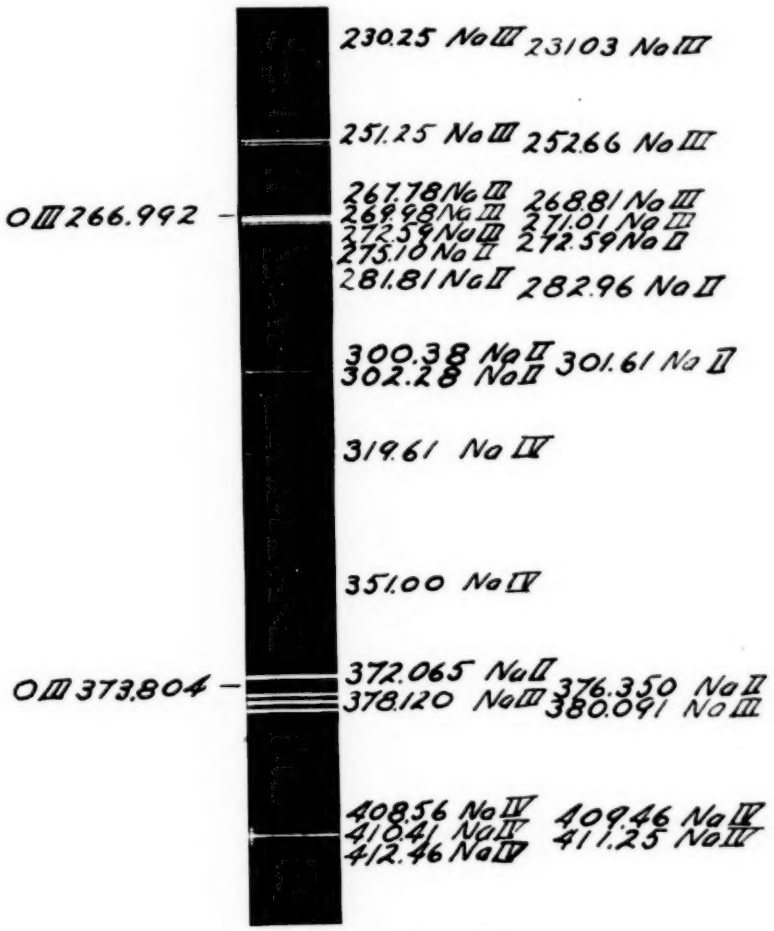

Fig. 1. Typical spectrogram.

With a very narrow slit and the pressure in the discharge chamber below 10^{-4} cm of Hg (as observed with an ionization gauge) plates were easily obtained which were free from fog and weak gas lines. Under these conditions

[8] J. Soderqvist and B. Edlen, Zeits. f. Physik **69**, 356 (1931).

[9] From a list of standard oxygen wave-lengths furnished through the courtesy of Dr. Bengt Edlen of Uppsala.

[10] A. Ericson and B. Edlen, Zeits. f. Physik **59**, 659 (1930).

only the prominent oxygen, carbon and aluminum lines appeared as impurities, which were used as standards in reducing the plates.

Na II (Neon-like)

In the region investigated one would expect to find, besides the prominent resonence transitions $s^2p^6\ {}^1S_0 - s^2p^5 3s\ {}^3P_1,\ {}^1P_1$, transitions from two or three of the three $3d$ levels with $J=1$ and possibly from higher s orbits than the $3s$.

It was found possible to form two series formulas of the type

$$\nu = \nu_0 - 4R/(m+\mu+\alpha/m)^2 \text{ where } m = 1, 2, 3, \cdots$$

whose limits differed by the same amount (in cm^{-1}) as the separation of the ground terms of Na III ($s^2p^5\ {}^2P_{1\,2,3\,2}$). In addition to the three pairs of transitions used in forming these series formulas a fourth pair and possibly a fifth pair were found. (The latter was later found to fit better into the term scheme of Na III.) The levels thus found correspond to the ms_2 and ms_4 levels of neon as given by Paschen,[11] whose limits are ${}^2P^\circ_{1\,2}$ and ${}^2P^\circ_{3\,2}$, respectively. From the value of the latter limit 47.068 volts has been obtained as the ionization potential of Na II. The lines resulting from transitions from these levels to the ground term $s^2p^6\ {}^1S_0$ can be seen easily on the plates (Fig. 1 typical). They are given in Table I and II and are shown diagrammatically in Fig. 2a.

Table I. *Observed and calculated transitions of Na II.*

I	λ (obs.)	ν (cm^{-1})	Config. and Terms	ν (calc.[t])
6	376.350[3]	265710	$s^2p^6\ {}^1S_0 - s^2p^5 3s\ {}^3P_1^\circ (s_4)$	265710
10	372.065[3]	268770	$s^2p^6\ {}^1S_0 - s^2p^5 3s\ {}^1P_1^\circ (s_2)$	268770
0	302.28	330830	$s^2p^6\ {}^1S_0 - s^2p^5 4s\ (s_4)$	330945
3	301.61	331540	$s^2p^6\ {}^1S_0 - s^2p^5 3d\ Z_{11}$	331502[1]
			$4s\ (s_2)$	332811
2	300.38	332910	$s^2p^6\ {}^1S_0 - s^2p^5$	
			$3d\ Z_2$	333050[1]
1	282.96	353260	$s^2p^6\ {}^1S_0 - s^2p^5 5s\ (s_4)$	353283
1	281.81	354850	$s^2p^6\ {}^1S_0 - s^2p^5 5s\ (s_2)$	354854
0	275.10	363500	$s^2p^6\ {}^1S_0 - s^2p^5 6s\ (s_4)$	363510
0	273.99	364960	$s^2p^6\ {}^1S_0 - s^2p^5 6s\ (s_2)$	364888
(0	271.01	369000	$s^2p^6\ {}^1S_0 - s^2p^5 7s\ (s_4)$	369028)*
(0	269.98	370400	$s^2p^6\ {}^1S_0 - s^2p^5 7s\ (s_2)$	370459)*

* Probably Na III.

[t] Calculated ν obtained from the following formulas:

$ms_2 \cdots \nu = 382800 - 4R/(m+0.963845-0.001872/m)^2$

$ms_4 \cdots \nu = 381430 - 4R/(m+0.949650-0.002057/m)^2$

in which $m = 1, 2, 3, \cdots$.

Of the three $3d$ levels with $J=1$ one should have the limit $s^2p^5\ {}^2P^\circ_{1\,2}$ and the other two the limit $s^2p^5\ {}^2P^\circ_{3\,2}$, of the latter two only the transition to the ground term from one of them is observed. This level is calculated to be 331,540 cm^{-1} above the ground term, and corresponds, within experimental error, to the Z_{11} term of Frisch.[1] The other $3d$ ($J=1$, ${}^2P^\circ_{1\,2}$ limit) falls too close to the $4s(s_2)$ level to be resolved, it would correspond to the Z_2 term of Frisch.

[11] Paschen-Goetz, Seriengesetze (1922).

The transition from this level to the ground term is evident only from the fact that the line classified as the $^1S_0-4s(s_2)$ transition is unusually wide for a line of that intensity. The $4s(s_2)$ and $4s(s_4)$ levels correspond to the Z_3 and

TABLE II. *Term values of Na II.*

Config.	Term	Term Value (cm^{-1})	Limit
s^2p^6	$^1S_0$	0	
s^2p^53s	$^3P_1(s_4)$	265710	$^2P^\circ_{3/2}$
s^2p^53s	$^1P_1$ (s_2)	268770	$^2P^\circ_{1/2}$
s^2p^54s	(s_4)	330830	$^2P^\circ_{3/2}$
s^2p^53d	Z_{11}	331540	$^2P^\circ_{3/2}$
s^2p^54s (and $3d$)	(s_2) and Z_2	332910	$^2P^\circ_{1/2}$
s^2p^55s	(s_4)	353260	$^2P^\circ_{3/2}$
s^2P^55s	(s_2)	354850	$^2P^\circ_{1/2}$
s^2p^56s	(s_4)	363500	$^2P^\circ_{3/2}$
s^2p^56s	(s_2)	364960	$^2P^\circ_{1/2}$
s^2p^57s	(s_4)	369000	$^2P^\circ_{3/2}$
s^2p^57s	(s_2)	370400	$^2P^\circ_{1/2}$

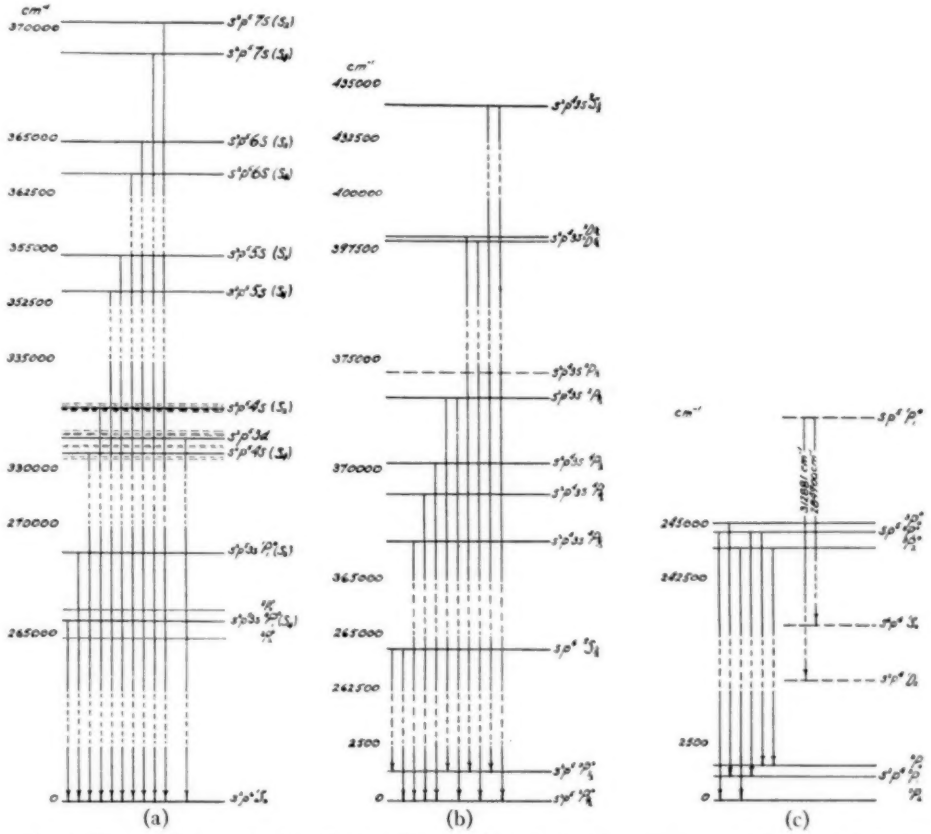

Fig. 2. Term schemes for Na II, Na III, and Na IV for transitions in the far ultraviolet.

Z_{14} levels of Frisch. The other $4s$ and $3d$ terms, which have been calculated from Frisch's values, are indicated by dotted lines in Fig. 2(a) and are given the following J values; $Z_{1,5,8,10,15}$ $J=2$, $Z_{4,9,12}$ $J=3$, Z_{13} $J=4$ and $Z_{6,7}$ $J=0$.

The levels in Fig. 2(a) between 335,000 and 330,000 cm^{-1} are Z_1 to Z_{16} reading down, $Z_{8,9}$ are indicated as one level.

Na III (FLUORINE-LIKE)

In addition to the previously observed transitions $2s-2p$ reported by Edlen and Ericson[4] and Mack and Sawyer,[5] lines have been found which can be classified as $s^2p^5-s^2p^43s$ transitions. These are given in Table III, shown diagrammatically in Fig. 2(b) and the term values are given in Table IV.

TABLE III. *Observed transitions of Na III.*

I	λ	ν (cm^{-1})	Config. and Terms
6	380.091[4]	263095	$s^2p^5\ ^2P^\circ_{1/2}-sp^6\ ^2S_{1/2}$
8	378.120[4]	264466	$s^2p^5\ ^2P^\circ_{3/2}-sp^6\ ^2S_{1/2}$
0	272.59	366840	$s^2p^5\ ^2P^\circ_{3/2}-s^2p^43s\ ^4P_{5/2}$
0*	271.01	369000	$s^2p^5\ ^2P^\circ_{3/2}-s^2p^43s\ ^4P_{3/2}$
0*	269.98	370400	$s^2p^5\ ^2P^\circ_{3/2}-s^2p^43s\ ^4P_{1/2}$
2	268.81	372060	$s^2p^5\ ^2P^\circ_{1/2}-s^2p^43s\ ^2P_{3/2}$
6	267.78	373430	$s^2p^5\ ^2P^\circ_{3/2}-s^2p^43s\ ^2P_{3/2}$
		374600[t]	$s^2p^5\ ^2P^\circ_{3/2}-s^2p^43s\ ^2P_{1/2}$
2	252.26	396410	$s^2p^5\ ^2P^\circ_{1/2}-s^2p^43s\ ^2D_{3/2}$
5	251.25	398010	$s^2p^5\ ^2P^\circ_{3/2}-s^2p^43s\ ^2D_{5/2,3/2}$
1	231.03	432840	$s^2p^5\ ^2P^\circ_{1/2}-s^2p^43s\ ^2S_{1/2}$
2	230.25	434210	$s^2p^5\ ^2P^\circ_{3/2}-s^2p^43s\ ^2S_{1/2}$

* Possibly Na II.
[t] Masked by O III line 266.992A.

The configuration s^2p^4ns theoretically yields inverted $^4P_{1/2,3/2,5/2}$, $^2P_{1/2,3/2}$ terms with limit at $s^2p^4\ ^3P$; $^2D_{3/2,5/2}$ terms with limit at $s^2p^4\ ^1D_2$; and a $^2S_{1/2}$ term with limit at $s^2p^4\ ^1S_0$. Lines are found which are considered to

TABLE IV. *Term values of Na III.*

Config.	Term	Term Value (cm^{-1})	Limit
s^2p^5	$^2P^\circ_{3/2}$	0	
s^2p^5	$^2P^\circ_{1/2}$	1370	
$s\ p^6$	$^2S_{1/2}$	264460	
s^2p^43s	$^4P_{5/2}$	366840	^3P
s^2p^43s	$^4P_{3/2}$	369000	^3P
s^2p^43s	$^4P_{1/2}$	370400	^3P
s^2p^43s	$^2P_{3/2}$	373430	^3P
s^2p^43s	$^2P_{1/2}$	[t]374600?	^3P
s^2p^43s	$^2D_{5/2}$	398010	^1D
s^2p^43s	$^2D_{3/2}$	398230	^1D
s^2p^43s	$^2S_{1/2}$	434210	^1S

[t] Masked by O III line 266.992A.

come from all these levels, for $n=3$, except from the $^2P_{1/2}$ level, and these levels fit well into a Moseley diagram with the same terms of other members of this isoelectronic sequence (F I[12] and Ne II[13]).

The transitions from the $^2P_{1/2}$ level to the $^2P^\circ_{3/2,1/2}$ levels are assumed to be masked by the prominent O III line at 266.992A and the line corresponding to the transition $^2P^\circ_{3/2}-{}^2P_{3/2}$ of Na III respectively. The relative position

[12] H. Dingle, Proc. Roy. Soc. **A117**, 411 (1927).
[13] T. L. deBruin and C. J. Bakker, Zeits. f. Physik **69**, 19 (1931).

of this $^2P_{1/2}$ level on this assumption is indicated by a dotted line in Fig. 2(b).

The lines here identified as corresponding to the transitions between the $^4P_{1/2,3/2}$ and the $^2P^\circ_{3/2}$ levels possibly may be the fifth members of the ms_2 and ms_4 series of Na II, but it seems more likely that they belong to Na III.

Na IV (OXYGEN-LIKE)

The PP° group at 244,000 cm^{-1} that had been found and identified as that of Na IV on photographs taken by Gale and Hoag,[14] during their investigation of multiply ionized lithium, was obtained on nearly all the plates taken during this investigation. The central line was not resolved, which made it difficult to determine exactly the position of the $^3P_1$ and $^3P_0^\circ$ levels.

In addition to the triplet levels there should be a $^1D_2$ and a $^1S_0$ level for the configuration s^2p^4, and a $^1P_1$ level for the configuration sp^5. Lines have been found which probably correspond to the allowed transitions between these levels, and these transitions fit well into a Moseley diagram with the same transitions of Ne III given by Boyce and Compton.[15] The actual position of these levels can not be given from the results obtained, but it is possible to place them roughly from the information obtained from the positions of the ^4P, ^2P, ^2D, and ^2S levels of Na III. This has been done in Fig. 2(c).

TABLE V. *Observed transitions of Na IV.*

I	λ	ν (cm^{-1})	Config. and Terms
3	412.46	242448	$s^2p^4\ ^3P_1-sp^5\ ^3P^\circ_2$
2	411.25	243161	$s^2p^4\ ^3P_0-sp^5\ ^3P^\circ_1$
6	410.41	243654	$s^2p^4\ ^3P_{2,1}-sp^5\ ^3P^\circ_{2,1}$
2	409.46	244224	$s^2p^4\ ^3P_1-sp^5\ ^3P^\circ_0$
3	408.56	244762	$s^2p^4\ ^3P_2-sp^5\ ^3P^\circ_1$
0	351.00	284900	$s^2p^4\ ^1S_0-sp^5\ ^1P^\circ_1$
3	319.61	312880	$s^2p^4\ ^1D_2-sp^5\ ^1P^\circ_1$

TABLE VI. *Term values of Na IV.*

Config.	Terms	Term Values (cm^{-1})
s^2p^4	$^3P_2$	0
s^2p^4	$^3P_1$	1110
s^2p^4	$^3P_0$	1600
s^2p^4	$^1D_2$	A
s^2p^4	$^1S_0$	$A+27980$
sp^5	$^3P^\circ_2$	244050
sp^5	$^3P^\circ_1$	244760
sp^5	$^3P^\circ_0$	245330
sp^5	$^1P^\circ_1$	$A+312880$

In conclusion the author wishes to express his appreciation to Dean Gale for suggesting the problem and for his helpful encouragement throughout the investigation, and to Professor R. S. Mulliken for his advice in the analysis.

Note added in proof: J. Soderqvest, Zeits. f. Physik **76,** 316 (1932), gives an analysis of the Na III spectrum which agrees well with the results given above.

[14] H. G. Gale and B. Hoag, Phys. Rev. **37,** 1703 (1931).

[15] J. C. Boyce and K. T. Compton, Proc. Nat. Acad. Sci. **15,** 656 (1929).

The Absorption Spectrum of Benzene in the Region of 6.75μ

By S. SILVERMAN
The Johns Hopkins University

(Received July 5, 1932)

The absorption band of benzene lying at 6.75μ has been investigated under high resolution for both liquid and gaseous states. The spectrum for the vapor shows three distinct branches with evidence of unresolved fine structure. The liquid shows a less regular spectrum with a definite shift towards longer wave-lengths. In addition, some new water vapor lines in the 6.26μ band are reported.

IN RECENT years an increasing amount of work has been done investigating the infrared absorption and Raman spectra of organic substances. The success which followed the unravelling of the fine structure of some of the more simple compounds led to attempts to resolve the spectra of molecules of increasing complexity. Among the group offering promise due to its complete symmetry is benzene, which has been investigated by a number of workers.[1,2,3,4,5,6] Particularly in the last two or three years, considerable work has been done in the near infrared in this laboratory by Barnes[6] and Leberknight.[7]* Continued improvements in apparatus and resolving power, consisting chiefly of the employment of the Pfund anastigmatic spectrometer with echelette gratings of high resolution, have led to discovery of new bands, and increased complexity in some of the older ones. These studies have thus far been restricted primarily to the region in the neighborhood of 3μ. Bands which previously were so broad as to permit, at best, mere designation as combinations of various vibrational frequencies began to show some evidence of vibration-rotation structure. As a result of several discussions with Dr. C. E. Leberknight, the writer felt that it might be profitable to examine in great detail one of the bands somewhat farther out. The band at 6.75μ, which is quite intense and hence probably represents a fundamental vibration, offered excellent possibilities.

For the purpose of this investigation, the grating spectrometer employing the resonance radiometer, which was used in a recent mapping of the absorption and reflection spectrum of calcite,[8] was found readily adaptable. The grating had 1364 lines per inch; the slit-width was 20A. As in this previous experiment, a magnesium-oxide filter was used to remove the higher

* In this work, which is soon to be published, the spectrum of benzene was investigated in solid, liquid and gaseous states in the region of 3μ under high resolution.

[1] Dougherty, Phys. Rev. **34,** 1549 (1929).
[2] J. Ellis, Phys. Rev. **27,** 298 (1926).
[3] K. W. F. Kohlrausch, Der Smekal-Raman Effekt (Springer 1931).
[4] Schaefer and Matossi, Das Ultrarote Spektrum. P. 270 ff.
[5] R. B. Barnes, Phys. Rev. **35,** 1524 (1930).
[6] R. B. Barnes, Phys. Rev. **36,** 296 (1930).
[7] C. E. Leberknight, unpublished results.
[8] S. Silverman, Phys. Rev. **39,** 72 (1932).

orders of shorter wave-lengths. The instrument was calibrated by means of visual observation of higher orders of the 5461 mercury line, and also by prominent atmospheric absorption lines.[9] The vapor cell was prepared by sealing polished rock-salt windows to the ends of a brass tube. The cement used was a clear lacquer which was found to be almost completely unattacked by the benzene. The optimum cell length was found to be about 22 mm, which length of vapor absorbed 50 percent of the incident energy in the neighborhood of the absorption maximum. A free surface of liquid benzene was kept continually in the bottom of the cell in order to maintain constantly saturation pressure. No difficulty due to condensation on the windows was experienced. A dummy cell was prepared to give a comparison set of readings, as all measurements were taken *cell-in* and *cell-out*. The liquid cell consisted of two flat plates of rock salt, separated by thin strips of silver-foil 0.01 mm thick. This thickness of liquid gives the equivalent molecular path length of 22 mm of gas; this is desirable, as it is essential for direct comparison of gas and liquid to have very much the same *molecular thickness* to traverse. The cell was made tight on 3 sides with lacquer, and the 4th, open, side was fed occasionally with liquid from a pipette; an identical dummy cell was also prepared. The cells maintained their performance unaltered throughout the duration of the experiment.

RESULTS

The absorption in the vapor cell shows the 6.75μ band to be clearly divided into three distinct bands lying at 6.683; 6.743; 6.790μ respectively; the band at 6.743 being somewhat broader and slightly more intense than

TABLE I. *Absorption maxima for benzene.*

Vapor λ	ν	Liquid λ	ν
6.683 ± 0.0015μ	1496.3 ± 0.4	6.643μ	1505.3 ± 0.4
		6.683	1496.3
6.743	1483.0	6.753	1480.8
6.790	1472.8	6.830	1468.1

its companions. All three of the branches show clear evidence of unresolved fine structure, with small but distinct maxima separated by intervals as small as 2 wave numbers. It is entirely probable, however, that the true fine structure of the band is such as to defy resolution by the instrument at our disposal; in which case these small maxima would have no meaning other than to indicate the presence of other fine structure. Inasmuch as the benzene is so complex and has such a large moment of inertia (in the neighborhood of $11 \times 10^{-39} \text{g} \times \text{cm}^2$) one would expect the structure to be very complicated and the lines to be densely packed.

The absorption of the liquid presented a less attractive map. The central band from the vapor absorption is sharpened slightly with a shift from 6.743 to 6.753μ. The band at 6.683 has been so altered as to bear little resemblence

[9] Plyler and Sleator, Phys. Rev. **37**, 1493 (1931).

to the gaseous state. It is much weaker, being nearly washed out, and shows two maxima: one at 6.643 and one at 6.683μ. The 3rd band has also changed so as to present an entirely new picture. It is much broader than its counterpart in the vapor state, and it is quite irregular in outline, with its maximum at 6.830μ. Its intensity is about that of the corresponding vapor band.

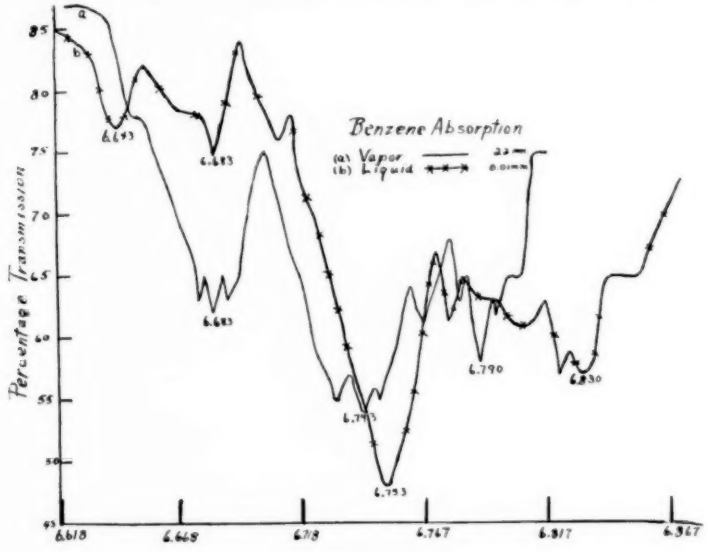

Fig. 1.

It is perhaps worthy of note that in the plotting of this spectrum many runs of the atmospheric absorption bands were obtained. An admirable check of many lines found recently by Plyler and Sleator[9] was obtained. In addition some new ones, marked by the above authors as missing, were observed. These are listed in Table II.

TABLE II. *New absorption lines in water vapor.*

λ	ν	λ	ν
$6.284 \pm 0.0015\mu$	1591.3 ± 0.4	$6.367 \pm 0.0015\mu$	1570.6 ± 0.4
6.294	1588.8	6.480	1543.2
6.299	1587.6	6.485	1542.0
6.313	1584.0	6.583	1519.1

In conclusion, it might be remarked that at present it appears impossible to derive a detailed description of the quantum states of the benzene molecule from the data at hand. The present investigation has shown the existence of hitherto undiscovered fine structure, and it is planned further to probe the spectrum with instruments of still higher resolution in an attempt to unravel the fine detail.

The writer takes great pleasure in expressing his thanks to Dr. C. E. Leberknight for many fruitful discussions concerning this experiment. He also wishes to acknowledge a Grant-in-aid of the National Research council which has helped make this investigation possible.

The Theory of the Faraday Effect in Molecules

By ROBERT SERBER
University of Wisconsin

(Received June 27, 1932)

In treating the Faraday effect two cases may be distinguished, depending upon whether the frequency of the incident light is near resonance or well removed from resonance with absorption lines of the molecule.

Frequency of incident light well removed from resonance with any absorption lines. In this case it is imperative to include the perturbation of the intensities by the magnetic field, as well as the perturbation of the energies. A general expression is obtained for the rotation by molecules (poly-, di-, or monatomic), of the form

$$V=\sum_{n'}\left\{\frac{\nu^2A(nn')}{(\nu(n'n)^2-\nu^2)^2}+\frac{\nu^2B(nn')}{\nu(n'n)^2-\nu^2}+\frac{\nu^2C(nn')}{T(\nu(n'n)^2-\nu^2)}\right\},$$

where V is the Verdet constant. This formula contains dia- and paramagnetic terms of the usual type, but augmented by terms arising from perturbation of the intensities. It contains, in addition, other diamagnetic terms which have the same frequency dependence as the paramagnetic terms. For atoms this expression reduces to that given by Rosenfeld. However for diatomic molecules our results differ from Kronig's, since we include the effects of the components of magnetic moment perpendicular to the axis of figure. The terms arising in this way were omitted by Kronig, although generally they are of the same order of magnitude as the contribution of the parallel component of the moment.

Independence of spin. When the over-all spin-multiplet width is small compared to kT/h the rotation is completely independent of spin. As a consequence the paramagnetic terms vanish for nonlinear polyatomic molecules, and for linear polyatomic and diatomic molecules in Σ states.

Magnitude of the rotation and comparison with experiment. The classical Becquerel formula for the Verdet constant is $V=\gamma(e/2mc^2)\nu\partial n/\partial\nu$, with $\gamma=1$. It is shown that the rotations, in the visible and near ultraviolet, of the gases for which data are available should be approximately representable by a formula of this form, provided γ is given the proper value. The γ value should lie between zero and one. This conclusion, in all cases but one, agrees with the known facts. The exception is oxygen, but the data are probably in error because of polymerization effects which seriously alter the absorption at high pressures.

Frequency of incident light near resonance with an absorption line. Here only the perturbation of the energies by the magnetic field need be considered. It is shown that the rotation in iodine vapour, observed by Wood, is due to rotational distortion of the excited $^3\Pi_0$ level, which partially uncouples the spin moment from the figure axis. The magnetic rotation spectrum of the alkalis, observed by Wood and Loomis, is also explained, in particular the quenching of lines of large rotational quantum number.

TWO different experimental procedures have been employed in measuring the Faraday rotation in gaseous molecules. One method uses a continuous band of incident frequencies, and a low gas pressure; rotation is then observed only in the immediate neighborhood of an absorption line. The other uses monochromatic incident radiation, and high pressures; it serves to mea-

sure the rotation in "transparent" regions of the spectrum. The first method is exemplified by Loomis's measurements of the magnetic rotation spectrum of the alkalis, the second by Siertsema's work on the rotation of hydrogen in the visible.

Correspondingly, the theory must distinguish two cases:

(I) Incident light near resonance with an absorption line of the molecule.

(II) Incident light well removed from resonance with any absorption line.

Anticipating our later results, we may remark that (I) is the simpler of the two, as here the rotation is caused by the Zeeman effect alone. In case (II) it is essential to include, in addition, the effect of the perturbation of the amplitudes (i.e., intensities) by the magnetic field.

§§1 to 5 of this paper deal with case (II). §1 discusses, in a non-mathematical way, the theoretical attack, the general conclusions, and the experimental data. §§2, 3, and 4 give the mathematical development of the theory. §5 is concerned with the magnitude of the rotation and with the application of the theory to a number of simple examples.

§6 treats case (I), in particular, the rotation of iodine as observed by Wood, and the work of Loomis mentioned above.

§1. Discussion of Theory and Experiment

The theory of the Faraday effect in atoms has been treated by Rosenfeld[1] and others. Rosenfeld found, for the case of multiplet widths small compared to kT/h, that when the frequency of the incident light is not near any absorption line the rotation can be expressed as a sum of terms of two types: the diamagnetic, characterized by independence of temperature, and the paramagnetic, proportional to $1/T$. The diamagnetic terms are given by

$$V = \frac{4\pi e N \nu^2}{3hmc^2} \sum_{n'} \frac{\nu(n'n) \left| P(nn') \right|^2}{(\nu(n'n)^2 - \nu^2)^2}, \tag{1}$$

where V, the Verdet constant, is the rotation per gauss per cm, the $P(nn')$ are the matrix elements of the resultant electric moment, and ν is the frequency of the incident light. Eq. (1) can also be written in the Becquerel form

$$V = \frac{e}{2mc^2} \nu \frac{\partial n}{\partial \nu},$$

in which n is the index of refraction, as given by the Kramers dispersion formula.[2] This value of V will be called the normal Verdet constant.

The purpose of the present paper will be to extend the theory to molecules. A start in this direction has already been made by Kronig,[3] who, under the same condition that ν is not too near the frequency of any line, finds a Verdet

[1] L. Rosenfeld, Zeits. f. Physik **57**, 835 (1930).

[2] See, for example, J. H. Van Vleck, *The Theory of Electric and Magnetic Susceptibilities*, p. 362.

[3] R. de L. Kronig, Zeits. f. Physik **45**, 458 and 508 (1927).

constant of only one-third the normal value.[4] This result seems unsatisfactory, for it does not agree with Rosenfeld's calculation in the limiting case of a central field. It will be shown that the error lies in Kronig's neglect of the components of magnetic moment perpendicular to the axis of figure of the diatomic molecule. Since in a central field the components of magnetic moment along any three orthogonal axes contribute equally to the rotation, neglect of two of these components will naturally lead to Kronig's result.

We shall suppose throughout that ν is well outside the Zeeman pattern of any line, i.e., that $\nu - \nu(n'n)$ is large compared to the Zeeman displacements. When only this restriction is made the rotation of any molecule[5] is found to be given by a formula of the form

$$V = B \sum_{nn'} \left\{ \frac{\nu^2 a(nn')}{(\nu(n'n)^2 - \nu^2)^2} + \frac{\nu^2 b(nn')}{\nu(n'n)^2 - \nu^2} + \frac{\nu^2 c(nn')}{T(\nu(n'n)^2 - \nu^2)} \right\} e^{-W_n/kT}, \quad (2)$$

with $B = 1/\sum_n e^{-W_n/kT}$. The three kinds of terms appearing in Eq. (2) will be called "a terms," "b terms," and "c terms," respectively. The a terms are the contributions of the Zeeman effect; the c terms are due to the altered distribution of molecules in the various normal states caused by the magnetic field. The b terms arise from the perturbation of the amplitude elements of the electric moment by the magnetic field. This perturbation is, of course, a consequence of the existence of matrix elements of the magnetic moment between the various states.

Definition of the term "magnetic interaction"

For brevity, when an element of the magnetic moment between two states exists, we shall speak of the magnetic interaction between the states.

Coalescence of *b* terms into *a* and *c* terms

The magnetic interaction between a state n' and a state n'' gives a rotation proportional to the difference quotient[6]

$$\frac{1}{\nu(n'n'')} \left\{ \frac{1}{\nu^2 - \nu(n'n)^2} - \frac{1}{\nu^2 - \nu(n''n)^2} \right\}. \quad (3)$$

If $\nu(n'n'')/(\nu - \nu(n'n))$ is small the difference quotient can be expanded in powers of this ratio (since $\nu(n'n'') = \nu(n'n) - \nu(n''n)$) giving

$$\frac{2\nu(n'n)}{(\nu^2 - \nu(n'n)^2)^2} \left\{ 1 - \frac{2\nu(n'n)\nu(n'n'')}{\nu^2 - \nu(n'n)^2} + \cdots \right\}.$$

[4] Kronig has calculated the rotation explicitly only for diatomic molecules in $^1\Sigma$ states. In comparing Kronig's result (p. 511, reference 3) with our Eq. (1), the factor 2 in his expression must be absorbed by summing over $\Lambda = \pm 1$ rather than only over $\Lambda = 1$. Making the substitution $|a_0(l_0 l_1)|^2 = 4|P_\xi(l_0 l_1)|^2$, and remembering that in a central field $|P_\xi(l_0 l_1)|^2 = \frac{1}{3}|P(l_0 l_1)|^2$, one readily verifies that the two expressions differ by a factor 1/3.

[5] Throughout this paper the term *molecule* is to be understood as including *atom*.

[6] It must be cautioned that this picture is incomplete, as not all b terms appear in the form of difference quotients (see Eq. (8)).

Neglecting terms after the first we see that the two b terms contained in Eq. (3) have reduced to a single a term. Similarly, b terms due to magnetic interactions between states with slightly different Boltzmann factors give rise to c terms when expanded in powers of $h\nu(n'n'')/kT$. Of course b terms caused by interactions between states of widely different energies cannot be simplified in this way.

The net result of the operations just described is the enrichment of a and c terms at the expense of b terms. These modified terms will be called A, B, and C terms to distinguish them from the a, b, and c terms. It should be noted that the A and C terms can not be ascribed any such simple origin as was possible for the a and c terms. Hereafter, whenever we refer to Eq. (2) we shall mean the equation modified in this way, rather than the equation as originally given.

Elimination of Boltzmann factors

The exponential factors drop out of Eq. (2) when the following conditions are satisfied:

a. The over-all spin-multiplet width is small compared to kT/h; or

a'. The separation between the two lowest spin-multiplet components is large compared to kT/h.

b. There are no electronic states with separations from the lowest state of the order of kT/h.

c. The separations between the rotational levels of the normal state are small compared to kT/h.

d. The molecule can be considered rigid (e.g., rotational distortion neglected).

e. The states of the molecule can be divided into *groups*.[7] A set of states $n_1, n_2, \cdots n_t$, will be said to constitute a group if $\nu(n_r n_s)$ is small compared to both $\nu - \nu(n_r p)$ and $\nu(n_r m)$, n_r and n_s representing any two members of the set, p one of the normal states, and m any state, normal or excited, not belonging to the set. Thus in Fig. 1 the states g form a group.

It is evident that condition (e) restricts us to case (II) discussed in the introduction, for if $\nu - \nu(n_r p)$ is too small (i.e., if the incident light is "near resonance with any absorption line") division of states into groups will be impossible. When ν is restricted to such a range that (e) is satisfied, the allowable spread of a group will be widely different in different parts of the spectrum. For example, groups lying near ν or near the normal level may consist of states differing only in their rotational quantum numbers, while groups far from ν and the normal level may include different vibrational states, or even states arising from different electronic configurations.

When either set of conditions, (a), (b), (c), (d), (e), or (a'), (b), (c), (d), (e), is met, the rotation is given by a formula of the form

$$V = \sum_{n'} \left\{ \frac{\nu^2 A(nn')}{(\nu(n'n)^2 - \nu^2)^2} + \frac{\nu^2 B(nn')}{\nu(n'n)^2 - \nu^2} + \frac{\nu^2 C(nn')}{T(\nu(n'n)^2 - \nu^2)} \right\}, \qquad (4)$$

[7] In dividing the states into groups not all states need be considered, but only those having nonvanishing terms in Eq. (8).

with $A(nn')$, $B(nn')$, $C(nn')$ constants independent of temperature. Both A and B terms are thus diamagnetic, the C terms paramagnetic. One must not be misled by the terminology into supposing that the signs of paramagnetic and diamagnetic terms are necessarily opposite, for this is not the case. The presence of diamagnetic B terms, having the same frequency dependence as the paramagnetic terms, has been generally overlooked in the previous theories (it was noted, however, by Van Vleck[8]), although, as will be shown later, the B terms are actually no less important than the more customary A terms.

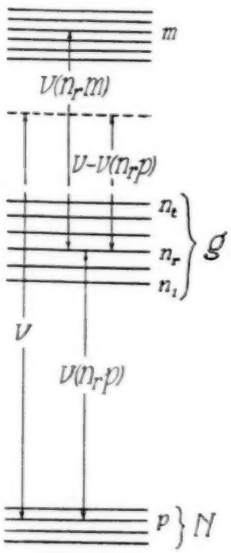

Fig. 1.

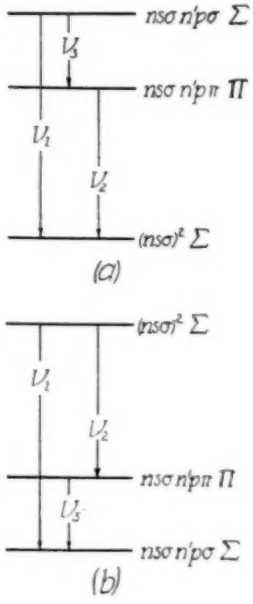

Fig. 2.

In virtue of condition (e) and in view of the discussion of Eq. (3), we can now say that the A terms are due to magnetic interactions between states lying in the same group, while B terms are due to interactions between states in different groups.

The A terms of Eq. (4) are of a more general type than the A terms obtained by Kronig and Rosenfeld, since ours include the interactions between various states in a group. These interactions were neglected by Kronig[9] and did not exist in the case considered by Rosenfeld. Rosenfeld's case of atoms with multiplet widths small compared to kT/h is simplified by the fact that M_L and M_s can be considered constants of the motion,[10] and so the z com-

[8] J. H. Van Vleck, reference 2, p. 370.

[9] Kronig, to be sure, included the elements of μ_z between states of different j, but not between states of different electronic quantum numbers. It is to the latter sort that we refer.

[10] Strictly speaking, this is true only if the magnetic field is strong enough to produce the Paschen-Back effect; however the distinction is trivial in view of the invariance of the spurs appearing in Eq. (9).

ponent of the magnetic moment has no nondiagonal elements. Thus there are no interaction terms like Eq. (3), with the consequence that the A terms reduce simply to the normal Verdet constant, while the B terms vanish entirely (see Eq. (9)).[11] Kronig's calculation of the A terms for diatomic molecules is valid in the limiting case of an axial field so far from central in character that the components of the magnetic moment perpendicular to the figure axis have elements only between states in different groups. Here obviously the A terms are due only to the parallel component of the moment, as Kronig assumed. The B terms will not vanish in this case, and, in fact, are of the same order as the A terms, although omitted by Kronig. Our A terms agree with Kronig's and Rosenfeld's in these limiting cases, but otherwise they are not the same. For example, for nonlinear polyatomic molecules the mean value of the magnetic moment along any axis is zero;[12] hence Kronig's method would give no rotation at all, although we obtain both A and B terms.

Independence of spin

An important characteristic of Eq. (2) (and consequently of Eq. (4)) is that, when (*a*), (*c*) and (*e*) are satisfied, it is completely independent of spin. In any calculation of the rotation, subject of course to these conditions, the spin can be regarded as completely uncoupled from the orbital angular momentum, and, in effect, forgotten completely. This result is analogous to the well-known theorem that the magnetic susceptibility is independent of the Paschen-Back effect, and like it is a consequence of the fact that we sum our expressions over all Zeeman components. In view of this property of the rotation the attempts to explain the anomalous behavior of oxygen as due to its spin are not justifiable. Another conclusion which can immediately be drawn is that the paramagnetic terms of Eq. (4) vanish for nonlinear polyatomic molecules, and for linear polyatomic molecules and diatomic molecules in Σ states. This is because the paramagnetic terms are due to the magnetic interactions between the normal states. Since spin need not be considered, these interactions are clearly zero in the cases indicated.

The absence of a spin-paramagnetic rotation is in sharp contrast to the presence of a spin term in the magnetic susceptibility under the same supposition of narrow multiplets. The difference arises because, under the circumstances, the spin and orbital moments can be regarded as completely independent systems. They thus will contribute additively to the susceptibility; on the other hand, the spin appears in the rotation only in cross terms with the orbit, and such cross terms average to zero.

Magnitude of the rotation

It frequently happens that the rotation has not been measured much beyond the visible, while all the $\nu(n'n)$ are in the far ultraviolet. The A and B

[11] Considering the phases proper to a central field, it is readily seen that, in this case, Eq. (9) is identical with Rosenfeld's expression.

[12] This statement might not hold if the molecule had a very high degree of symmetry; however, whenever we consider nonlinear polyatomic molecules we shall assume that this is not the case.

terms are then practically indistinguishable, the net result of the B terms being to change the apparent values of the $A(nn')$. Thus the diamagnetic terms of Eq. (4) will have, effectively, the frequency dependence, $\nu^2/(\nu(n'n)^2-\nu^2)^2$, of the Becquerel formula. In consequence, as will be shown more fully in §5, the rotation can often be represented fairly well by the Becquerel formula with an anomalous value of e/m.

In general our knowledge of the molecule is not sufficient to permit explicit calculation of all the terms required by Eq. (4), but simple considerations lead to the conclusion that the Verdet constant should ordinarily be less than the normal value. The experimental results in all cases confirm this. The reason is roughly as follows: The rotation is largely due to the nearest intense group of lines in the ultraviolet, which are heavily weighted compared to those further out. If all the lines lay close to this nearest group a normal Verdet constant would result, as is shown in §5. The effect of removing some of the lines further into the ultraviolet, where in fact they belong, is to diminish greatly their contribution to the rotation. If the field is not central this diminution is greater than the corresponding decrease in $\partial n/\partial \nu$, and so leads to a smaller Verdet constant.

Discussion of experiment[13]

Siertsema's measurements of the rotation in hydrogen in the visible are representable almost exactly by the normal Verdet constant. This result, remarkable in its agreement with the classical theory, will be discussed in §5. However Sirk's measurements in the ultraviolet show some evidence of the presence of a B term. The magnitude of the observed rotation in nitrogen is 63 percent of the normal Verdet constant, i.e., the Becquerel formula is valid if we insert a factor 0.63. As the measurements have not been carried beyond the visible no differentiation between A and B terms is possible. The case of N_2O is similar. Carbon dioxide has been observed in the ultraviolet, but not far enough to give any conclusive evidence as to the presence or absence of B terms (see §5).

Oxygen, on the other hand, is definitely anomalous. The measurements of Siertsema and Sirks in the visible and ultraviolet cannot be fitted by Eq. (4) using the observed absorption frequencies, and, as we have seen, this cannot be blamed on the spin. However the experimental data are open to serious objection because of the high gas pressures used: Siertsema, working in the visible, used a pressure of 100 atmospheres; Sirks, 80 atmospheres in the visible, 40 in the ultraviolet below 2800A. At these pressures a considerable amount of oxygen would be in the form of the polymer O_4.[13a] The equilibrium constant is somewhat uncertain; at 80 atmospheres the estimates of the

[13] An excellent account of the experimental data on the Faraday effect has been given by C. G. Darwin and W. H. Watson, Proc. Roy. Soc. **114A**, 474 (1927). The reader is referred to this paper for references to the literature.

[13a] The existence of this polymer was kindly called to my attention by Professor R. Ladenburg.

partial pressure of O_4 range from 1 to 10 percent of the total pressure.[14] According to Wulf,[14] O_4 shows continuous absorption below 2400A, as well as a number of bands extending towards longer wave-lengths. Moreover, the source of light used by Sirks and Siertsema was a quartz mercury arc, and Warburg[15] has shown that at high pressures the 2537A line is efficacious in producing ozone. Ozone shows strong absorption in the infrared, and in the ultraviolet beginning at about 2800A. Sirks found, in his 230 cm column of oxygen at 80 atmospheres, that absorption began at 2805A; in fact it was for this reason that he was compelled to reduce the pressure for his shorter wave-length measurements. At 40 atmospheres the absorption had moved down to 2654A. O_2 shows no absorption in this region, but both O_4 and O_3 bands have been reported at 2810A and 2654A;[16] these might readily account for Sirk's results.

In view of these facts we believe the existing measurements of the rotation entirely unreliable; solution of the problem must await more unambiguous data.

Monatomic gases should, according to Rosenfeld, have a normal Verdet constant. This has been verified for neon, although at only one wave-length, 5460A. The same result has also been found for argon.[17]

In general the rotations in the large number of liquids and solids cited by Darwin are not accurately representable by the Becquerel formula, even with an anomalous value of e/m. There are two obvious reasons for this: first, the $A(nn')$ are not proportional to the f values of the Kramers dispersion formula; second, B terms are also present.

§2. Derivation of the General Formula for the Rotation

Let the magnetic field and the light ray be directed along the z axis. The rotation of the plane of polarization per centimeter is[18]

$$\theta = CB \sum_{nn'} \tau(n'n) \left[P_x(nn') P_y(n'n) \right] e^{-W_n/kT}, \tag{5}$$

where

$$B = N / \sum_n e^{-W_n/kT}, \quad C = 4\pi^2 \nu^2 i / ch,$$

and $P_x(nn')$, $P_y(nn')$ are the elements of the x and y components of the electric moment in the presence of the magnetic field. Here, and throughout this paper, the square brackets have the meaning

$$\left[P_x(nn') P_y(n'n) \right] = P_x(nn') P_y(n'n) - P_y(nn') P_x(n'n);$$

and

$$\tau(n'n) = 1/(\nu^2 - \nu(n'n)^2).$$

[11] O. R. Wulf, Proc. Nat. Acad. **14**, 356, 609, 614 (1928); Jour. Am. Chem. Soc. (II) **50**, 2596 (1928).

[15] References to Warburg's work are given by Wulf, reference 14.

[16] Wulf, reference 14; D. Chalonge and M. Lambrey, Comptes Rendus **184,** 1165 (1927).

[17] R. de Mallemann, L. Gabiano, and F. Suhner; Comptes Rendus **194,** 861 (1932).

[18] H. A. Kramers, Kon. Acad. Wet. Amsterdam **33,** 959 (1930). Kramer's Eq. (34) should be multiplied by 4π, as can be seen from his Eq. (32).

We expand P_x, P_y, $\nu(n'n)$, W_n, B in power series of the form $P_x = P_x^0 + \mathfrak{H}P_x^{(1)} + \cdots$; then, under the supposition that $\nu - \nu(n'n)$ is large compared to the Zeeman splitting, the terms of Eq. (5) linear in $\mathfrak{H}$ give

$$\begin{aligned} V = \theta/\mathfrak{H} = CB^0 \sum_{nn'} \{ & \tau^0(n'n)([P_x^0(nn')P_y^{(1)}(n'n)] + [P_x^{(1)}(nn')P_y^0(n'n)]) \\ & + 2\nu^0(n'n)\nu^{(1)}(n'n)\tau^0(n'n)^2[P_x^0(nn')P_y^0(n'n)] \\ & - (W_n^{(1)}/kT)\tau^0(n'n)[P_x^0(nn')P_y^0(n'n)]\} e^{-W_n^0/kT}. \end{aligned} \tag{6}$$

$P_x^{(1)}(nn')$ is expressed in terms of the unperturbed amplitudes by means of[19]

$$P_x^{(1)}(nn') = \frac{1}{h} \sum_{n''}{}' \left\{ \frac{H^{(1)}(nn'')P_x^0(n''n')}{\nu^0(nn'')} - \frac{P_x^0(nn'')H^{(1)}(n''n')}{\nu^0(n''n')} \right\}. \tag{7}$$

The prime on the summation sign indicates that $n'' = n$ and $n'' = n'$ are to be omitted from the summation. Denoting the z component of the magnetic moment by μ_z, we have $H^{(1)}(nn') = -\mu_z(nn')$. Using these, and a similar expression for $P_y^{(1)}(nn')$, we obtain

$$\begin{aligned} V = & - (CB^0/h) \sum_{nn'n''}{}' \nu^0(n'n'')^{-1}[P_x^0(nn')\mu_z(n'n'')P_y^0(n''n)] \\ & \{\tau^0(n'n) - \tau^0(n''n)\} e^{-W_n^0/kT} \\ & - (2CB^0/h) \sum_{nn'} \nu^0(n'n)\tau^0(n'n)^2[P_x^0(nn')\mu_z(n'n')P_y^0(n'n)]e^{-W_n^0/kT} \\ & + (CB^0/h) \sum_{nn'n''}{}' \nu^0(n''n)^{-1}\tau^0(n'n) \{[P_x^0(nn')P_y^0(n'n'')]\mu_z(n''n) \\ & + \mu_z(nn'')[P_x^0(n''n')P_y^0(n'n)]\} e^{-W_n^0/kT} \\ & + (2CB^0/h) \sum_{nn'} \nu^0(n'n)\tau^0(n'n)^2\mu_z(nn)[P_x^0(nn')P_y^0(n'n)]e^{-W_n^0/kT} \\ & + (CB^0/kT) \sum_{nn'} \tau^0(n'n)\mu_z(nn)[P_x^0(nn')P_y^0(n'n)]e^{-W_n^0/kT}. \end{aligned} \tag{8}$$

Here we have extended our definition of the square bracket to include

$$\begin{aligned} [P_x^0(nn')\mu_z(n'n'')P_y^0(n''n)] = & P_x^0(nn')\mu_z(n'n'')P_y^0(n''n) \\ & - P_y^0(nn')\mu_z(n'n'')P_x^0(n''n). \end{aligned}$$

In accordance with our division of states into groups, all matrix elements will now be written (dropping henceforth the superscript 0) in the form $P_x(nk;n'k')$, where n and n' represent the quantum numbers which are the same for all states in a group, k and k' the quantum numbers which differentiate the various states within a group.

The terms of the first sum in Eq. (8) for which $n'' = n'$ (although, of course, $k'' \neq k'$) can be simplified by expanding the factor in curly brackets in powers of $\nu(n'k';n'k'')/(\nu^2 - \nu(n'k';nk)^2)$. To simplify the terms of the third sum for which $n'' = n$ ($k'' \neq k$) the method of pairing terms previously used by Van Vleck[20] is employed.

[19] See, for example, Born and Jordan, *Elementare Quantenmechanik*, p. 198.

[20] J. H. Van Vleck, reference 2, p. 191; Phys. Rev. **29**, 727 (1927).

The pair of terms

$$(1/h)\nu(nk''; nk)^{-1}\tau(n'k'; nk)\{[P_x(nk; n'k')P_y(n'k'; nk'')]\mu_z(nk''; nk) + \mu_z(nk; nk'')[P_x(nk''; n'k')P_y(n'k'; nk)]\}e^{-W_{nk}/kT}$$
$$+ (1/h)\nu(nk; nk'')^{-1}\tau(n'k'; nk'')\{[P_x(nk''; n'k')P_y(n'k'; nk)]\mu_z(nk; nk'') + \mu_z(nk''; nk)[P_x(nk; n'k')P_y(n'k'; nk'')]\}e^{-W_{nk''}/kT}$$

can be written

$$\{[P_x(nk; n'k')P_y(n'k'; nk'')]\mu_z(nk''; nk) + \mu_z(nk; nk'')[P_x(nk''; n'k')P_y(n'k'; nk)]\}$$
$$\frac{1}{h\nu(nk''; nk)}\left\{\frac{e^{-W_{nk}/kT}}{\nu^2 - \nu(n'k'; nk)^2} - \frac{e^{-W_{nk''}/kT}}{\nu^2 - \nu(n'k'; nk'')^2}\right\}.$$

Putting

$$W_{nk''} = W_{nk} + h\nu(nk''; nk),$$
$$\nu(n'k'; nk'') = \nu(n'k'; nk) - \nu(nk''; nk)$$

and expanding gives (the first bracket representing the first line of the above expression)

$$\{\}\{\}\left\{\frac{1}{2kT}\,\frac{e^{-W_{nk}/kT}}{\nu^2 - \nu(n'k'; nk)^2}\left[1 + \left(1 - \frac{h\nu(nk''; nk)}{kT}\right)\right]\right.$$
$$\left. + \frac{2\nu(n'k'; nk)e^{-W_{nk}/kT}}{h(\nu^2 - \nu(n'k'; nk)^2)^2}\left[1 - \frac{h\nu(nk''; nk)}{kT}\right]\right\}$$

plus higher order terms which are very small. Apart from them, this is the same as

$$\{[P_x(nk; n'k')P_y(n'k'; nk'']\mu_z(nk''; nk) + \mu_z(nk; nk'')[P_x(nk''; n'k')P_y(n'k'; nk)]\}$$
$$\{(1/h)\nu(n'k'; nk)\tau(n'k'; nk)^2 + (1/2kT)\tau(n'k'; nk)\}e^{-W_{nk}/kT}$$
$$+ \{[P_x(nk''; n'k')P_y(n'k'; nk)]\mu_z(nk; nk'') + \mu_z(nk''; nk)[P_x(nk; n'k')P_y(n'k'; nk'')]\}$$
$$\{(1/h)\nu(n'k'; nk'')\tau(n'k'; nk'')^2 + (1/2kT)\tau(n'k'; nk'')\}e^{-W_{nk''}/kT}.$$

The purpose of these manipulations is to remove all small ν's from the denominators of Eq. (8). A primed sum is no longer required for the terms written in this form, since the diagonal terms (i.e., $k''=k$) are already present in Eq. (8): namely, the fourth and fifth sums there appearing. The expansion of the first sum of Eq. (8) leads to a similar simplification, the diagonal terms being contained in the second sum.

It is now convenient to introduce the übermatrix notation used, for example, in Born and Jordan's *Elementare Quantenmechanik*. In this notation $P_x^{(nn')}$ signifies the matrix of all the elements $P_x(nk;n'k')$ having a given n and n'. Sp is an abbreviation for *spur*.

One finds, on carrying out the operations described above that Eq. (8) becomes

$$\begin{aligned}
V = {} & (CB/h)\sum_{n'}\nu(n'n)\tau(n'n)^2\ \mathrm{Sp}\left\{(-2[P_x^{(nn')}\mu_z^{(n'n')}P_y^{(n'n)}]\right. \\
& \left. + [P_x^{(nn')}P_y^{(n'n)}]\mu_z^{(nn)} + \mu_z^{(nn)}[P_x^{(nn')}P_y^{(n'n)}])e^{-W^{(n)}/kT}\right\} \\
& + (CB/h)\sum_{n'n''(n'\neq n'')} - \nu(n'n'')^{-1}\{\tau(n'n) - \tau(n''n)\} \\
& \mathrm{Sp}\left\{[P_x^{(nn')}\mu_z^{(n'n'')}P_y^{(n''n)}]e^{-W^{(n)}/kT}\right\} \\
& + \nu(n''n)^{-1}\tau(n'n)\ \mathrm{Sp}\left\{([P_x^{(nn')}P_y^{(n'n'')}]\mu_z^{(n''n)}\right. \\
& \left. + \mu_z^{(nn'')}[P_x^{(n''n')}P_y^{(n'n)}])e^{-W^{(n)}/kT}\right\} \\
& + (CB/2kT)\sum_{n'}\tau(n'n)\ \mathrm{Sp}\left\{([P_x^{(nn')}P_y^{(n'n)}]\mu_z^{(nn)}\right. \\
& \left. + \mu_z^{(nn)}[P_x^{(nn')}P_y^{(n'n)}])e^{-W^{(n)}/kT}\right\}.
\end{aligned} \tag{9}$$

As all small ν's have been removed from the denominators of Eq. (8) we have been able, in Eq. (9), to write $\nu(n'k';nk)=\nu(n'n)$. In the first sum of Eq. (9) small terms involving $\nu(nk';nk)$ have been omitted. This corresponds to neglecting the pure rotation spectrum.

§3. Independence of Spin

The spurs appearing in Eq. (9) are invariant of a transformation to a system of representation appropriate to strong fields. If the over-all spin-multiplet width is small compared to kT/h the matrix $e^{-W^{(n)}/kT}$ is independent of spin. Then the "strong field" representation the spin appears only in μ_z, which breaks up into two parts, $\mu_{lz}+\mu_{sz}$, of which only the second contains the spin. On summing over m_s this term vanishes, since μ_{sz} is a diagonal matrix with elements ranging from $-2\beta s$ to $2\beta s$. Thus, when the over-all multiplet width is small and when ν is not near resonance with any line, the rotation is independent of the spin.[21] This result, of course, is valid for all field strengths (barring saturation effects).

In §5, dealing with the magnitude of the rotation, we shall consider only narrow multiplets; μ_z may accordingly be taken as representing only that part of the magnetic moment due to the orbital angular momentum.

§4. Rotation in Rigid Molecules

We will make the approximation of supposing the molecule rigid, that is, we suppose the "internal" wave functions, which are expressed in terms of a coordinate system rotating with the molecule, independent of j. Then the summation over j, m, j', m', j'', m'' implied in Eq. (9) can be readily performed by a method given by Niessen.[22] Let x', y', z' be the rotating system of coordinates. On applying Niessen's method to Eq. (9) we find[23]

$$
\begin{aligned}
V = {} & (CN/3hg)\sum_{x'y'z'}\sum_{n'}\nu(n'n)\tau(n'n)^2\,\mathrm{Sp}\,\{-2[P_{x'}^{(nn')}\mu_{z'}^{(n'n')}P_{y'}^{(n'n)}] \\
& + [P_{x'}^{(nn')}P_{y'}^{(n'n)}]\mu_{z'}^{(nn)} + \mu_{z'}^{(nn)}[P_{x'}^{(nn')}P_{y'}^{(n'n)}]\} \\
& + (CN/3hg)\sum_{x'y'z'}\sum_{n'n''(n''\neq n')} - \nu(n'n'')^{-1}\{\tau(n'n)-\tau(n''n)\} \\
& \mathrm{Sp}\,[P_{x'}^{(nn')}\mu_{z'}^{(n'n'')}P_{y'}^{(n''n)}] + \nu(n''n)^{-1}\tau(n'n) \\
& \mathrm{Sp}\,\{[P_{x'}^{(nn')}P_{y'}^{(n'n'')}]\mu_{z'}^{(n''n)} + \mu_{z'}^{(nn'')}[P_{x'}^{(n''n')}P_{y'}^{(n'n)}]\} \\
& + (CN/6kTg)\sum_{x'y'z'}\sum_{n'}\tau(n'n)\,\mathrm{Sp}\,\{[P_{x'}^{(nn')}P_{y'}^{(n'n)}]\mu_{z'}^{(nn)} \\
& + \mu_{z'}^{(nn)}[P_{x'}^{(nn')}P_{y'}^{(n'n)}]\}\,.
\end{aligned}
\tag{10}
$$

The symbol $\sum_{x'y'z'}$ indicates a summation of the three terms obtained by a cyclic interchange of x', y', z'. g is the statistical weight of the normal state

[21] This result has been given, for central fields, by Rosenfeld, reference 1, and in the old quantum theory, also for central fields, by Darwin, Proc. Roy. Soc. **112A**, 814 (1926).

[22] K. F. Niessen, Phys. Rev. **34**, 253 (1929). Niessen's derivation is valid only for diatomic molecules, but the proof can be given for the general case.

[23] It should be noted that Eq. (10) holds when either condition (*a*) or (*a'*) is satisfied.

of the stationary molecule. The elements of matrices such as $P_{x'}^{(nn')}$ are, of course, independent of j, m, j', m'.

Making a simple rearrangement of the terms in the second sum of Eq. (10), we find the explicit expression for the $A(nn')$, $B(nn')$, $C(nn')$ of Eq. (4):

$$A(nn') = (CN/3hgv^2) \sum_{x'y'z'} \nu(n'n) \operatorname{Sp}\{-2[P_{x'}^{(nn')}\mu_{z'}^{(n'n')}P_{y'}^{(n'n)}] + [P_{x'}^{(nn')}P_{y'}^{(n'n)}]\mu_{z'}^{(nn)} + \mu_{z'}^{(nn)}[P_{x'}^{(nn')}P_{y'}^{(n'n)}]\}$$

$$B(nn') = (CN/3hgv^2) \sum_{x'y'z'} \sum_{n''(n''\neq n')} -\nu(n'n'')^{-1} \operatorname{Sp}\{[P_{x'}^{(nn')}\mu_{z'}^{(n'n'')}P_{y'}^{(n''n)} + [P_{x'}^{(nn'')}\mu_{z'}^{(n''n')}P_{y'}^{(n'n)}]\} + \nu(n''n)^{-1} \operatorname{Sp}\{[P_{x'}^{(nn')}P_{y'}^{(n'n'')}]\mu_{z'}^{(n''n)} + \mu_{z'}^{(nn'')}[P_{x'}^{(n''n')}P_{y'}^{(n'n)}]\}$$

$$C(nn') = (CN/6kgv^2) \sum_{x'y'z'} \operatorname{Sp}\{[P_{x'}^{(nn')}P_{y'}^{(n'n)}]\mu_{z'}^{(nn)} + \mu_{z'}^{(nn)}[P_{x'}^{(nn')}P_{y'}^{(n'n)}]\}.$$

§5. Magnitude of the Rotation

For nonlinear polyatomic molecules the matrix $\mu^{(nn)}$ will be zero, there being no "precession frequencies" which are not large compared to kT/h. Thus the $C(nn')$ will vanish. Diatomic molecules and linear polyatomic molecules in Σ states will also have no elements in $\mu^{(nn)}$ different from zero, so the $C(nn')$ again vanish. In these cases there will be no paramagnetic rotation.

The work of Rosenfeld and Kronig give limiting values for the $A(nn')$. We have shown in §1 that in a central field the $A(nn')$ have just the values which give the normal Verdet constant, and in the other limiting case (for diatomic molecules) of an extreme axial field the $A(nn')$ are reduced to one-third the previous value (the three terms of the $\sum_{x'y'z'}$ sum reducing to a single term), unless both n and n' are Σ states, in which case $A(nn')$ vanishes entirely.[24] The $A(nn')$ of polyatomic molecules similarly vanish for sufficiently asymmetrical fields.

The whole question of the magnitude of the rotation is greatly clarified by consideration of a few simple examples. The molecular wave function (in the x', y', z' system) will be supposed the product of the hydrogenic wave functions of the individual electrons. This makes Λ a constant of the motion.

Let the normal state be $(ns\sigma)^2\Sigma$, as in the hydrogen molecule. Take for excited states $ns\sigma n'p\pi\Pi$ and $ns\sigma n'p\sigma\Sigma$, and let ν_1, ν_2, ν_3 be respectively the $ns\sigma n'p\sigma\Sigma - (ns\sigma)^2\Sigma$, $ns\sigma n'p\pi\Pi - (ns\sigma)^2\Sigma$, $ns\sigma n'p\sigma\Sigma - ns\sigma n'p\pi\Pi$ separations. This situation is illustrated in Fig. 2 (*a*). No assumption will be made as to the relative magnitudes of ν_1 and ν_2, other than that condition (*e*) is satisfied; they must accordingly be considered as belonging to two different groups. This procedure, of course, is valid even when $\nu_1 - \nu_2$ (i.e., ν_3) is small. Using the well-known hydrogenic moment matrices we readily find from Eq. (10),[25]

[24] We are thinking here of the practically important case, in which the normal state is a Σ state. In general the one-third remaining after passage to the axial field limit will be divided among the states of different Λ into which the central field group breaks up.

$$V = \frac{4\pi eN\nu^2}{3hmc^2}\left\{\frac{P^2}{\nu_3(\nu_2^2 - \nu^2)} - \frac{P^2}{\nu_3(\nu_1^2 - \nu^2)} + \frac{\nu_2 P^2}{(\nu_2^2 - \nu^2)^2}\right\}, \tag{11}$$

where $P^2 = 2\left|P_{x'}(n'p\pi, ns\sigma)\right|^2$ in the notation of footnote (25).

The normal Verdet constant is

$$V_n = \frac{4\pi eN\nu^2}{3hmc^2}\left\{\frac{\nu_1 P^2}{(\nu_1^2 - \nu^2)^2} + \frac{2\nu_2 P^2}{(\nu_2^2 - \nu^2)^2}\right\}. \tag{12}$$

The asymptotic properties discussed above are easily verified. If ν_3 is made small compared to $\nu_1 - \nu$, Eqs. (11) and (12) both reduce to

$$V = V_n = 4\pi eN\nu^2\nu_2 P^2/hmc^2(\nu_2^2 - \nu^2)^2;$$

thus V is just the normal Verdet constant. If ν_3 is very large, so that the first two terms of Eq. (11) and the first term of Eq. (12) are negligible, the rotation, as given by Eq. (11), is reduced to one-third the above value, which is Kronig's result. In this case $V = \frac{1}{2}V_n$ (the index of refraction being reduced to 2/3 its central field value, while the rotation is reduced to 1/3).

If γ is defined by $\gamma = V/V_n$, we have seen that $\gamma = 1$ for a central field, and $\gamma = 0.5$ for an extreme axial field.[26] In intermediate cases γ will lie between these values. For example if we take $\nu_1 = 2\nu_2$, $\nu = \nu_2/6$ we find $\gamma = 0.817$. Taking $\nu = \nu_2/4$ gives $\gamma = 0.813$. If ν_2 corresponds to a line at 1000A these two values of ν correspond to 6000A and 4000A respectively. This simple calculation strikingly illustrates the point made in §1 that A and B terms are, in such a frequency range, practically indistinguishable. Further, it shows very clearly why a Becquerel formula with an anomalous value of e/m is approximately valid for many substances. If we put $\nu = \nu_2/2.5$, corresponding to $\lambda = 2500$A, we obtain $\gamma = 0.79$. Thus even measurements this far in the ultraviolet would be of little value in distinguishing between Eq. (11) and the modified Becquerel formula.

Magnetic interactions between some of the excited states may be due to the "core," or part of the molecule exclusive of the excited electron, for when we remove an electron from a closed shell the residuum may have a magnetic moment. Of course states which have different core-configurations are greatly different in energy, and so the magnetic interactions of the core may easily connect widely separated levels. On the other hand, a normal Verdet constant requires narrow, rather than wide, separations. The essential difference

[25] For example, denoting the normal state by ψ_1, the II state by ψ_2, and the wave functions of the individual electrons by $(n|x_i)$ we have

$$\begin{aligned} \psi_1 &= (ns\sigma|x_1)(ns\sigma|x_2), \quad \psi_2 = (ns\sigma|x_1)(n'p\pi|x_2), \\ P_x(12) &= -ef\int\psi_1^*(x_1 + x_2)\psi_2 d\tau_1 d\tau_2 = -ef(ns\sigma|x_2)^* x_2(n'p\pi|x_2)d\tau_2 \\ &= P_{x_2}(ns\sigma; n'p\pi). \end{aligned}$$

The elements such as $P_{x_2}(ns\sigma; n'p\pi)$ are given in all the standard texts, e.g., H. Weyl, *The Theory of Groups and Quantum Mechanics*, p. 200.

[26] If the Σ state is taken as the lower of the excited states γ would range from 1 to 0 (we are supposing $\nu < \nu_1, \nu_2$). For polyatomic molecules also, γ would be expected to range from 1 to 0. These figures are exclusive of negative terms, which will be discussed later.

between the rotations in atoms and molecules lies in the spread, in molecules, of levels which coincide in atoms; and the more complicated the core the larger this spread is likely to be. One would therefore expect the rough rule that molecules with complicated cores have lower values of γ than simpler molecules. The data confirm this, the γ values for H_2, N_2, CO_2, N_2O being respectively 1.00, 0.63, 0.56, 0.34.

The central field behaviour of hydrogen in the visible is now readily explained, for the core consists of a single electron in a σ state, and thus plays no part in determining the rotation. As one would anticipate, the potential energy curves[27] show that the excited $1s\sigma 2p\sigma\Sigma$ and $1s\sigma 2p\pi\Pi$ states lie quite close to each other as compared to their separation from the normal state. Since there is little possibility of exciting the core electron to obtain other states which could contribute to the rotation, the rotation is evidently due almost entirely to the two excited states mentioned above; and, as we have seen, these closely spaced levels should give a normal Verdet constant.

As an example of the case in which the core does have a magnetic moment we shall take for the normal state $(np\pi)^4(np\sigma)^2\Sigma$, the nitrogen configuration, and for excited states $(np\pi)^3(n\not{p}\sigma)^2n's\sigma\Pi$ and $(np\pi)^4\, n\not{p}\sigma n's\sigma\Sigma$. Magnetic interactions between these states will evidently be due to the core of the II state. Proceeding exactly as in the previous example we again find the rotation to be given by Eq. (11). In a central field the energies of our two excited states will coincide, and a normal Verdet constant will result: in such a field no distinction need be made between the magnetic moment of the core and the magnetic moment of a valence electron. In the axial field of a diatomic molecule the energies of the excited states will be widely different, since these states have different core configurations; γ will thus be considerably less than unity. This result, as contrasted with the result obtained for the hydrogen molecule, illustrates the effect of a complex core in diminishing the Verdet constant.

When we deal with homonuclear diatomic molecules another factor may enter which we have not yet considered. For such molecules $P(nn')$ has elements only between the normal state and states of opposite symmetry with respect to reflection of the electrons in the origin. States n'' of the same symmetry as the normal state will have no effect on the refraction, but Eq. (10) shows that they will affect the magnitude of the rotation if the elements $\mu_z(nn'')$ are not negligible, although no terms containing $\tau(n''n)$ will appear.

A situation in which μ_z has elements between the normal states and an excited group of states can be obtained by inverting the energy levels of our first example, so that the $(ns\sigma)^2\Sigma$ state lies above the $ns\sigma n'p\pi\Pi$ and $ns\sigma n'p\sigma\Sigma$ states, as is shown in Fig. 2(b). Eq. (11) then holds only if ν_3 is small compared to kT/h, so that there is no difference in the concentrations of the molecules in the $ns\sigma n'p\pi\Pi$ and $ns\sigma n'p\sigma\Sigma$ states.[28] The second term of Eq. (11) is then due to molecules in the latter state, the first and third to those in the former.

[27] R. S. Mulliken, Rev. Mod. Phys. **4**, 1 (1932).

[28] A weight factor 1/3 should be included in Eq. (11) in this case. There will also be a paramagnetic term; however it is of no interest for our purposes.

However if the II state is the higher of the two, that is if ν_3 is positive and large compared to kT/h, the first and third terms vanish and we are left with a negative B term. A negative B term is also obtained if the Σ state is the higher.

In our examples the effect of magnetic interactions between two excited levels is to give, when $\nu<\nu_1, \nu_2$ or $\nu>\nu_1, \nu_2$, two B terms which, although they are of opposite sign, give a net rotation which is positive; when $\nu_2<\nu<\nu_1$, two negative B terms. The effect of interaction between the normal state and an excited state of frequency ν_3 is to give a negative B term when $\nu<\nu_1$, a positive term when $\nu>\nu_1$. Negative B terms may account for the negative rotation of $TiCl_4$.

It is of some interest to calculate the rotation under the assumption that all excited levels lie in the same group. Suppose the electric moments have elements only between the normal states, n, k, and a group of states, n', k', having the same n'. Under this hypothesis the second sum of Eq. (10) vanishes, and the teilmatrices appearing in the remaining terms can be replaced by the complete matrices (the spur, of course, is still taken only over the normal states). The third sum of Eq. (10), and the second and third terms of the first sum, are zero in virtue of the commutability of the coordinates. On summing over all electrons we have

$$\begin{aligned} P_x\mu_z P_y - P_y\mu_z P_x &= -(e^3/2mc)\sum_{ijk} x_i(x_j p_{yj} - y_j p_{xj})y_k - y_k(x_j p_{yj} - y_j p_{xj})x_i \\ &= -(e^3/2mc)\sum_{ijk} x_i x_j(p_{yj}y_k - y_k p_{yj}) + y_k y_j(p_{xj}x_i - x_i p_{xj}) \\ &= -(e^3 h/4\pi mci)\sum_{ij}(x_i x_j + y_i y_j) = -(eh/4\pi mci)(P_x^2 + P_y^2). \end{aligned}$$

Adding the terms obtained by cyclic interchange of x, y, z, we find

$$V = \frac{4\pi eN\nu^2}{3hmc^2}\,\frac{\nu(n'n)}{(\nu^2 - \nu(n'n)^2)^2}\,\frac{1}{g}\sum_{kk'}|\,P(nk;\,n'k')\,|^2,$$

which is just the normal Verdet constant.

§6. Rotation Near an Absorption Line

Going back to Eq. (6) we see that when ν is close to one of the $\nu(n'n)$ the rotation is

$$V = 2CB\sum_{m,m'}\frac{\nu(n'n)\nu^{(1)}(n'm';\,nm)\,[P_x(nm;\,n'm')P_y(n'm';\,nm)]}{(\nu^2 - \nu(n'n)^2)^2}\,e^{-W_n/kT}, \quad (13)$$

for, since this term contains $1/(\nu^2-\nu(n'n)^2)^2$ rather than $1/(\nu^2-\nu(n'n)^2)$, it is very much larger than all the others. The rotation thus depends only on the Zeeman effect, the perturbation of the amplitudes being negligible.

Rotation in iodine

The iodine lines observed by Wood[29] come from a $^3\Pi_0 - {}^1\Sigma$ transition, and so exhibit no Zeeman effect if we use the "rigid molecule" approximation. Actually, the Zeeman effect, and consequently the optical rotation, is due to rotational distortion, that is, to the effect of molecular rotation in uncoupling the spin from the nuclear axis of figure. The suggestion that rotational distortion is responsible for the behaviour of iodine was originally made by Kemble,[30] but an adequate mechanism was lacking, as at the time the transition was mistakenly classified as $^1\Sigma - {}^1\Sigma$. Kemble supposed that the orbital moment, rather than the spin moment, was uncoupled by the molecular rotation, but it now seems much more probable that spin uncoupling is the preponderant effect.

We shall use the rotating system of axes, x', y', z', previously employed by Van Vleck;[31] the z component of the spin in fixed axes is given in terms of this rotating system by

$$s_z = s_{y'} \sin\theta + s_{z'} \cos\theta,$$

θ denoting the angle between the axis of figure of the molecule and the fixed axis z. The term involving $s_{z'}$ gives the spin part of the ordinary rigid molecule Zeeman effect. In our case this just cancels the effect of the orbital angular momentum, since $\Omega=0$ in the $^3\Pi_0$ state; we shall not be further interested in this term. The matrix $s_{y'} \sin\theta$ can be written

$$(s_{y'} \sin\theta)(\sigma_s jm; \sigma_s' j'm') = 2s_{y'}(\sigma_s\sigma_s') L(\sigma_s jm; \sigma_s' j'm').$$

The elements $L(\sigma_s jm; \sigma_s' j'm')$ are defined and evaluated in a paper by Rademacher and Reiche.[32] As the multiplet separations of the $^3\Pi_0$ state of iodine are very wide, only the first order perturbation of s_z by the molecular rotation is required. This is given by a formula similar to Eq. (7), from which we find for the diagonal elements of $s_z^{(1)}$, when $\Omega=0$, $\sigma_l=1$,

$$\begin{aligned} s_z^{(1)}(-1jm; -1jm) &= 2H^{(1)}(-10)L(0jm; -1jm)s_{y'}(0-1)/h\nu(-10) \\ &\quad + 2L(-1jm; 0jm)s_{y'}(-10)H^{(1)}(0-1)/h\nu(-10) \\ &= 4H^{(1)}(-10)L(0jm; -1jm)s_{y'}(0-1)/h\nu(-10), \end{aligned}$$

since all the quantities involved are real.

It is convenient to write $s_z^{(1)}(\sigma_s jm; \sigma_s' j'm')$, $L(\sigma_s jm; \sigma_s' j'm')$, and $\nu(\sigma_s\sigma_s')$ in terms of Ω rather than σ_s. The elements appearing above are, in this notation, $s_z^{(1)}(0jm; 0jm)$, $L(1jm; 0jm)$ and $\nu(01)$. We then have[33]

$$s_{y'}(\sigma_s; \sigma_s \pm 1) = \tfrac{1}{2}[S(S+1) - \sigma_s(\sigma_s \pm 1)]^{1/2};$$

$$H^{(1)}(\sigma_s; \sigma_s \pm 1) = b[j(j+1) - \Omega(\Omega \pm 1)]^{1/2}[S(S+1) - \sigma_s(\sigma_s \pm 1)]^{1/2};\ b = h^2/8\pi^2 Mr^2;$$

$$L(1jm; 0jm) = -m/2[j(j+1)]^{1/2};$$

and from these

$$s_z^{(1)}(0jm; 0jm) = -2bm/h\nu(01).$$

[29] R. W. Wood and G. Ribaud, Phil. Mag. **27,** 1009 (1914).

[30] E. C. Kemble, Bull. Nat. Res. Council 57: Molecular Spectra in Gases, Chap. VII.

[31] J. H. Van Vleck, Phys. Rev. **33,** 467 (1929). The primed and unprimed systems of his Eq. (5) will be interchanged, to accord with our previous notation. We shall follow this paper in our choice of phases for $H^{(1)}$ and $s_{y'}$, and in notation: σ_l will denote the component of angular momentum along the figure axis, σ_s the component of spin along the figure axis, $\Omega=\sigma_l+\sigma_s$.

[32] H. Rademacher and F. Reiche, Zeits. f. Physik **41,** 453 (1927). See Eq. (13) and the table on p. 475.

[33] Van Vleck, reference 31, Eqs. (30) and (31). From Rademacher and Reiche's table we find $L(1jm; 0jm) = |m|/2[j(j+1)]^{1/2}$. The minus sign must be taken when $m>0$ to match Van Vleck's phases for $H^{(1)}$ (see Van Vleck's footnote (25)).

Using the fact that $L(1jm;\,0jm) = L(-1jm;\,0jm)$, it is readily verified that the same result is obtained when $\sigma_l = -1$.

Thus for our ${}^3\Pi_0 - {}^1\Sigma$ transition

$$\nu^{(1)}(j'm';\,jm) = -4\beta bm'/h^2\nu(01),$$

β being the Bohr magneton number.

The elements of the electric moment appearing in Eq. (13) are the familiar amplitudes of the symmetric top, given, for example, by Kronig.[34] The terms different from zero are

$$[P_x(j, m; j+1, m \pm 1)P_y(j+1, m \pm 1; j, m)] = \mp \frac{iP^2}{2} \frac{(j \pm m + 2)(j \pm m + 1)}{(2j+1)(2j+3)},$$

$$[P_x(j, m; j-1, m \pm 1)P_y(j-1, m \pm 1; j, m)] = \mp \frac{iP^2}{2} \frac{(j \mp m + 2)(j \mp m + 1)}{(2j+1)(2j+3)},$$

where $P^2 = |P_{y'}({}^1\Sigma, {}^3\Pi_0)|^2$.

The rotation is found by substituting these expressions in Eq. (13) and summing over all values of m, the result being multiplied by two, since the two upper states, $\sigma_l = \pm 1$, contribute equally to the rotation. In this way we obtain

$$V = -\frac{8\pi c b \nu_1 P^2 \nu^2 B e^{-W_j/kT}}{hmc^2\nu_2(\nu^2 - \nu_1^2)^2} \sum_{m=-j}^{j} \frac{(m+1)(j+m+2)(j+m+1)}{(2j+1)(2j+3)} - \frac{(m-1)(j-m+2)(j-m+1)}{(2j+1)(2j+3)},$$

with $\nu_1 = \nu({}^3\Pi_0, {}^1\Sigma)$, $\nu_2 = \nu({}^3\Pi_0, {}^3\Pi_1)$ (i.e., $\nu(01)$ in our previous notation), for the R branch, and an analogous expression for the P branch. Performing the summations,

$$V = \mp \frac{16\pi c b \nu_1 P^2 \nu^2 B e^{-W_{j\pm1}/kT} j(j+1)}{3hmc^2\nu_2(\nu^2 - \nu_1^2)^2}.$$

j here is the j of the ${}^3\Pi_0$ level; the minus sign is to be taken for the R branch, the plus for the P. Our theory thus agrees with Wood's observations in giving positive (normal) rotations for the lines of the P branch, and negative (abnormal) rotations for the R branch.

Magnetic rotation spectra of the alkalis

The calculation of the rotations in the alkali vapours is similar. The lines observed by Wood and Loomis[35] are ${}^1\Pi - {}^1\Sigma$ transitions. Here the Zeeman effect is given by the well-known formula $W^{(1)}(\Lambda jm) = \beta\Lambda^2 m/j(j+1)$. We have

[34] Kronig, reference 3. The phases we use are

$$P_{y'}(\Omega, j, m;\,\Omega', j', m \pm 1) = \pm iP_{x'}(\Omega, j, m;\,\Omega', j', m \pm 1).$$

[35] F. W. Loomis, Phys. Rev. **31,** 323 (1928); Loomis and Nusbaum, ibid. **38,** 1447 (1931); **39,** 89 (1932).

$$v^{(1)}(1j'm';0jm) = \beta m' \quad hj'(j'+1),$$

$$|P_x(j,m;j-1,m\mp1)P_y(j-1,m\mp1;jm)| = \pm\frac{iP^2}{2}\frac{(j-1)(j\pm m)(j\pm m-1)}{j(2j-1)(2j+1)},$$

$$|P_x(j,m;j+1,m\mp1)P_y(j+1,m\mp1;jm)| = \pm\frac{iP^2}{2}\frac{(j+2)(j\mp m+2)(j\mp m+1)}{(j+1)(2j+1)(2j+3)},$$

$$|P_x(j,m;j,m\mp1)P_y(j,m\mp1;jm)| = \pm\frac{iP^2}{2}\frac{(j\mp m+1)(j\pm m)}{j(j+1)},$$

$$P^2 = |P_x(^1\Sigma,\ ^1\Pi)|^2.$$

The rotations are, in terms of the j of the normal state,

$$\Gamma = \frac{4\pi c\nu_1 P^2\nu^2 Be^{-W_j/kT}f(j)}{3hmc^2(\nu^2-\nu_1^2)^2},$$

$$f(j) = (j+2)(j+1) \qquad R \text{ branch},$$

$$f(j) = -(j-1)j \qquad P \text{ branch},$$

$$f(j) = (2j+1)j(j+1) \quad Q \text{ branch},$$

$$\nu_1 = \nu(^1\Pi,\ ^1\Sigma).$$

The signs of the rotations of the R and P branches are just opposite those found for iodine. These signs are confirmed by Wood's observations of the rotation in Na_2.

It may seem a little surprising that, aside from the Boltzmann factor $e^{-W_j/kT}$, the rotations of the P and R branches are nearly independent of j when j is large. However it must be remembered that although the over-all width of the Zeeman pattern decreases as $1/j$, the number of components increases linearly with j. The angle of rotation is small, only a few degrees, hence the intensities, which are proportional to $\sin^2\theta$, vary with j approximately as $\{f(j)e^{-W_j/kT}\}^2$.[36] As the intensities in the absorption spectrum vary as $(2j+1)e^{-W_j/kT}$, the intensities of lines of large j in the P and R branches of the magnetic rotation spectrum are weighted adversely, as compared to the absorption spectrum, by a factor $e^{-W_j/kT}/(2j+1)$, and so are, comparatively, greatly reduced. It is perhaps worthy of remark that the intensity of the rotation spectrum is proportional to the square of the density, rather than the first power. The intensities of the Q branch decrease much more rapidly than those of the R and P branches, which accounts for the fact that the Q branch is not observed in the rotation spectrum. For small j the R branch is considerably more intense than the P. This, together with the piling up of the R lines at the heads of the bands, explains why sometimes the R branch alone is observed. The present theory is thus adequate to account for the principle characteristics of the magnetic rotation spectrum.

I am deeply indebted to Professor J. H. Van Vleck, under whose direction this work was done.

[36] It should be noted that, since the separations between lines increase with j, the density of lines on a photographic plate will decrease even more rapidly than the intensities.

Experiments on the Nature of Ferromagnetism

By FRANCIS BITTER
Westinghouse Research Laboratories, East Pittsburgh, Pennsylvania

(Received May 31, 1932)

Irregularities in the magnetization of ferromagnetic crystals were studied by means of magnetic Fe_2O_3 particles about 1μ in diameter suspended in ethyl acetate. On iron crystals the particles settle along parallel lines spaced about 0.1 mm apart and more or less at right angles to the applied field. On nickel crystals the pattern is similar, but the lines split up into more complicated structures as the applied field is increased. On cobalt crystals straight lines are obtained on some crystals, and spotty patterns on others. The spots arrange themselves in rows when the crystals are magnetized. The patterns can be destroyed by relatively slight surface strains. There is some evidence that in the straight line patterns the direction of the lines is related to the direction of magnetization. An explanation of these effects is not known.

THE object of the experiments described below was to find any irregularities or inhomogeneities that exist in the magnetization of ferromagnetic crystals.

APPARATUS AND MATERIALS

The method used was the old magnetic powder method. In order to reveal small details, the particles must be small and have as large a magnetic moment as possible without causing them to form chains in the direction of the magnetic field. They must further be suspended in some medium that will allow them to settle according to the pattern of the field. Particles of red Fe_2O_3 having diameters in the neighborhood of 1μ were found very satisfactory.[1] These were suspended in ethyl acetate, which, because of its low viscosity, allows the particles to settle fairly rapidly and without undue disturbance from currents in the liquid. Observations were made by magnetizing a flat sample in the direction of its length and placing a drop of the suspension on the surface of the crystal to be investigated. In order to be certain that the patterns obtained were determined by the sample investigated rather than by the interaction of the Fe_2O_3 particles, observations were made with particles of different size, and of different substances suspended in various liquids, and with no liquid at all. In all cases the same patterns were observed.

A few samples of iron were prepared by elongating small annealed slabs about 3 percent and annealing in hydrogen just below the $\alpha-\gamma$ transformation point. This material was very pure, having a total impurity before the above treatment of about 0.01 percent, chiefly Si. Some samples were ground flat and annealed. All other samples were made by melting in alundum troughs in an electrically-heated alundum tube furnace through which purified dry hydrogen flowed continuously. In order to observe the effects re-

[1] F. Bitter, Phys. Rev. **38**, 1903 (1931).

ported below, it is desirable to have a shiny, smooth, unstrained surface. Hydrogen was used to prevent surface tarnish due to oxidation. Considerable hydrogen was absorbed while the samples were molten, and given off during solidification, producing cavities in the ingots and locally imperfect surfaces. In most cases, however, at least a part of the sample was satisfactory.

I should like to express my indebtedness to various members of the Laboratories for their assistance—to Mr. L. McCulloch for preparing the Fe_2O_3 powder; to Dr. V. Hicks for making an x-ray examination of this powder; to Miss M. Ferguson for taking the best of the photographs reproduced below; to Mr. P. G. McVetty for stretching the strain-annealed samples of iron; and especially to Mr. A. A. Frey, who built the furnaces and prepared most of the samples investigated.

Results

Iron

In a sample of iron having small grains, whether annealed or not, irregular patterns are found. The deposits do not follow any obvious structural features, such as grain boundaries. If, however, the grains are somewhat larger, and unstrained, deposits like that shown in Fig. 1 are formed, which, for larger fields, degenerate into irregular patterns. In Fig. 1 some of the

Fig. 1. Deposit on a sample of 4 percent Fe-Si with large grains. Field horizontal. Approximate magnification ×2. Deposits are black in all photographs.

grains are crossed by systems of parallel lines more or less at right angles to the direction of the applied field. The lines are not spaced perfectly evenly, but are of the order of 0.1 mm apart. Fig. 2 shows the deposit obtained near a grain boundary on an Fe-Si sample, and Fig. 3 shows the slip lines obtained on a similar sample after a slight reduction by cold rolling. The similarity is rather striking. In both cases there is a tendency for the lines to continue in a changed direction after crossing a grain boundary.

In general, the deposits on iron are indefinite, and it often occurs that no regular patterns are observed at all. Better results were obtained with an alloy containing 4 percent Si than with pure iron. An attempt was made to determine how the pattern changed as the direction of magnetization was

varied. As a rule the pattern was obscured, but on several crystals three sets of lines were observed all told. Further observation is required to establish the generality of this result.

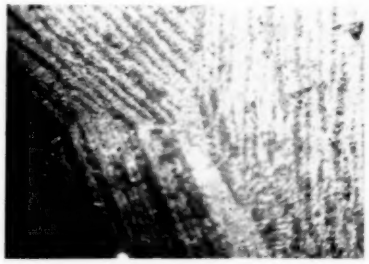

Fig. 2.

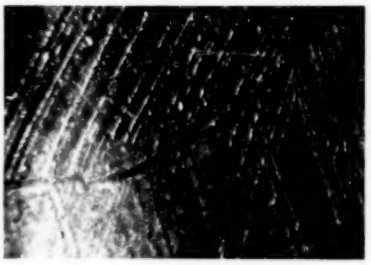

Fig. 3.

Fig. 2. Deposit on a 4 percent Fe-Si sample near a grain boundary. Field horizontal. Approximate magnification ×10.

Fig. 3. Slip lines in a 4 percent Fe-Si sample. Approximate magnification ×10.

Cobalt

Typical deposits on cobalt are shown in Figs. 4–6. These illustrate the state of affairs before a magnetic field is applied. In Fig. 4 the spots vary a good deal in size. Fig. 5 shows grain boundaries, and the tendency for the

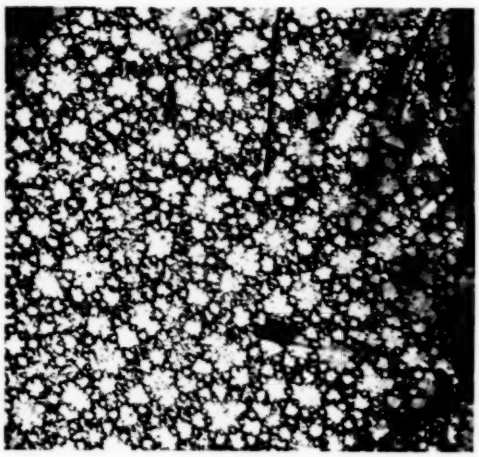

Fig. 4.

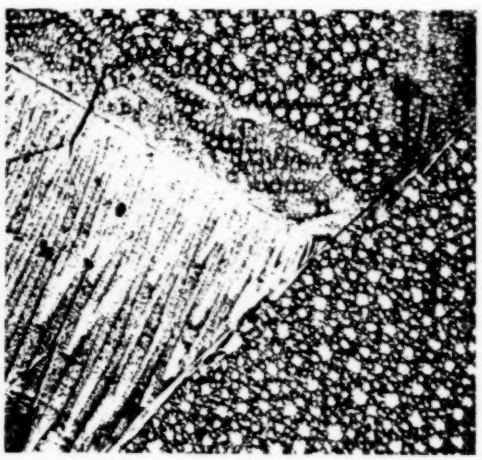

Fig. 5.

spots to form a hexagonal array. Also a grain having a straight line pattern is shown. Fig. 6 shows transition patterns between the spotty and the straight line types. Just what difference exists between samples showing different patterns is not known. One sample containing 20 percent of iron showed no pattern whatsoever. Until further evidence is obtained, we may make the reasonable assumption that the irregularities are produced by strains, impurities, or other imperfections. In Figs. 7–9 the effect of magnetization on

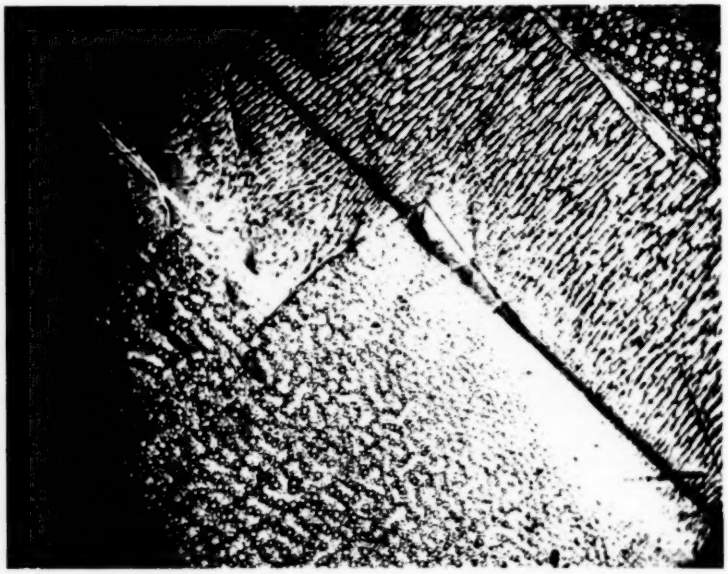

Fig. 6.

Fig. 4–6. Deposits on unmagnetized cobalt crystals. Magnification approximately ×70.

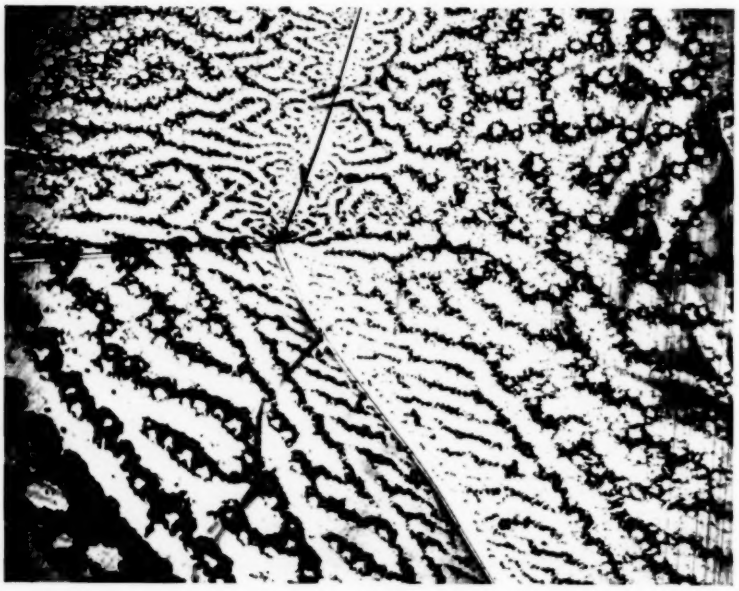

Fig. 7. Deposit on magnetized cobalt near a grain boundary. Approximate magnification ×80.

the spotty type of deposit is shown, the magnetization being stronger in Fig. 9 than in Fig. 8. Fig. 7 shows the distorting effect of the grain boundary. The line pattern illustrated in Fig. 5 is affected little if at all by magnetization, and has in no case been observed to change its direction on the crystal surface as the direction of the applied field was varied.

Fig. 8.

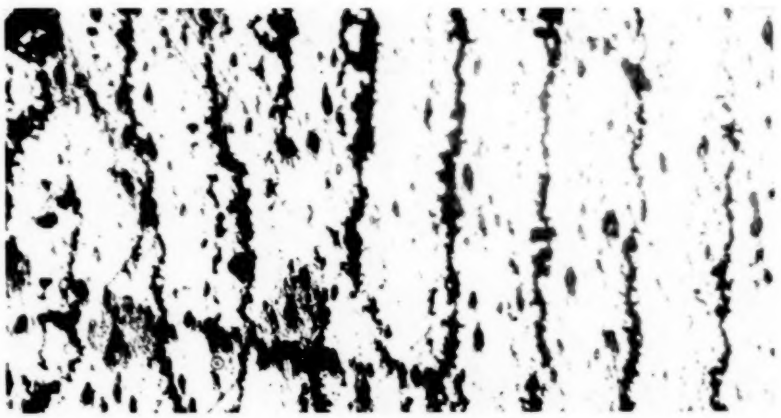

Fig. 9.

Fig. 8 and 9. Deposits on a magnetized cobalt crystal. Approximate magnification ×160.

Nickel

A typical deposit on nickel before being exposed to any magnetic field other than that of the earth is shown in Fig. 10. On magnetization the patterns become more definite, as shown in Figs. 11a and 11b. Sometimes the lines are curved, especially near grain boundaries, and sometimes they show a break as is the case for one of the lines in Fig. 10. It quite often happens that the spacing of the lines changes progressively from one side of a crystal to the other, as can be seen in Fig. 11a. These lines are not associated with

fixed places in a crystal. This is illustrated in Fig. 12 in which photographs of three different deposits on the same region are superposed. It seems quite generally true that the position of the lines changes after demagnetization.

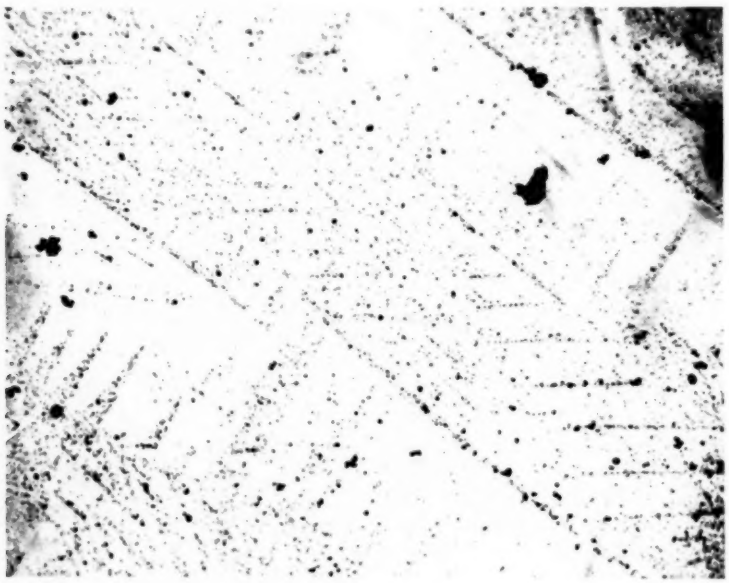

Fig. 10. Deposit on a nickel crystal before magnetization. Approximate magnification ×80.

Some samples in the shape of disks were prepared, and magnetized in eight directions at 45° intervals. The deposits were photographed and the total number of directions in which lines appeared was determined for five crystals.

a b

Figs. 11a and 11b. Typical deposits on nickel with the applied field acting in a horizontal direction. Approximate magnification ×65.

In each case the lines appeared in four directions all told. In those positions in which two such directions made nearly equal angles with the applied field chevron patterns like that shown in Fig. 13 appeared.

If successive patterns are obtained in the same region in gradually increasing fields without demagnetization between observations, the phenomenon shown in Fig. 14 is found. The wavy marks on the photographs are surface irregularities that are of no interest here except insofar as they may be used as a reference system fixed in the crystal. In the twelve photographs shown the applied field increases progressively, being smallest in 1 and largest in 12. The position of the lines as shown in the first photograph does not change radically. The lines, however, split up as the magnetizing field is increased, first into two, then four, and on the original photograph, No. 12, each of the original lines is seen to consist of eight components. In addition a new line appears between each of the main groups in photograph No. 7 and splits into two components also. The smallest splitting here shown is deter-

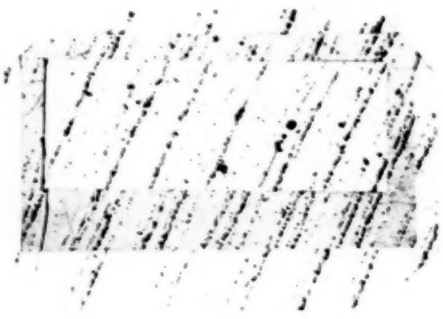

Fig. 12. Superposed photographs of deposits obtained on the same region at different times, the sample being demagnetized after each observation.

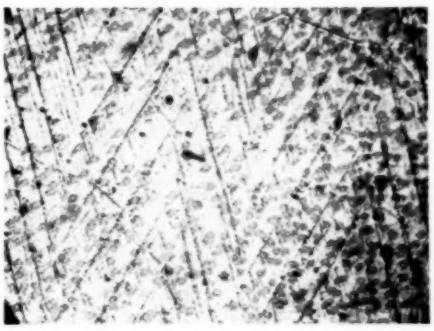

Fig. 13. Peculiar pattern obtained on a nickel crystal.

mined by the method, and it seems very probable that much more detail exists than is here indicated. To obtain these results it is essential not to demagnetize the sample between observations. The sample consisted of crystals having linear dimensions of from 1 to 4 cm imbedded in a large slab, 27 cm$\times$4 cm$\times$1 cm. It was consequently possible to measure only the intensity of magnetization of the aggregate. This was done with a fluxmeter and the value of $I = 350$ or about 75 percent of saturation was obtained for the conditions under which deposit No. 12 was produced. Magnetization of this intensity is confined to the directions of easiest magnetization within the crystal.

Alloys containing 10 percent, 20 percent, and 30 percent of iron were prepared by melting and slow cooling. That containing 10 percent of iron showed patterns typical of nickel, but less distinctly than usual. No patterns whatsoever could be found on the other samples.

The effects are exceedingly sensitive to strain. Some samples that were lightly pressed by a C-clamp no longer gave any patterns, nor was anything to be found on polished samples until they had been annealed.

Discussion

If it is quite generally true, as has been found in a few cases, that the line patterns can appear in three directions in iron, in four directions in nickel, and in only one direction in cobalt, it seems reasonable to assume that they are somehow related to the three (100) axes in iron, the four (111) axes in nickel, and the single (0001) axis in cobalt. This assumption is supported by

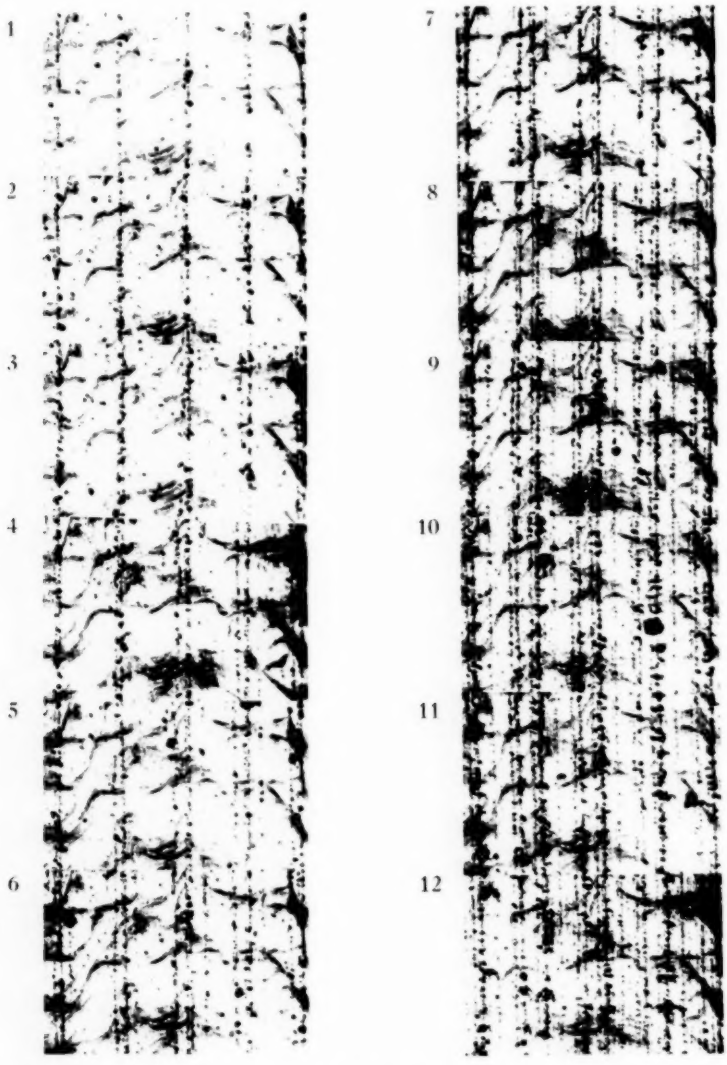

Fig. 14. Twelve photographs of the same region, the applied field being gradually increased between observations.

the fact that in each case the axis mentioned has a special significance magnetically—it is the direction of easiest magnetization within the crystal. Taking into consideration the above material, and the fact that the lines are

sometimes curved or broken, we suggest the hypothesis that inhomogeneities occur along planes perpendicular to the direction of magnetization, and that the lines observed are parallel to the intersection of such planes with the surface under observation. In the fields used the direction of magnetization probably differed in no case appreciably from the direction of easiest magnetization. The above hypothesis fits into the observation that in nickel and cobalt alloying tends to destroy the pattern, for the effect of a foreign substance must, as a rule, be to introduce local fluctuations in the direction and intensity of magnetization. This reasoning can be applied to the observations on iron if we suppose that it is exceptionally difficult to produce a satisfactorily uniform crystal of iron, and that the addition of silicon tends to remove certain imperfections. The above discussion does not take into account the spotty pattern obtained on certain cobalt crystals. It seems likely that this is more complicated in its origin, and occurs whenever the hexagonal axis is normal to the surface of the crystal.

From the observations so far made, it is not possible to determine the nature of the inhomogeneities revealed. They may be changes in direction or intensity of magnetization, or both. Bearing in mind that in this discussion a change in direction, to be detected as such, must cover a region large compared to 1μ, it is probable that we have to do with changes in direction in cases like that shown in Fig. 13, but that in patterns like that shown in Fig. 11 there is only a change in intensity. It is most important to settle definitely the nature of the inhomogeneities by further and more detailed observations.

The origin of the patterns obtained is of course even more obscure. The conception is current that ferromagnetic crystals are made up of spontaneously magnetized regions whose directions of magnetization are distributed among the various energetically possible orientations. Magnetization is then supposed to result partly from a growth of some of these regions at the expense of their neighbors,[2] partly from changes in the direction of magnetization of each region. It seems a little difficult to fit this picture into the above photographs unless the regions are smaller than 1μ. The secondary structures suggested by Zwicky[3] offer a different attack on the problem. Finally, we must remember that a crystal consists of atoms in different excited states, that the various periodic motions which its constituent atoms and electrons perform most probably are coupled together in a variety of ways, and that in addition there must be a certain amount of electromagnetic radiation present. Any of these factors may have an influence in determining the equilibrium configuration of a crystal, and it is perhaps the most important aspect of experiments such as the above to furnish evidence from which conclusions on these points may eventually be drawn.

[2] F. Bloch, Zeits. f. Physik. **74,** 295 (1932).
[3] F. Zwicky, Phys. Rev. **38,** 1772 (1932).

Thermoelectric Power of Single Crystal Bismuth Near the Melting Point

By ADOLF SOROOS
Physical Laboratory, University of Iowa

(Received June 14, 1932)

By investigating directly the thermoelectric power of bismuth single crystals near the melting point a transition region is found in which the thermoelectric power changes gradually from that characteristic of the solid to that characteristic of the *final* liquid state. The region extends from the melting point to about 8° above it. As an explanation it is supposed that a definite crystal structure persists into the liquid state.

INTRODUCTION

IN measuring the thermal e.m.f. of bismuth single crystals against constantan as a reference metal, Boydston[1] found certain irregularities in the e.m.f.-temperature curves in the region just beyond the melting point. As an explanation he says, "It appears, in fact, as if some crystalline arrangement still persists in the molten metal as shown by a transition region between the thermal e.m.f. of solid and liquid."

Goetz[2] makes use of a similar explanation for certain effects observed in his study of the factors influencing the growth and perfection of bismuth crystals. He found that if he used a seed crystal with regions of twinning to inoculate a molten rod he would invariably obtain a crystal which still showed the twin orientation unless he melted the seed back considerably beyond the region of twinning so that this region was at a much higher temperature than the melting point. He also found that a polycrystalline rod melted and raised to a temperature just slightly above the melting point, recrystallized, on cooling, into a rod which had the "same position and same orientation of the prominent crystal elements" as the original rod. If he heated the specimen considerably above the melting point, however, he found an entirely new arrangement on recrystallization.

Although Boydston observed only slight deviations of thermal e.m.f. from what is expected on the basis of an abrupt change at the melting point, it is obvious that these deviations must be accompanied by relatively large changes in the derived thermoelectric power curve. For this reason it seemed advisable to investigate directly the thermoelectric power of bismuth crystals over a temperature range extending on both sides of the melting point with the hope of definitely establishing the phenomenon foreshadowed by Boydston.

The method devised to do this consists in measuring the thermal e.m.f. over a small temperature interval at successive mean temperatures in the

[1] R. W. Boydston, Phys. Rev. **30**, 911 (1927).
[2] A. Goetz, Phys. Rev. **35**, 193 (1930).

desired region. The observed e.m.f. divided by the temperature interval gives directly the mean thermoelectric power at the mean temperature. By use of a small enough temperature interval the resolution can be made sufficiently high to justify considering this mean thermoelectric power as the actual.

Apparatus and Method

The experimental arrangement is shown in Fig. 1. The bismuth crystal, *BB*, has its ends fused to two copper blocks, *AA*. In fusing, the copper surface is cleaned with a flux ($ZnCl_2$) and then with the end of the crystal pressed lightly against the block, the latter is heated until the bismuth just begins to melt. A little added pressure with the finger tip at this point insures a good contact. The crystal structure is not altered at the junction. Two holes *a*, *b* were drilled into the ends of each copper block, with the bottoms of the holes separated from the surface onto which the bismuth was fused by a thickness of copper of about 0.5 mm. Into the holes, *aa*, were inserted the two junctions of a constantan—copper thermocouple which measured the difference in temperature of the two ends of the bismuth rod. These junctions were en-

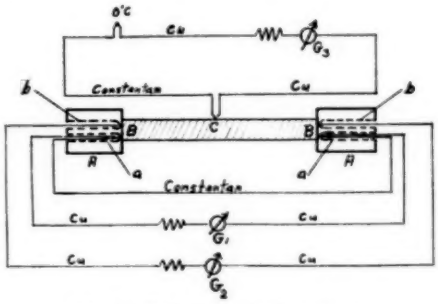

Fig. 1. Diagram of apparatus.

closed in small Pyrex glass tubes, the copper and constantan wires being separated by thin strips of mica. To the bottoms of the holes, *bb*, were silver soldered copper wires which completed the bismuth-copper thermal e.m.f. circuit. These wires were insulated from the side walls of the holes by small Pyrex tubes. This latter procedure was necessary in order to make sure that the effective junctions of this bismuth-copper couple should be at the surface of separation between the copper block and bismuth crystal. A second copper-constantan circuit had one junction placed at *C*, the other junction being maintained at zero degrees.

The electrical circuits are also pictured in Fig. 1. The reading of the galvanometer, G_1, is proportional to the temperature difference between the ends of the bismuth crystal, the reading of galvanometer, G_2, is proportional to the e.m.f. of the bismuth-copper circuit, and the reading of the galvanometer, G_3, is proportional to the mean temperature of the crystal.

The crystals were grown by a method similar to that described by Kapitza.[3] A groove[4] in an asbestos block was used for a mold. Crystals were

[3] P. Kapitza, Proc. Roy. Soc. **A119,** 358 (1929).

[4] The cross section was almost V-shaped, but with a rounded bottom.

grown of three brands of bismuth, Mallinckrodt C.P.,[5] a special silver-free[6] and Kahlbaum's best.

The results given below are for only the first brand, preliminary work[7] having shown no essential difference in the behavior of the others. The crystals were about 0.5 cm^2 in cross section and either 10 or 20 cm long. The longer ones were cut in half and a separate determination made on each piece.

In making a determination the crystal was put into an asbestos holder and placed in a horizontal furnace. The temperature gradient in the furnace was so controlled by auxiliary coils that the temperature difference between the ends of the crystal could be kept at about 1°C. The furnace temperature was allowed to pass slowly through the region under investigation. The time required to take the crystal through the desired temperature range (260° to 290°C) was about one hour.

Results and Discussions

Measurements were made on six single crystals ranging in orientation[8] from 29° to 69°. These results are shown in Fig. 2. All crystals at a temperature sufficiently above the melting point, (i.e., in the region 280°–290°) showed a constant thermoelectric power against copper of 4.5 microvolts per degree (within 1 microvolt per degree). This has therefore been taken as a zero point and the ordinates of the curves depict the excess values above this constant level. While the curves are plotted against mean temperature, this is not obtained directly from the readings of the thermocouple, *C*, Fig. 1. This couple could not be placed in thermal contact with the crystal, and while for any one crystal it is believed that its readings give a correct measure of the rising temperature these readings may differ from the actual temperature of the center of the crystal by a presumably constant and small but undetermined amount. The observed curves have therefore been so adjusted in plotting Fig. 2 that they agree in mean temperature at the point where the final constant value is reached. This adjustment does not amount for any crystal to more than about 2° difference between the adjusted temperature scale and the indication of thermocouple, *C*, Fig. 1. The location of the melting point (271°C) as shown on the figure actually coincides with the reading of thermocouple *C* in the case of the 40° crystal. Moreover, it occurs, for this crystal, about 0.5° above the first sharp break which is then interpreted as coinciding with the beginning of the melting process. For no other crystal is the onset of melting so sharply marked. Even without such an adjustment,

[5] This is the same grade of bismuth that Boydston used and has the same stated analysis. Other work in this laboratory has shown that the silver content may be much less than the 0.04 percent maximum limit.

[6] The writer has to thank the U.S.S. Lead Refinery for this material. The analysis given with it shows: Pb 0.005 percent, Ag 0.0006 percent, Cu, Fe 0.000 percent.

[7] In this preliminary work about fifteen crystals were investigated, the experimental set-up being improved from time to time. As soon as a reliable arrangement was obtained the set of crystals reported on herein was grown and measured. The preliminary results were all in agreement with the final ones in their general characteristics.

[8] Angle between the trigonal axis and the length of the specimen.

however, the general character of the results is unchanged. To avoid confusion, the curves in Fig. 2 are plotted with an arbitrary displacement in the scale of ordinates between successive curves. Four of the crystals were sufficiently long for two determinations to be made, the circles indicating determinations made on the half onto which the nucleus had been fused during growth and crosses indicating the second half of the same crystal.

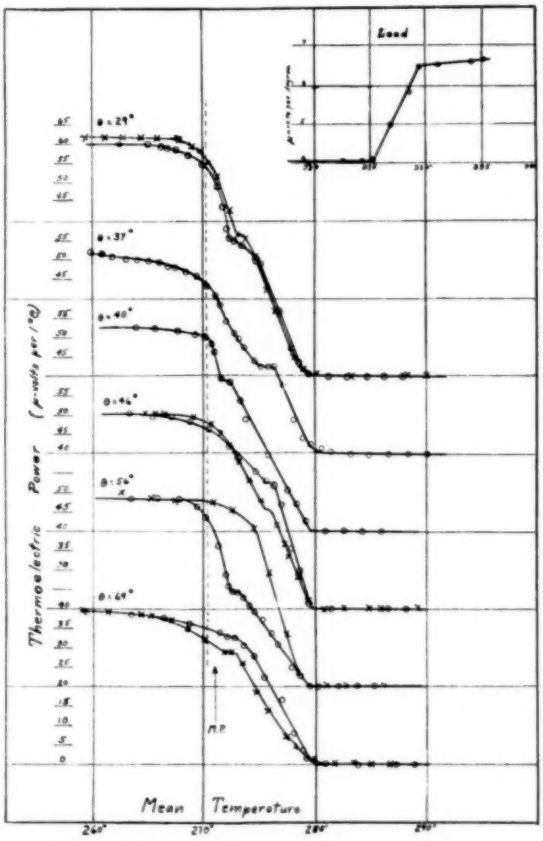

Fig. 2. Thermoelectric power as a function of temperature.

It is clear from Fig. 2 that bismuth is abnormal in its thermoelectric behavior in the region just above the melting point. For most substances which melt at a definite temperature, the thermoelectric power changes abruptly at the melting point or the thermal e.m.f. curve suffers an abrupt change in slope.[9,10] For the crystals shown here, however, the curves before settling down to a practically constant final liquid value pass through a transition region which lasts for approximately 8°C. This is exactly the effect predicted by Boydston. This transition of thermoelectric power, of course, takes place entirely in the liquid state since the crystal is completely melted when the mean temperature (temperature at center of crystal) is 0.5° above 270°, since

[9] E. G. Linder, Phys. Rev. **29,** 554 (1927).
[10] T. R. Harrison and P. D. Foote, J.O.S.A. and R.S.I., **7,** 389 (1923).

the difference in temperature between the two ends of the crystal is only one degree.

On account of the doubt of the exact indication of thermocouple *C* and from the general appearance of the curves in Fig. 2 one might be inclined to believe that the melting process was not complete until the final constant value of the thermoelectric power had been reached and that the observed effect all lies in a region below the melting point and is, therefore, characteristic of the solid and not the liquid state. That this is not the case was verified by an independent experiment. A separate determination was made on a 90° crystal and as all of the curves show a small constant portion shortly after melting, the determination was stopped when that place was reached. The holder containing the crystal was then quickly taken from the furnace, tipped on its side and jarred a little. There was only one possible place where the liquid could seep out through the holder and this was at the position where the thermocouple *C* was inserted. It was found that the liquid had indeed forced its way out and on examining the material remaining in the holder, it was found recrystallized into a changed orientation[11] from what it was at the beginning. This seems conclusive evidence that the transition region belongs to the liquid state.

It seemed desirable also to make a check on the apparatus to be sure that the results obtained were not due to some peculiarity in the apparatus itself. To check this point a determination was made on a specimen of polycrystalline lead. The results of this determination are shown in the curve in the upper right corner of Fig. 2. Since the thermoelectric power of lead against copper is small, a temperature difference between the ends of the specimen of 4°C had to be used in order to obtain a conveniently large galvanometer deflection. This made the resolution much less than that for any of the bismuth crystals. The result obtained for lead, however, is the one to be expected on the assumption of no transition region existing. The thermoelectric power passes directly from the solid value to the liquid value without a change of slope in this region and the temperature interval of this change corresponds almost exactly to the temperature difference of the ends of the lead rod. The fact that the transition is not shown by a line parallel to the ordinate axis, is, of course, due to the finite resolution.

The above results yield incidently a value of *2.6* microvolts per 1°C for the thermoelectric power of solid against liquid lead at the melting point.

As a matter of interest a plot has been made, Fig. 3 of the thermoelectric power of the solid crystals just below the melting point against the square of the cosine of the orientation angle. To do this ordinates were read from Fig. 2 for the value of temperature shown by the dotted line. This is 0.25° below the temperature at which the hotter end of the crystals start to melt. The points lie on a straight line, confirming the Voigt-Thomson relation. This is in agreement with Boydston though at variance with the slight deviation from

[11] Doubtless from tipping and jarring. From Goetz's observation it should remain the same if undisturbed.

the law later found by Bridgman[12] and Fagan and Collins.[13] It does, however, give the writer considerable confidence in the method used to adjust the mean temperature scale. A numerical comparison[14] of Boydston's and the writer's data shows that at the melting point the former obtains:

$$e_{\parallel} - e_1 = 70 \text{ microvolts/degree}^{15}$$

$$e_{\perp} - e_1 = 29 \text{ microvolts/degree}$$

while the writer obtains:

$$e_{\parallel} - e_1 = 65.5 \text{ microvolts/degree}$$

$$e_{\perp} - e_1 = 31.0 \text{ microvolts/degree.}$$

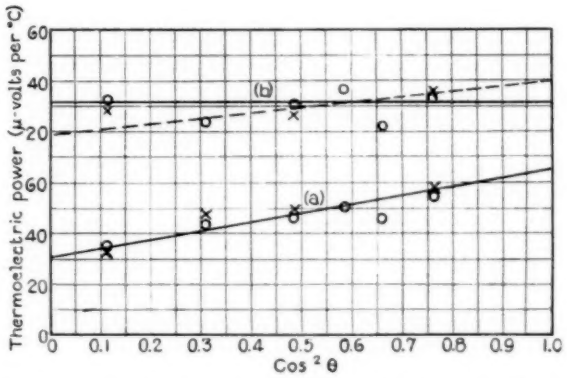

Fig. 3. Thermoelectric power as a function of $\cos^2\theta$. (a) At the melting point. (b) At the *knee* of the curves of Fig. 2.

The results then show that the thermal e.m.f. curve of bismuth does not change its shape as abruptly and in as clearly defined a fashion as in the case of zinc, tin, lead and some other substances. The thermoelectric power before settling down to a final constant value passes through a transition region lasting for a temperature interval of about 8°C above the melting point. Moreover, this settling down is gradual. The curves for differently oriented crystals preserve their individuality for several degrees above the melting point. Although it is only quite close to the final liquid stage that the curves become practically identical there is within the transition region a feature common to all but one of the curves of Fig. 2, namely a slight *knee* or practically stationary value of thermoelectric power. This seems to indicate a definite phase, or intermediate liquid state, existing for a temperature range of about one degree. If this is the case it ought to occur at the same tempera-

[12] P. W. Bridgman, Proc. Amer. Acad. of A. and S. **63,** 351 (1929).

[13] H. D. Fagan and T. R. D. Collins, Phys. Rev. **35,** 421 (1930).

[14] Boydston's values for comparison were obtained by plotting his data for $e_1 - e_\perp$ against $\cos^2\theta$ and then extrapolating the straight line to the ordinates of 0° and 90° crystals.

[15] $e = dE/dT$, the thermoelectric power, E being the thermal e.m.f., e_1 = thermoelectric power of liquid bismuth, $e_{\parallel}$ = thermoelectric power of crystal of 0° orientation, $e_\perp$ = thermoelectric power of 90° crystal.

ture for all the crystals. Although it obviously does not do so its significance can be tested in another fashion. This is shown in Fig. 3b in which the value of the thermoelectric power at the knee is plotted against $\cos^2 \theta$. A definite intermediate liquid phase might be expected to give either (1) a straight line (dotted in the figure) with a positive slope indicating that the liquid is still very much like its *parent crystal* (2) a straight line (solid line in the figure) of zero slope, indicating that an identical state has been reached for all crystals. Unfortunately the observed data do not decide unambiguously between these two suppositions. In spite of this the existence of a knee at all strongly supports the idea of an intermediate state. It may be noted that this knee was also obtained for most of the crystals which were studied in the preliminary work previously mentioned.

The writer believes that the existence of a transition region extending from the melting point to about 8° above it, is established by the foregoing and that the explanation which has already been advanced is adequate to explain this phenomenon. Up to 8° beyond the melting point the liquid retains, but in decreasing measure, the organization of the crystal from which it is derived. Beyond that point the state of the liquid is independent of its previous history. It is practically impossible to think of any state or condition of the liquid, other than that postulated, which could give rise to such a transition region. It must be noted however, that the thermoelectric effect must be particularly well suited to observe this phenomenon as the appearance of a transition region for other properties which depend on crystal orientation has not been observed, so far as the writer knows. W. L. Webster's study[16] of the change in magnetic susceptibility in solidifying bismuth apparently shows no transition region for this quantity of the type shown here, but a sudden change occurring at the melting point. It may be, however, that a degree of organization suitable for modifying the thermoelectric effect may have little effect on susceptibility. Moreover, Webster was looking for an effect said to occur 10° below the melting point and not for one above.

It may be said finally that only x-ray diffraction can give positive and unambiguous proof of the explanation offered to explain the transition region.

The writer wishes to express his most sincere thanks to Professor E. P. T. Tyndall, who suggested the problem and under whose direction the work was carried out.

[16] W. L. Webster, Proc. Roy. Soc. **A133,** 162 (1931).

The Acoustic Resonator Interferometer: II. Ultrasonic Velocity and Absorption in Gases

By J. C. HUBBARD
The Johns Hopkins University

(Received June 13, 1932)

The derivation of the equivalent electric network of the acoustic resonator interferometer in Part I of this paper has made it possible to develop the theory for the current in a simple resonant circuit in which the electrodes of the piezoelectric plate of the interferometer are connected to the terminals of the variable condenser of the circuit. The special case of this theory in which the circuit is excited at a constant frequency determined by the crevasse frequency of the resonator plate in its given situation with respect to electrodes and associated circuit, when the acoustic path in the interferometer is *detuned* and the resonant circuit is tuned so that its resonant maximum occurs at the same frequency, takes an especially simple form and leads to a direct procedure for determination of ultrasonic velocity and absorption in a gas in terms only of current in the resonant circuit and path-length in the interferometer, all circuit and interferometer constants dropping out. The values of current as a function of path-length obtained experimentally are in complete accord with the theory and data for ultrasonic absorption in air and in CO_2 so far obtained are in agreement with the meager data available by other methods. The role of the coefficient of reflection at the fluid-reflector surface is discussed.

I. EXPERIMENTAL OBJECTIVES AND METHODS

THE vibration of a column of fluid of variable length, one end of which is bounded by a vibrating plane face of an electrical vibrator such as a piezoelectric plate, the other end being bounded by a plane reflector parallel to the vibrating face of the plate, has been considered in Part I[1] of the present paper, and the equivalent electric network of the system was there shown to be the same as that of the quartz plate alone with modified resistance and capacity coefficients. Such a system, associated with an appropriate driving circuit, may be termed an acoustic resonator interferometer, and has already been used for the measurement of compressional velocities in liquids,[2,3,4,5] and in gases,[6] of absorption coefficients in gases,[6] and of the modification of velocity in liquids due to scattering.[5] Specific consideration of some of the methods of measurement of absorption in gases and of the role of the reflection coefficient at the boundary of the fluid will be given in the

[1] J. C. Hubbard, Phys. Rev. **38**, 1011–1019 (1931). Part I will be referred to hereinafter as I.

[2] J. C. Hubbard and A. L. Loomis, Phil. Mag. **5**, 1178–1190 (1928); and A. L. Loomis and J. C. Hubbard, J.O.S.A. and R.S.I. **17**, 295–307 (1928).

[3] E. B. Freyer with J. C. Hubbard and D. H. Andrews, Jour. Am. Chem. Soc. **51**, 759–770 (1929). E. B. Freyer, *ibid.* **53**, 1313–1319 (1931).

[4] E. Klein and W. D. Hershberger, Phys. Rev. **37**, 760–774 (1931).

[5] C. R. Randall, Bur. Stand. Jour. Res. **8**, 79–99 (1932).

[6] J. C. Hubbard, Phys. Rev. **35**, 1442 (1930); **36**, 1668–1669 (1930).

present paper. Mr. W. D. Hershberger[7] has presented independently an analysis of the motion of the fluid column and of its reaction on the piezoelectric plate, his treatment being somewhat more restricted than that of the author, particularly in that he does not consider the effects of coefficients of reflection at the fluid-reflector surface of value less than unity.

Among the methods of measurement which have been used, undoubtedly the simplest is that in which the interferometer electrodes are connected to the terminals of a variable condenser which is part of a simple resonant circuit driven by an oscillation generator of suitable frequency. The measurements consist in this case of a determination of current in the resonant circuit as a function of the length r of the fluid column.[2,3,4,6] The current readings pass through sharp maxima (for gases, minima for liquids) or peaks as r is increased, these peaks having been interpreted as marking the value of r, for resonance in the fluid, successive resonant positions of the reflector being one-half wave-length apart. An analysis of this method for gases is given in the present paper.

In a second method, far more sensitive than the first, the interferometer electrodes are connected to a secondary coil coupled to the primary of an oscillation generator. As r is varied a cyclical variation of frequency of the generator takes place which is compensated by the variation of a vernier condenser in parallel with the capacity of the generator, constancy of frequency being assured by using the double heterodyne beat method.[2,3,6] From the variation of vernier condenser readings as a function of r the acoustic behavior of the medium is deduced. The theory of this method will be given in a later paper.

A third method[5] makes use of the current in the leads to the interferometer itself as a function of r, the circuits being otherwise as in the first method described above. Klein and Hershberger[4] report a variety of experiments in which a number of methods were employed, the interferometer system being treated as an impedance in alternating current measurements.

It is essential that the power dissipated in the acoustic system be so small as to produce negligible temperature effects. In practice it has been found possible to reach the limits of accuracy imposed by the sensitiveness of the thermocouple and galvanometer used in the first method with amounts of power several orders smaller than that which is capable of influencing the results. The power necessary in the second method is still much smaller.

The most important factor causing a departure of the acoustic system from that theoretically expected is to be found in the conditions at the electrodes of the piezoelectric plate. This factor need not be considered if the electrodes are of sufficiently small mass and if their attachment to the plate is of such nature as not materially to modify the crevasse. As will be seen the constants of the crystal including the effect of electrode mounting upon the position and shape of the crevasse may be eliminated from consideration in determinations of velocity and absorption.

[7] W. D. Hershberger, J. Acous. Soc. Am. **3**, 263–268 (1931).

II. Method of Forced Vibrations. Ultrasonic Velocity and Absorption in a Gas

As shown in I the acoustic interferometer may be represented by an electric network consisting of a fixed capacity K_1 shunted by a series consisting of the fictitious inductance L, capacity K' and resistance R', where

$$R' = R + AB\rho v P \tag{1}$$

$$1/K' = 1/K + AB\rho v\omega Q \tag{2}$$

R and K being the fictitious series resistance and capacity respectively of the quartz plate itself, A the cross section of the fluid column, B a constant of quartz, and ρ and v, respectively the density of the fluid and the wave velocity in it.

P and Q have the values, in general, with $x=0$ in I, Eqs. (12) and (13), respectively

$$P = \frac{1 - \gamma^3 e^{-4r\alpha} + \gamma(1-\gamma)e^{-2r\alpha}\cos(2r\omega/v)}{1 - 2\gamma^2 e^{-2r\alpha}\cos(2r\omega/v) + \gamma^4 e^{-4r\alpha}} \tag{3}$$

$$Q = \frac{\gamma(1+\gamma)\sin(2r\omega/v)}{1 - 2\gamma^2 e^{-2r\alpha}\cos(2r\omega/v) + \gamma^4 e^{-4r\alpha}} \tag{4}$$

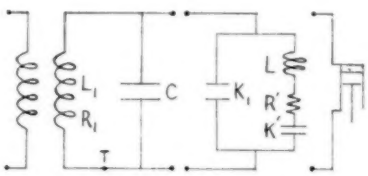

Fig. 1. Resonator circuit with interferometer replaced by its equivalent electric network.

where α is the attenuation factor of particle velocity in the fluid and is equal to one-half the coefficient of absorption, and γ is the coefficient of reflection of particle velocity between the fluid and the reflecting plate. The distance r is that between the vibrating plate and the reflector, i.e., the length of the fluid column.

Let the electrodes of the piezoelectric plate be connected to the terminals of the variable condenser C of the resonant circuit L_1, R_1, C, Fig. 1. The resistance R_1 includes the resistance of the vacuum thermocouple T which is inserted between C and L_1 on the grounded side of the interferometer. Let the inductance L_1 be loosely coupled to the output of an oscillation generator which may be kept at any desired frequency, so that in L_1 we have the induced e.m.f., $E = E_0 e^{i\omega t}$. We have for the impedances of the various branches of the circuit, putting $\theta = j\omega$: $Z = L_1\theta + R_1$; $Z_1 = 1/K_1\theta$; $Z_2 = L\theta + R' + 1/K'\theta$; $Z_3 = 1/C\theta$.

Solving for i_0, the amplitude of current in the L_1R_1 branch, including the thermocouple heater, we have

$$i_0^2 = \frac{E_0^2\left\{R'^2K'^2\omega^2 + \left[1 - LK'\omega^2 + \frac{K'}{C+K_1}\right]^2\right\}\omega^2}{\left\{\left[\frac{1-(C+K_1)L_1\omega^2}{C+K_1}(1-LK'\omega^2) - \left(R_1R'K' + \frac{L_1K'}{C+K_1}\right)\omega^2\right]^2\right.} \qquad (5)$$
$$\left. + \left[R'K'\frac{1-(C+K_1)L_1\omega^2}{C+K_1} + R_1(1-LK'\omega^2) + \frac{R_1K'}{C+K_1}\right]^2\omega^2\right\}.$$

Putting $I_0 = E_0/R_1$, the maximum value of i_0 at resonance with the interferometer disconnected, and also putting

$$p = 1 - (C+K_1)L_1\omega^2 \qquad (6)$$

$$q = 1 - LK'\omega^2,\ q_0 = 1 - LK\omega^2 \qquad (7)$$

$$\phi_1 = R_1(C+K_1)\omega \qquad (8)$$

$$\phi_2 = R'K'\omega \qquad (9)$$

and

$$\sigma = i_0/I_0$$

we have

$$\sigma^2 = \frac{\phi_1^2[\phi_2^2 + (q + K'/(C+K_1))^2]}{[pq - \phi_1\phi_2 - (1-p)K'/(C+K_1)]^2 + [\phi_2 p + \phi_1(q + K'/(C+K_1))]^2} \qquad (10)$$

Eq. (10) is an exact description of the current amplitude in the thermocouple heater relative to the current amplitude at resonance in the resonant circuit with the interferometer disconnected, as a function of the decrements of the oscillating circuit and of the interferometer system, of the departure from resonance in the two systems, of the pure capacity $C+K_1$, and of the fictitious capacity K' of the acoustic system. This equation is similar to the one deduced by D. W. Dye[8] for the piezoelectric resonator in a resonant circuit but is complicated by the inclusion of the modified R', K' and ϕ_2 terms introduced because of the interferometer system. Dye's analysis includes a capacity K_2 between the resonator and the resonant electrical circuit to account for the effect of variable electrode distance from the quartz plate. This capacity is here suppressed, the electrode conditions being maintained constant.

In view of the exhaustive study which Dye has made of his equation no extended discussion of its analogue, Eq. (10), is necessary here. It should be pointed out, however, that in general σ^2 as a function of the frequency rises to the usual resonance maximum for $p=0$, and that further, if $q+K'/(C+K_1) = 0$ in the same neighborhood there will be a sharp minimum or *crevasse* in the resonance curve. This crevasse is extraordinarily narrow because of the extremely small value of ϕ_2 as compared to ϕ_1, and at its center σ^2 falls to a small fraction of its value on either side. By repeated adjustment of C and ω it is possible to find the value of the frequency for which p and $q+K'/(C+K_1)$

[8] D. W. Dye, Proc. Phys. Soc. Lond. **38,** 399–458 (1926).

are zero simultaneously, provided the reflecting plate is set at a distance $r=(2n+1)\lambda/4$, so that P and Q are both equal to zero and $K'=K$, making $q=q_0$. In practice it is sufficient to find a crevasse for any setting of r, whereupon a rough determination of $\lambda/2$ is made. The setting of r is now made at $\lambda/4$, then by successive adjustment of C and ω the crevasse is made symmetrical. The interferometer is then disconnected and C is varied, ω being kept constant, until i_0 has the maximum value I_0, which is determined. The interferometer is then reconnected and C is adjusted to its former value for a symmetrical crevasse, which completes the adjustment necessary for a determination of σ^2 as a function of r. A series of observations of i taken under these conditions is shown in Fig. 2, curves I and II, in which only maxima

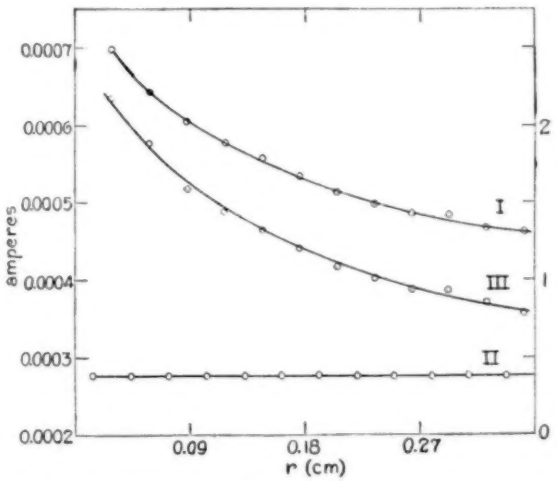

Fig. 2. Curves I and II, maximum and minimum galvanometer readings as a function of r. Curve III, representation of Eq. (17) as a function of the same observations.

and minima of current are shown. The behavior in the immediate neighborhood of a maximum for the same case is shown in Fig. 4, Insert a, the abscissa scale being magnified twentyfold. In the preliminary adjustments just described, we have made $p=0$, $q_0+K/(C+K_1)=0$, and, remembering Eqs. (1), (6) and (7), $q+K'/(C+K_1)=K'AB\rho v\omega Q$, so that

$$\sigma^2 = \frac{(1+SP)^2+S^2Q^2}{[1+SP+1/R\omega\phi_1(C+K_1)]^2+S^2Q^2} \tag{11}$$

where

$$S = AB\rho v/R. \tag{12}$$

When the reflector is at a distance $r=(2n+1)\lambda/4$ from the face of the vibrating plate, if n is small, $P=$ zero to a very close approximation, and $Q=0$.[9] Let σ_0 be the value of σ for this reflector position. We have then

[9] See I, Figs. 2 and 3. These figures were drawn for the case in which γ was assumed to be unity. As we shall see later the statement made above is practically always valid for gases.

$$\sigma_0 = 1/[1 + 1/R\omega\phi_1(C + K_1)]$$

or

$$R\omega\phi_1(C + K_1) = \sigma_0/(1 - \sigma_0). \tag{13}$$

The value of σ given by Eq. (11) under the prescribed conditions will have maximum values, σ_m, for values of r such that $Q=0$ and $P=P_m$ given by

$$P_m = (1 + \gamma e^{-2r\alpha})/(1 - \gamma^2 e^{-2r\alpha}). \tag{14}$$

We then have

$$\sigma_m = (1 + SP_m)/[1 + SP_m + (1 - \sigma_0)/\sigma_0], \text{ or}$$

$$S = AB\rho v/R = [\sigma_m(1 - \sigma_0)/(1 - \sigma_m)\sigma_0 - 1]/P_m = \text{constant}. \tag{15}$$

Putting $\gamma = e^{-\beta}$, Eq. (14) becomes $P_m = e^{\beta/2}[\cosh(r\alpha+\beta/2)]/\sinh(r\alpha+\beta)$, or, to a very close approximation, unless r is large

$$P_m = (1 + \beta/2)/(r\alpha + \beta). \tag{16}$$

This value of P_m inserted in Eq. (15) would lead at once to a determination of α and β if we had the means of accurate determination of A, assumed to be the area of the vibrating plate exposed to the fluid. As is well known, only a small portion of the surface of a piezoelectric plate as ordinarily cut is in vibration in a given mode[10,11] though by optical means it can be shown that the entire cross section of the column of a fluid in an interferometer is set into resonant vibration and presumably reacts upon the crystal over the whole of its exposed face. Hershberger[12] has recently pointed out that the assumption that A is to be taken as the area of the plate exposed to the fluid is not valid. As we shall see, however, it is sufficient to assume an effective A, which is constant. In the absence of knowledge of its magnitude we have then in Eq. (15) only a means of computing the relative effects of absorption and reflection. For, substituting P_m from Eq. (16) into (15), we have

$$[(1 - \sigma_0)/\sigma_0][\sigma_m/(1 - \sigma_m) - \sigma_0/(1 - \sigma_0)](r\alpha/\beta + 1) = S' \tag{17}$$

where

$$S' = S(1 + \beta/2)/\beta = \text{constant}. \tag{18}$$

Eq. (17) enables us at once to compute α/β from a series of observations of values of σ_m and the corresponding values of r, and the mean value of σ_0. Fig. 2, curve III, shows the observations of Fig. 2, curves I and II, in terms of Eq. (17), the smooth curve passing through the maxima being the hyperbola given by Eq. (17), where $\alpha/\beta=6.276$, and $S'=2.548$. All types of acoustic interferometers which have been used by the method described here yield results for gases in entire accord with the theory showing that within the limits of errors of observation the quantities entering into S', Eq. (18), may be considered as constant.

[10] Nat. Phys. Lab. Report for 1928.

[11] P. Vigoureux, Quartz Resonators and Oscillators, London (1931).

[12] W. D. Hershberger, Physics **2**, 269–273 (1932).

Having determined α/β from a given series of observations, it remains to be seen how α and β may separately be determined. Putting $(1-\sigma_0)/\sigma_0=a$, combining Eqs. (11) and (13), and solving for $1+SP$, we have

$$1 + SP = (a/b)\{1 + [1 + b - (QSb/a)^2]^{1/2}\} \quad . \quad (19)$$

where $b=(1-\sigma^2)/\sigma^2$. Remembering Eq. (15), it is seen that in (19) we have a relation, free of all circuit and interferometer constants, involving only galvanometer readings, values of r, and the values of α and β. Having determined the ratio α/β from a series of observations, using Eq. (17), we may assume a value of α, from which we may compute β and S'. The corresponding value of S is then found by means of Eq. (18). Choosing any value of σ on the r, σ curve, preferably at about one-half the altitude of a peak, we compute the value of b. The corresponding value of r is found from the curve for use in computing P and Q. These functions involve r both in the hyperbolic and circular functions composing them. The argument, $2r\omega/v$ of the circular functions may be found directly if the frequency is known, but may be found independently of frequency from the interferometric determination of $\lambda/2$, since $\theta=2r\omega/v=4\Delta r\pi/\lambda$, where Δr is the distance from the point for which σ is chosen to the axis of the peak, or one-half the peak width, since, owing to its extreme narrowness, the symmetry of the peak is not affected by damping to a determinate degree. It is now possible to compute the left and right hand sides of Eq. (19). If the left hand side is larger than the right, the tentative value of α which was chosen is too large, etc. Successive trials lead, usually in three or four steps, to the region of intersection of the curves of the two sides of this equation plotted as functions of α, when by interpolation the value of α satisfying the equation is found. The process may be shortened by noting that $1+SP$ must lie between the values a/b and $(a/b)[1+(1+b)^{1/2}]$ and by using the approximations $P=4(r\alpha+\beta)/[4(r\alpha+\beta)^2+\theta^2]$, and $Q=2\theta/[4(r\alpha+\beta)^2+\theta^2]$ in all but the last two steps.

Measurement of velocity

The values of r for successive values of maximum σ^2 given by Eq. (11) are, to a degree of precision beyond experimental measurement, independent of the damping,[13] except in excessively absorbing media, and are determined by the maximum values of P, which in turn occur when $\cos 2r\omega/v=1$, or when $r=n\lambda/2$. It then remains to measure the frequency in order to evaluate the velocity v.

III. Experimental Tests of the Theory

Three interferometers have been built for the purpose of testing the theory. As the results obtained from all of them differ in no important detail, no extensive description of them will be given.

Interferometer *I*, Fig. 3a, was designed for operation in the open air. It consists of the quartz plate Q resting upon a grounded electrode mounted at the top of a Bakelite support. This support is attached to a plate provided

[13] Cf. also C. D. Reid, Phys. Rev. **35,** 829 (1930).

with adjusting screws so that the face of the plate may be made parallel to the plate glass reflector R. This adjustment was made by viewing fringes in sodium light passed through R and falling upon Q when the two were close together and R was started in retreat from the crystal. The supports for R and Q are mounted upon the ways of a micrometer comparator of great accuracy made by the late Professor H. A. Rowland. The screw is provided with a large head divided into 100 parts, and has a fine adjustment making possible measurements to 10^{-4} mm. This interferometer was particularly useful in testing the effect of various methods of crystal mounting and types of electrodes. Its great accuracy and fine adjustment were used both with the method described in this paper, the crystal being used as a resonator, and with the crystal used as an oscillator, after the methods of Pierce[14] in order to test the effect of variation of velocity with reflector distance reported by

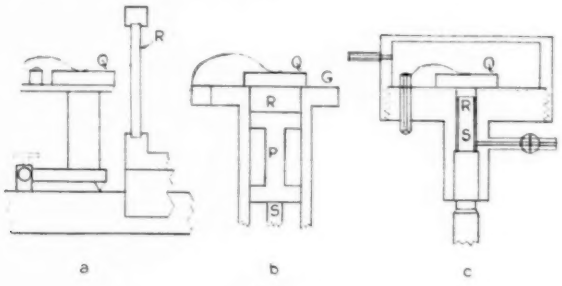

Fig. 3.

Reid.[13] The effect found by Reid was of decreasing amount with increase of frequency, being small with the highest frequencies which he employed. As the frequencies so far used in this laboratory are much higher the effect to be expected might be so small as to escape detection. So far, in the range 400 to 700 k.c. no such effect has been detected by either the resonator or oscillator method, although the interferometer distance has been varied from the face of the crystals used to a distance of 10 cm.

Interferometer II, Fig. 3b, was designed to give the largest possible reaction upon the crystal by the fluid column. It consists of a solid cylinder of brass in which a concentric hole 1″ in diameter was bored. The upper end of the cylinder was ground plane. Upon it rests the crystal Q, the lower face of which is gold sputtered providing the grounded electrode. Contact is made with the upper electrode by means of a light spring. The plunger P is close fitting, with end R ground plane and parallel to the surface G. P is displaced by the micrometer screw S.

Interferometer III, Fig. 3c, was designed to test the effect of the removal of water vapor and CO_2 from the air and to study other gases at room temperature. The end of the micrometer screw serves as the reflector, its parallelism to the surface upon which the crystal rests being tested by sodium fringes, with an optical flat in place of the sputtered crystal. The air or other gas to be tested enters a small channel at the side of the screw, passing up-

[14] G. W. Pierce, Proc. Am. Acad. **60,** 269–302 (1925).

ward and through a small slot under the crystal and into the chamber above, from which it escapes.

The constant frequency oscillator consists of a dynatron oscillator with secondary output connected to the inner grid of a UX222 tube having 45 volts applied to the outer grid. The output of this tube is amplified in two stages of resistance capacity coupling, with nonregenerative tuned output in the last stage. Loosely coupled to the output is the coil L_1 of the resonant circuit which excites the interferometer. Minute variation of the frequency of the dynatron oscillator is provided by a precision condenser of large capacity in series with the condenser of the dynatron circuit. In addition a vernier condenser of very small capacity and with a linear scale of 50 cm length is connected in parallel with the precision condenser so that rapid adjustment for symmetry of crevasse may be made. Currents are measured by a Western Electric vacuum thermocouple and a galvanometer provided with a number of shunts.

Connection to the interferometer is made through a mercury switch, which serves also at any time to connect the interferometer into a Pierce circuit so that studies by both the resonator and oscillator method may be compared, the crystal being under identical conditions. The results of these comparative studies will be presented in another paper.

The most general conclusion which can be drawn from the experiments so

TABLE I. *Galvanometer and screw readings. 597 k.c. First twelve rows give i_m with corresponding peak number m. Column (1), room air, interferometer II: (2), room air, interferometer III: (3), dry air: (4), dry, CO_2—free air: (5), CO_2.*

m	(1)	(2)	(3)	(4)	(5)
1	0.001484	0.000720	0.000698	0.000703	0.000653
2	1432	674	642	647	541
3	1383	634	603	614	484
4	1344	603	577	583	444
5	1295	582	557	557	420
6	1255	563	534	540	394
7	1211	539	513	514	386
8	1163	524	498	498	377
9	1119	508	485	486	
10	1094	504	484	483	
11	1050	492	467	470	
12	1020	483	462	456	
t°C	22.2	23.3	24.0	24.0	23.3
$\lambda/2$	0.02928	0.02944	0.02941	0.02944	0.02389
i_0	0.000235	0.000310	0.000278	0.000279	0.000304
I_0	0.002398	0.002329	0.002275	0.002293	0.002275
r cm	0.2343	0.3538	0.3529	0.3533	0.1433
$2\,\Delta r$	0.00322	0.00159*	0.00157	0.00156	0.00200
i	0.0006	0.000375	0.000350	0.000350	0.000350
r cm	0.3514				
$2\,\Delta r$	0.00325				
i	0.0006				

* Peak structure not satisfactory owing to rapid drift of frequency and necessity of repeated correction.

far carried out is that for every case investigated, in the frequency range 400–700 k.c. and with all three of the interferometers just described, the results for the maxima and minima of the σ, r curve can be expressed within experimental error by the hyperbolic relation given in Eq. (17). The value of α/β and of S' for any set of observations may be determined by the method of least squares. Table I gives the original data for five cases at the frequency 597 k.c. The computed values of α/β and S' for each of the sets are given in Table II. Fig. 2 is drawn for the results of column (3). Fig. 4, Inserts (a) and (b), show the structures respectively of the 12th peak for dry air, and the 6th peak for CO_2. From these and other similar peaks the data for $2\Delta r$ in Table I are obtained. For the purpose of comparison of different sets of results taken

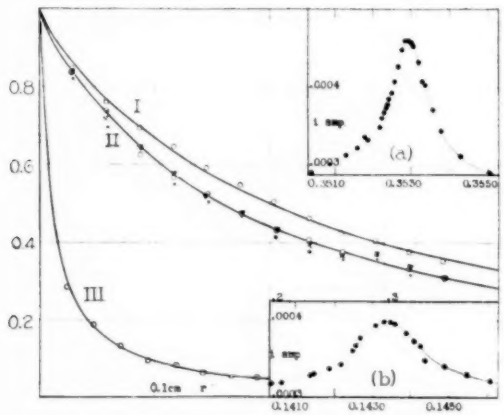

Fig. 4. Reduced observations compared with $1/(r\alpha/\beta+1)$.

Curve I, room air in interferometer II; Curve II, with circles, dry air in interferometer III; Curve III, CO_2 in interferometer III. Insert (a), twelfth current peak for dry air; Insert (b), sixth current peak for CO_2.

with different gases or under different conditions, as with different interferometers, we may plot $[(1-\sigma_0)/\sigma_0][\sigma_m/(1-\sigma_m)-\sigma_0/(1-\sigma_0)]/S'$ as a function of r. This should be compared with its theoretical equivalent, $1/(r\alpha/\beta+1)$. Fig. 4 shows as an example the first of the above functions for the observations of Table I indicated by circles, points, etc., and full curves, I, II, III, for $1/(r\alpha/\beta+1)$ for three of the sets corresponding respectively to columns (1), (3) and (5) of Table I. It is to be noted that all such curves start with ordinate unity at $r=0$.

Absorption measurements

Having determined α/β, it is possible, as has been explained, to find the separate values of α and β from some value of σ and its corresponding r by a method of graphic interpolation. The accuracy with which these quantities may be obtained is affected by the constancy with which the frequency and amplitude of the driving circuit may be maintained. In the absence of a piezo-electrically driven generator of required frequency for driving the resonant circuit containing the interferometer, it has been the practise to test the

constancy of frequency at the conclusion of readings for each peak by setting r at the nearest value of $(2n+1)\lambda/4$ and noting whether i is at the minimum value i_0. To test whether the amplitude of output has been changed, the interferometer is disconnected and a reading of I_0 is taken, corresponding to the resonance maximum of the interferometer circuit. If either i_0 or I_0 has changed the intervening observations are rejected. This practise has entailed a loss of time and labor, making it highly desirable to use crystals for driving the generator. However, since the particular crevasse of a given crystal most suitable for interferometric work is often not at one of the principal frequencies of the crystal, the process of accumulation of plates for driving purposes involves first a careful exploration of crevasses for their suitability in the interferometer, and then of preparing oscillator plates, one for each frequency which can be used.

The results given in Table I were taken with a rectangular plate. The crystal was an excellent oscillator and no other crevasses were observed in the neighborhood of its principal crevasse frequency. The peaks were symmetrical and showed no evidence at any time of having any satellites. This crystal was therefore regarded as being particularly suitable for the present purpose of illustration of the theory. The values of α/β, S', α, and γ computed from the results given in Table I are shown in Table II.

TABLE II. *Absorption and reflection coefficients. $\nu = 597$ k.c.*

	Interferometer	Gas	t°C	$\lambda/2$ cm	α/β	S'	α	γ
1	II	Room air	22.2	0.02928	5.045	16.63	0.130	0.9745
2	III	Room air	23.3	0.02944	6.384	2.262	0.106*	0.9836
3	"	Dry air	24.0	0.02941	6.276	2.548	0.110	0.9827
4	"	Dry CO_2 free air	24.0	0.02944	6.312	2.561	0.108	0.9831
5	"	CO_2	23.3	0.02389	94.78	5.705	0.702	0.99261

* See remark under Table I.

Data on absorption are very meager. From Neklepajew[15] we have for dry air, $\mu = 0.00073/\lambda^2$, which for $\lambda/2 = 0.02941$ gives $\mu = 0.211$. For α this gives 0.105, in fair agreement with the value 0.110 for dry air in Table II. For CO_2, we have the calculations of Herzfeld and Rice[16] from the velocity measurements of Pierce[14] and by extrapolation from the results of Abello[17] giving respectively for μ, $3\times10^{-12}\nu^2$ and $5.6\times10^{-12}\nu^2$. We have, for $\nu = 5.97 \times 10^5$, from the former, $\alpha = 0.54$, and from the latter $\alpha = 1.0$. These results may be compared with $\alpha = 0.702$ for CO_2 in Table II.

The coefficient of reflection

An interesting feature of these experiments is the large departure from unity of the coefficient of reflection γ. If we take as the coefficient of reflection of air waves at a surface of brass, $\gamma = (R_1 - R_2)/(R_1 + R_2)$, where R_1 for brass

[15] N. Neklepajew, Ann. d. Physik **35,** 175–181 (1911).
[16] K. F. Herzfeld and F. O. Rice, Phys. Rev. **31,** 695 (1928).
[17] T. P. Abello, Proc. Nat. Acad. Sci. **13,** 699 (1927).

is $\rho v = 8.5 \times 3.65 \times 10^5 = 3.1 \times 10^6$, and for air, $R_2 = 40$, we expect γ to be $1 - 1.3 \times 10^{-5}$. The departure from unity in these experiments is actually several orders greater, as may be seen from Table II. In explanation of this we may recall that we are dealing with a resonant system, and that it is to be expected that resonance in the reflector system will result in a motion of the reflector surface depending upon the dimensions and material of the reflector. The coefficient of reflection in terms of motion of reflector surface is considered in Part I of this paper. It is to be noted in Table II that γ changes abruptly from interferometer II to III, and from air to CO_2. Similar changes are noted in passing from one frequency to another. It would be of interest in this connection to use as a reflector a second piezoelectric plate of quartz so that the amplitude of vibration of the reflecting surface could be studied directly. The equations developed for this case, where it was assumed that the reflector was rigid, I, Eqs. (17) and (18) do not apply in so far as γ is not unity. From I, Eqs. (12) and (13) we have putting $x = r$,

$$P_r = \left[(1+\gamma)(1-\gamma^2 e^{-2r\alpha})e^{-r\alpha} \cos (r\omega/v)\right] / \left[1 - 2\gamma^2 e^{-2r\alpha} \cos (2r\omega/v) + \gamma^4 e^{-4r\alpha}\right] \quad (20)$$

$$Q_r = \left[(1+\gamma)(1+\gamma^2 e^{-2r\alpha})e^{-r\alpha} \sin (r\omega/v)\right] / \left[1 - 2\gamma^2 e^{-2r\alpha} \cos (2r\omega/v) + \gamma^4 e^{-4r\alpha}\right]. \quad (21)$$

These equations, with Eqs. (1) and (2) applied to the reflector, considering its network in combination with a suitable thermogalvanometer connected to its electrodes, would make practicable a detailed study of reflection phenomena. Grossmann and Wien[18] have used a piezoelectric plate as reflector for the study of frequency variation of a radiating crystal oscillator as a function of reflector distance. Grossmann[19] has used an arrangement of two crystals as source and detector for the study of absorption in CO_2, but at this writing details of his method and procedure are not available.

It is of interest to compare the effect on the observations of using different cross sections of fluid column. From Eq. (12), $A = SR/B\rho v$, and from Eq. (13), $R = \sigma_0/(1-\sigma_0)\omega\phi_1(C+K_1)$. In changing under the same conditions from one interferometer to another, $B\rho v$ and $\omega\phi_1(C+K_1)$ remain practically unchanged, so that the areas of cross section of the two columns should be in proportion to the respective values of $S\sigma_0/(1-\sigma_0)$, or $S'\sigma_0\beta/(1-\sigma_0)(1+\beta/2)$. For interferometer II, room air, we have $S' = 16.63$, $\beta = 0.0258$, $\sigma_0/(1-\sigma_0) = 0.1086$, and for interferometer III these quantities have the respective values 2.262, 0.0166, 0.1537, implying a ratio of cross section of interferometer II to III of 8.03. The actual areas were 5.07 and 0.707 cm², having a ratio 7.18. The agreement of these figures is closer than might be expected in view of the remarks following Eq. (16). The particular crystal for which the above numbers are cited vibrates vigorously for the mode considered at two points near opposite corners of its rectangular area, little trace of motion being found over much of its surface. In using such a crystal with interferometer III it is necessary to adjust the crystal so that one of its vibrating areas is exposed to the gas. The nearness to equality of the ratios given above and

[18] E. Grossmann and M. Wien, Phys. Zeits. **32,** 377–378 (1931).

[19] E. Grossmann, Phys. Zeits. **33,** 202 (1932).

similar values in many other cases point to the conclusion that what we have called the effective value of A is nearly equal to the actual area exposed to radiation. It seems probable that this equality would be exact with crystals cut in the manner described by Straubel[20] in which case the absolute value of S in Eq. (15) could be determined and the coefficient of absorption of the gas could be evaluated directly from observations of maxima and minima of σ, using Eqs. (15) and (16), thus avoiding the laborious procedure of analysis of peak form.

A study is in progress, with the methods here outlined, of the ultrasonic absorption constants of several gases, considered as functions of frequency and temperature.

My thanks are expressed to the Rumford Committee of the American Academy of Arts and Sciences for a grant with which the quartz crystals used in this work were obtained, and to Mr. Milton Lipnick, a graduate student of the Johns Hopkins University for assistance on many occasions.

[20] H. Straubel, Phys. Zeits. **32,** 222 (1931).

Mutual Impedance of Grounded Wires above the Surface of the Earth

By RONALD M. FOSTER
American Telephone and Telegraph Company

(Received July 27, 1932)

A FORMULA already established for the mutual impedance of any grounded thin wires lying on the surface of the earth[1] has now been extended to include wires lying in horizontal planes above the surface and grounded by vertical wires at their four end-points. With the same basic assumptions and the same general method of derivation as before, the extended formula is found to be:

$$Z_{12} = \int\int \left[\frac{d^2Q(r, H, h)}{dS\, ds} + \cos\epsilon\, N(r, H, h)\right] dS\, ds,$$

where

$$Q(r, H, h) = Q_0(r) + Q_1(r, H + h) - Q_2(r, |H - h|),$$

$$N(r, H, h) = N_0(r) + N_1(r, H + h) - N_2(r, |H - h|),$$

$$Q_0(r) = \rho/2\pi r,$$

$$Q_1(r, h) = \frac{i\omega\nu}{4\pi}\int_0^\infty \left\{\frac{h}{\mu} - \frac{1 - e^{-h\mu}}{\mu^2}\left[\frac{(\mu^2 + \Gamma^2)^{1/2} - \mu}{(\mu^2 + \Gamma^2)^{1/2} + \mu}\right]\right\} J_0(r\mu)d\mu,$$

$$Q_2(r, h) = \frac{i\omega\nu}{4\pi}\left[h \log \frac{(r^2 + h^2)^{1/2} + h}{r} - (r^2 + h^2)^{1/2} + r\right],$$

$$N_0(r) = \frac{\rho}{2\pi r^2}[1 - (1 + \Gamma r)e^{-\Gamma r}],$$

$$N_1(r, h) = \frac{i\omega\nu}{4\pi}\int_0^\infty (1 - e^{-h\mu})\left[\frac{(\mu^2 + \Gamma^2)^{1/2} - \mu}{(\mu^2 + \Gamma^2)^{1/2} + \mu}\right] J_0(r\mu)d\mu,$$

$$N_2(r, h) = \frac{i\omega\nu}{4\pi}\left[\frac{1}{r} - \frac{1}{(r^2 + h^2)^{1/2}}\right].$$

The integrations in the iterated integral are extended over the two wires S and s, lying in planes at heights H and h, respectively. The elements dS and ds are separated by the horizontal distance r and include the angle ϵ between their directions The resistivity of the earth is ρ; the inductivities of the air and of the earth are each assumed to be equal to that of free space, ν. The propagation constant of plane electromagnetic waves in the earth is Γ, which

[1] R. M. Foster, Bull. Amer. Math. Soc. **36,** 367–368 (1930); Bell System Tech. J. **10,** 408–419 (1931).

equals $(i\omega\nu/\rho)^{1/2}$. All distances are measured in meters, Z_{12} in ohms, and ρ in meter-ohms; ν has the value 1.256 microhenries per meter; ω is equal to 2π times the frequency.

For zero heights, the functions Q and N reduce to Q_0 and N_0, which are the values previously obtained for wires on the surface. For any heights but with low frequencies the formula gives the direct-current mutual impedance as found by G. A. Campbell.[2] For any heights but with one wire of infinite length the formula gives the mutual impedance as published independently by F. Pollaczek,[3] J. R. Carson,[4] and G. Haberland.[5]

[2] G. A. Campbell, Bell System Tech. J. **2,** 1–30 (1923).
[3] F. Pollaczek, Elekt. Nachr. Tech. **3,** 339–359 (1926).
[4] J. R. Carson, Bell System Tech. J. **5,** 539–554 (1926).
[5] G. Haberland, Zeit. angew. Math. **6,** 366–379 (1926).

LETTERS TO THE EDITOR

Prompt publication of brief reports of important discoveries in physics may be secured by addressing them to this department. Closing dates for this department are, for the first issue of the month, the twenty-eighth of the preceding month; for the second issue, the thirteenth of the month. The Board of Editors does not hold itself responsible for the opinions expressed by the correspondents.

The Frequency of Resonance Radiation

It is of considerable importance in many astrophysical studies to know whether the atom emits as resonance radiation exactly the same frequency which it absorbs. If one supposes, following Eddington, that it does emit this precise frequency, then an atom which absorbs light of frequency slightly off "resonance" will also emit off resonance. A preliminary test was made by illuminating mercury vapor with a line (2536A) having a narrow and sharp reversal, and observing the resonance radiation. This was accomplished by using a water-cooled quartz arc shining through a quartz absorption cell onto the resonance chamber. The temperature of the absorption cell could be regulated electrically and with ice, and consequently the vapor pressure of the absorbing column of mercury vapor could be controlled. With the absorption cell cold (0°C) resonance radiation was observed; and as the temperature of the cell was raised the resonance radiation became fainter, until at 45°C the resonance could barely be detected on a long exposure photograph. This absorption cell produces a narrow and sharp reversal in the center of the emission line of the arc, the amount of the reversal being of course determined by the temperature of the cell. Yet at no time was any reversal of the line in resonance observed. Careful tests were made for stray scattered light. The spectrograph used was of the quartz Cornu prism type with a dispersion of about 3A per mm at λ2536.

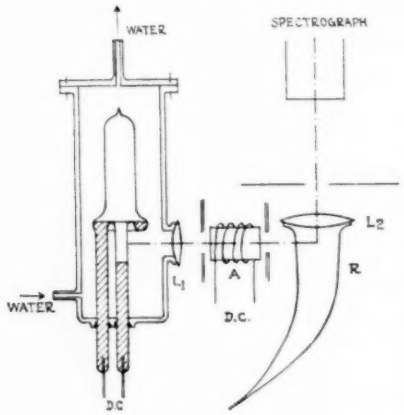

Fig. 1.

The physical interpretation of this effect is not fully understood. If one supposes a slight change in frequency to take place between the acts of absorption and emission, then energy which is absorbed in the wings would be reradiated in the center, as observed. The difference in energy between that of the absorbed and reradiated quantum presumably appears as thermal energy of motion. It will be noted that this change in energy, though apparently small, is far greater than the extremely minute Doppler width of mercury vapor at room temperature could possibly account for. If on the other hand we postulate detailed balancing and require the exact frequency absorbed to be reemitted, then the emission of a nonreversed line becomes something of a puzzle unless the upper state is more sharply quantized than the ground state—an improbable eventuality.

It is proposed to continue these experiments with a spectrograph of greater dispersion and to attempt to resolve the resonance radiated line more completely.

S. A. KORFF

Carnegie Institution of Washington,
Mt. Wilson Observatory,
July 10, 1932.

Use of Argon in the Ionization Method of Measuring Cosmic Rays

In designing apparatus for a cosmic-ray survey, we had occasion to study argon under pressure as material for the ionization chamber. The results of preliminary measurements showed that this gas was much more strongly ionized than either air or nitrogen, which have been used hitherto. A study was made of the ionization-pressure curves of argon and air. The source of ionization was about one milligram of radium at a distance of one meter. Even at the highest pressure (95 atmospheres) of argon that was used the curve was still rapidly rising.

The following current intensity ratios were obtained from our own measurements and from measurements of others on air and nitrogen, for a pressure of 95 atmospheres:

$$I_{(\text{argon})}/I_{(\text{air})} = 3.22;$$
$$I_{(\text{nitrogen})}/I_{(\text{air})} = 1.48$$
$$I_{(\text{argon})}/I_{(\text{nitrogen})} = 2.17$$

When the ionization chamber was first filled with argon to a high pressure, the ionization current increased with time. The value on fresh filling was only about 50 percent of the final steady value; after 3 hours it was about 87 percent and the final steady value was reached in about a day. This effect depends obviously upon how much the gas is stirred in filling the bomb. In view of this effect our ionization-pressure data have been taken in the direction of decreasing pressures.

When no electric field was applied across the ionization chamber, ions produced in argon at high pressure under exposure to gamma-rays remained uncombined for many minutes. This is in accord with the small recombination coefficient that had been found for argon at low pressures. This effect was also found in air but to a less degree.

An initial recombination of ions in air and nitrogen at high pressure before they are separated by diffusion has been used to account for the fact that in these gases the effective ionization is not proportional to the pressure. It is reasonable to suppose that in argon the low recombination rate makes improbable such initial recombination, with the result that the ionization continues to increase with pressure over a much wider range.

This small speed of recombination in argon allows a relatively large concentration of ions to form under the action of an ionizing source before equilibrium is reached. If now a potential is put onto the ionization chamber, the initial current is many times the value of the steady final current, which is ordinarily used to measure the rate of formation of ions. This cumulative action suggests the properties of a photographic plate, and indicates its possible application in the measurement of weak ionization currents.

ARTHUR H. COMPTON
JOHN J. HOPFIELD
University of Chicago,
July 18, 1932.

Strain and Magnetic Orientation

Previous work[1] has shown that tension establishes the axial as the preferred direction of magnetization in a 15 Ni 85 Fe wire, but this direction is unique in other respects such as symmetry of internal strains and partial crystal orientation. More recently further experiments with large Barkhausen discontinuities have given striking and direct confirmation of the view that a large elastic strain establishes a preferred orientation independent of other factors.

The NiFe wire, lying with its axis in the OH direction, Fig. 1, was strained by twisting, with the result that, referred to the surface of the wire, the maximum elongation lay in the *OP* direction. In this state the wire exhibits self-propagating changes of magnetization under the influence of longitudinal magnetic fields as described previously, an important feature of the phenomenon being the limiting ("critical") field below which reversal cannot proceed. The critical field values for 1, 2, and 3 turns of one end of an 80 cm long, 0.019 cm radius wire are shown in Fig. 1 at H_{01}, H_{02}, H_{03}, respectively. In the present experiments, however, a transverse field was added by passing current through the wire itself. Only the value H_t of this field at the surface of the wire will be considered.

In the presence of this field a new set of critical longitudinal fields was found. For

[1] K. S. Sixtus and L. Tonks, Phys. Rev. **37**, 930 (1931).

instance, with $H_t = H_t'$, H was increased so that the terminus of the vector representing the total field traversed RQ from left to right. No jump was found for 1 turn; the jump first became possible at h_2 for 2 turns, and for 3 turns the discontinuity occurred against an opposing longitudinal field!

Confining attention to the 2-turn case, we have in OH_2 and OH_{02} two vector critical fields.

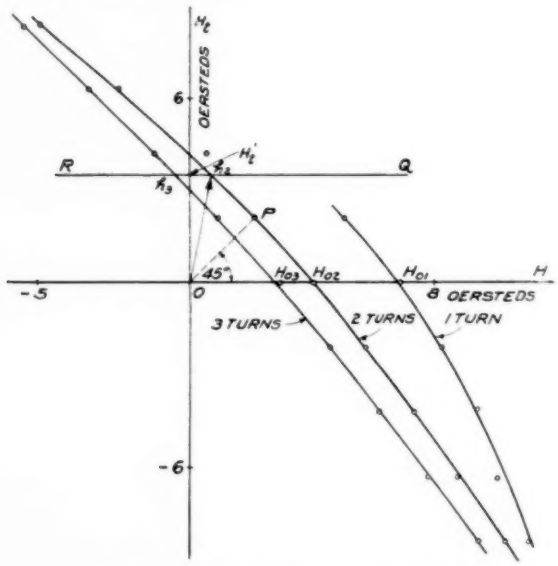

Fig. 1. Vector critical fields in twisted NiFe wire.

By using other values of H_t the curve joining h_2 and H_{02} was filled in. This curve is the same whether H_t is constant and H is increased in obtaining it, or vice versa.

The significant features of the curve are that (1) it approximates to a straight line and (2) it makes 45° with the axes. The parallelism of the 1- and 3-turn curves with the 2-turn curve shows that this is no accident. As it is a straight line, the components, taken along the direction of its normal, of all the vector critical fields are equal, and as it is at 45°, this direction coincides with OP, the direction of a principal strain. It follows that the component of the applied field in the direction of maximum elongation is solely effective in causing the large Barkhausen jump.

Characteristics were also obtained for a wire twisted while under strong tension. For zero torsion H_t was without effect, the characteristic being a straight line parallel to the H_t axis. For increasing torsion the lines inclined toward the H_t axis, the angle of inclination agreeing well with that calculated for the deviation of the principal strain from the axis.

These results lead naturally to the view that within the range of magnetic fields used and with sufficient strain applied, the magnetic intensity lies in the direction of maximum elongation, and that transverse fields are ineffective in aiding the reversal of magnetization under these conditions.

LEWI TONKS
K. J. SIXTUS

Research Laboratory,
General Electric Company,
Schenectady, New York,
July 29, 1932.

Electrons as Cosmic Rays

Professor A. H. Compton's fundamentally interesting experiments on the variation of cosmic-ray intensity with latitude raises once more, as he suggests, the possibility of cosmic rays being electrons. In addition to the bearing of such a hypothesis upon variations with altitude and with latitude, certain other matters suggest themselves as interesting for consideration.

In 1924, in connection with a theory of the

absence of ionization[1] by electrons of sufficiently high energy, the writer pointed out that an electron with velocity only 40 meters per second less than the velocity of light, i.e., with energy corresponding to 10^9 volts, could not approach the earth's surface at the equator nearer than a point at a distance of 8 earth's radii from the earth's center when projected from infinity towards the earth's surface in the magnetic equatorial plane. For the most favorable direction of projection in that plane at infinity, an electron would have to possess 10^{10} volts velocity in order to reach the surface. A. Bramley and the writer[2] having given evidence from the wave mechanics supporting the conclusion that electrons of energy comparable with this amount may be incapable of ionizing, as formerly surmised by the writer[1] for energies of the order 10^9 volts on the basis of the classical electrodynamics. Such a conclusion would render more reasonable an explanation of the maintenance of the earth's charge by the influx of such electrons, since it would relieve us of the difficulty following from the large ionization which the 1500 electrons per square centimeter per second, necessary to account for the earth's charge, would otherwise cause. Another point of interest involves the idea that for such electrons, considered as primary cosmic radiation, the action of ionization would have to occur through the intervention of secondaries shot out only occasionally by the primaries. The operation of the primaries would thus become more closely comparable with that characteristic of photons.

The actual experimental observation of secondary electrons of energies comparable with 10^9 volts, by Professor Millikan and his collaborators, raises many interesting questions. Such electrons would describe, in the earth's magnetic field, circles or helices of radius 10^7 cm; and their energy, on the basis of 16 volts per ion and 50 ions per centimeter of path at atmospheric pressure, would enable them to travel distances comparable with the whole thickness of the homogeneous atmosphere, and indeed distances forming at least appreciable fractions of the whole circumference of the circular orbits into which they are bent. The conclusions following from the foregoing considerations may best be illustrated in limited space by reference to Fig. 1, where in each case the circle represents the complete orbit of the electron if there were no absorption in earth or air (for simplicity, we consider orbits in the magnetic equatorial plane). The dotted line represents the earth's surface, and the point O, the point of emission of a secondary in the atmosphere. Even for the case of symmetrical emission of secondaries by primaries in all directions in the lower hemisphere, there will not be symmetrical emission of secondaries with respect to a plane passing through the magnetic poles. Thus, consider a case where the electron path (shown by the thick line) is one eighth of the circumference. Corresponding to an electron striking the earth at 45° from east to west as in Fig. 1*A*, there will be an electron striking at 45° from west to east as in *B*. But corresponding to an electron striking tangentially from east to west as at *C*, there will be no electron striking tangentially from west to east. Such an electron would have to have come from below the surface of the earth as at *D*, and to have been emitted partially upwards. A lack of symmetry in favor of vertical emission of secondaries would enhance still further the considerations here cited.

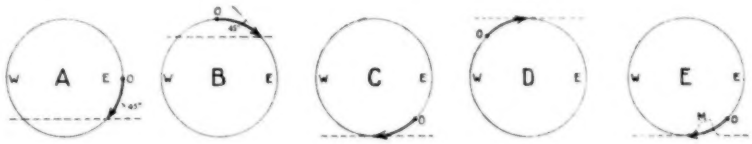

Fig. 1.

[1] W. F. G. Swann, Phil. Mag. [6] **47,** 306–319 (1924). Very exhaustive treatments of the orbits of electrons in the earth's magnetic field have been given by C. Stormer on the theoretical side and by K. Birkeland on the experimental side, in papers extending as far back as 1904. These have to do chiefly with the positions of the auroral zones.

[2] W. F. G. Swann and A. Bramley, Phys. Rev. **41,** 393 (1932). Read before the New Haven Meeting of the Am. Phys. Soc. on June 23, 1932.

Since the orbits of these high energy electrons are determined entirely by their relativistic mass, and are otherwise independent of the velocity since that velocity is practically equal to that of light, and since the mass is proportional to the energy for these electrons, the orbits will be the same for protons as for electrons of the same energy, except that they will be described in the opposite sense.

It is of interest to observe that in the case of observations on a high mountain, radiations coming from electrons which have passed their lowest point should be directed slightly upwards. It is also of interest to note the shielding effect to be expected from a mountain M for such conditions as are represented in Fig. 1 E.

W. F. G. SWANN
Bartol Research Foundation of
The Franklin Institute,
August 1, 1932.

BOOK REVIEWS

The Partial Differential Equations of Mathematical Physics. H. BATEMAN. Pp. 522+xxii. Figs. 29. Cambridge University Press, 1932. Price. $10.50.

To quote from the preface, "in this book the analysis has been developed chiefly with the aim of obtaining exact analytical expressions for the solution of the boundary value problems of mathematical physics." The volume is hence a valuable and comprehensive compendium of the mathematical technique which has been developed for solving the equations of classical physics. Professor Bateman is preeminently qualified to write a monograph of this character, since his ability is well known in finding new closed solutions of complicated equations. Among the subjects treated are Sommerfeld's method of handling diffraction problems, conformal representation, use of Green's functions, toroidal coordinates, etc. In practically all cases, physical problems are cited to which the mathematical analysis is applicable. For instance, the first section of the chapter on non-linear equations bears the caption "Riccati's equation, motion of a resisting medium, fall of an aeroplane, bimolecular chemical reactions, lines of force of a moving electric pole, examples." This is typical of the diversity of physical illustrations, although no attempt is made to draw upon the quantum mechanics of atomic structure. As the author intimates in the introduction, some of the differential equations and functions which are treated are, nevertheless, encountered in quantum mechanics; i.e., the confluent hypergeometric function. The great generality of the mathematical methods permits a high degree of comprehensiveness, but, coupled with the varied and scattered character of the physical illustrations, perhaps makes the style somewhat difficult in places. The author index of over four hundred names shows careful documentation of modern mathematical investigations on boundary value problems. The volume as a whole is focused upon exact solutions, but contains an introduction of eight pages on methods of approximation for the solution of differential equations, such as the Ritz method, least squares, etc.

J. H. VAN VLECK
University of Wisconsin

Die Relativitätstheorie. LUDWIG HOPF. (Volume XIV of **Verständliche Wissenschaft.**) Pp. 148+viii. Figs. 30. Springer, Berlin, 1931. Price RM 4.80.

This first physical volume to apear in Springer's series of semi-popular scientific expositions shows to what extent even such an abstruse discipline as the theory of relativity can be presented in a form readily understandable by the educated layman. An illuminating survey of the fundamental viewpoints of classical mechanics and electrodynamics is followed by a popular exposition of the special theory of relativity which is, in the opinion of the reviewer and within the scope of his experience in this field, the best of its kind; the only mathematics involved (elementary algebra and geometry!) is contained in several scattered paragraphs of fine print, one of which begins with the explanatory sentence "Auch hier sei eine kurze Rechnung für den Leser, der den Pythoagoräischen Lehrsatz und den Begriff der Wurzel noch Kennt, eingeschaltet." The remainder of the book is devoted to the more general theory, and although it falls somewhat behind the previous portions in clarity and fitness, is perhaps as successful an attempt as could be expected under the severe restrictions imposed.

H. P. ROBERTSON
Princeton University

Die gruppentheoretische Methode in der Quantenmechanik. B. L. VAN DER WAERDEN. (Volume XXXVI of **Die Grundlehren der mathemitschen Wissenschaften in Einzeldarstellungen.**). Pp. 157+viii. Figs. 7. Springer, Berlin. 1932. Price RM 9.–RM 9.90.

The appearance of van der Waerden's excellent exposition of the applications of group theory in quantum mechanics will be welcomed by those who wish to survey the field without subjecting themselves to the more strenuous task of digesting the more extended treatises of

Weyl or Wigner. This little book is characterized by a directness of attack which offers the interested reader a shortcut to those portions of the mathematical theory which are of immediate application in the theory of atomic and (diatomic) molecular spectra.

A short introductory account of the Schrödinger formulation of quantum mechanics is followed by a brief exposition of those theorems of the theory of groups and their representations which are to be employed in the sequel. A shortcut to the important theorems concerning the reduction of a representation into its irreducible constituents is obtained by restricting the proof of preliminary lemmas to the case of an "additive (Abelian) group with operators." These sections are followed by an explicit derivation of the complete set of irreducible representations of the rotation and Lorentz groups, and of the selection and intensity rules resulting from the former. The Lorentz group and its representations are discussed with the aid of the so-called spinor analysis, in a form immediately applicable in the following (fourth) chapter of the Pauli-Darwin and Dirac theories of the spinning electron. After a discussion of the relativistic invariance and the solution of Dirac's equations, the author drops back to the nonrelativistic Pauli-Darwin theory for a derivation of the Hund theory of atomic spectra—insofar as it does not involve the Pauli exclusion principle. This exclusion principle, which is of course bound up with the theory of the representations of the symmetric permutation group, is dealt with in Chapter V from the Dirac-Slater points of view which enable one to avoid much of the general theory of this group; the Hund vector model is then completed by the incorporation of these considerations into the scheme derived in the previous chapter. The sixth and last chapter is devoted to a brief development of the corresponding theory for the spectra of diatomic molecules.

The scope of the present book transcends that of Wigner's by the inclusion of some twenty pages on molecular spectra, and has therefore to obtain its end by the sacrifice of much of the illuminating detail contained in the latter. On the other hand, it is narrower in scope than that of Weyl—to which it bears a greater resemblance in notation, method and choice of material—but insofar as it does deal with the same topics it does so by presenting only that portion of the theory which is absolutely necessary for the applications under consideration. While it may therefore send the otherwise uninitiated reader to other treatises for a more thorough background, van der Waerden's logically self-contained and on the whole praiseworthy account of the applications of group theory to quantum mechanics should be of considerable assistance to the physicist or chemist who wishes to gain an insight into the field for himself—and who is not wholly untutored in the ways of mathematicians.

H. P. Robertson
Princeton University

CURRENT LITERATURE OF PHYSICS

Extracts from the Tables of Contents of Some of our Contemporaries

PROCEEDINGS OF THE ROYAL SOCIETY

SERIES A, VOL. 137, NO. A831 — JULY 1, 1932

Lunar Diurnal Variation of Atmospheric Temperature at Batavia, 1866–1928. By **S. Chapman** 1
Homogeneous Catalysis of Gaseous Reactions. By **F. F. Musgrave and C. N. Hinshelwood** 25
Some Measurements of Upper-Atmospheric Ionization. By **E. V. Appleton and R. Naismith** 36
On a Large Scale Crystalline Structure in Certain Glasses of Exceptional Composition. By **Lord Rayleigh.** (Plates 1–3) 55
On Protein Monolayers. By **A. H. Hughes and E. K. Rideal** (Plate 4) 62
Alternative to the Rejection of Observations. By **H. Jeffreys** 78
Oxidation of Carbon Monoxide. By **G. Hadman, H. W. Thompson and C. N. Hinshelwood** 87
Fluorescent Excitation of Mercury by the Resonance Frequency and by Lower Frequencies.—IV. By **Lord Rayleigh.** (Plates 5 and 6) 101
Method of Measuring the Effective Resistance of a Condenser at Radio Frequencies, and of Measuring the Resistance of Long Straight Wires. By **E. B. Moullin** 116
Electrolytic Valve Action and Electrolytic Rectifiers. By **E. Newbury** (Plates 7–9) 134
Some Tests on the Stability of Thin Strip Material under Shearing Forces in the Plane of the Strip. By **H. J. Gough and H. L. Cox** 145
Long Wave Transmission, Treated by Phase Integral Methods. By **T. L. Eckersley** 158
Excitation Function of Helium. By **J. H. Lees.** (Plate 10) 173
Notes on the Excitation Processes in Helium. By **J. H. Lees and H. W. B. Skinner** 186
X-ray Absorption Coefficients in the Range 0.3 to 2.0A. By **L. H. Martin and K. C. Lang** 199
On the Hyperfine Structure of Certain Hg I Lines in the Electrodeless Discharge. By **T. S. Subbaraya and T. G. Srinivasa Iyengar.** (Plate 11) 216
Experiments with High Velocity Positive Ions. II—The Disintegration of Elements by High Velocity Protons. By **J. D. Cockcraft and E. T. S. Walton.** (Plate 12) 229

NATURE

VOL. 130, NO. 3272 — JULY 16, 1932

Letters to the Editor:

Raman Spectrum of Nitrous Oxide. By **A. Langseth and J. Rud Nielsen** 92
Dielectric Constant of Liquid and Solid Nitrobenzene. By **A. Piekara** 93
Connection between the Eötvös Magnitudes. By **O. F. T. Roberts** 94
Confirmation of the Space-Group of Epsomite. By **William H. Barnes and R. G. Hunter** . 96
X-ray Study of Mannitol, Dulcitol, and Mannose. By **Thora C. Marwick** 96
National Physical Laboratory, Teddington. **Inspection by the General Board** 102

NATURE

VOL. 130, NO. 3273 — JULY 23, 1932

Total Solar Eclipse of Aug. 31, 1932. By **F. J. M. Stratton** 116

Letters to the Editor:

Constitution of Tantalum and Niobium. By **F. W. Aston** 130
Vibrations in Solid Rods. By **George S. Field** 130

Mean Lives of the Lowest Metastable States in Neutral Oxygen, and Intensities of Lines Arising Therefrom. By **A. F. Stevenson** 131
Layer-chain Structures of Thallium Di-Alkyl Halides. By **H. M. Powell and D. M. Crowfoot** 131
Energy of Dissociation of Nitrogen. By **T. C. Sutton** 132

ZEITSCHRIFT FÜR PHYSIK

VOL. 76, NOS. 9 AND 10 — JUNE 27, 1932

Influence of Temperature and of Field Strength on the Electrical Conductivity of Amber. By **F. Seidl** 565
Structure of Thin Crystal Layers. By **F. Kirchner** 576
Effect of a Magnetic Field on the Resistance of Photoelectric Contact Layer and Crystal Cells. By **E. Rupp** 597
Structure Sensitiveness of the Ultraviolet Discoloration and of the Excitation of Salt Crystals. By **Hans Joachim Schröder** 608
Quantum Theoretical Considerations in the Problem of the Aromatic and Unsaturated Compounds. By **Erich Hückel** 628
Short Space Charge Field of an Auxiliary Discharge as a Condensing Lens for Cathode Rays. By **Bodo von Borries and Ernst Ruska** 649
Relativistic Correction to the Laws of Image Formation of a Magnetic Condenser Lens for Cathode Rays. By **F. Ollendorff and G. Wendt** 655
Recombination of Ions in Air at Low Pressures. By **Ernst Lenz** 660
Derivation of Planck's Radiation Law without Quantum Hypothesis on the Basis of the Classical Statistics. By **G. Schweikert** 679
Piezoelectric Experiments by the Method of Giebe and Scheibe. By **A. Hettich and H. Steinmetz** 688

DIE NATURWISSENSCHAFTEN

VOL. 20, NO. 28 — JULY 8, 1932

Recognition of the True Nature of Optical Imagery and Its Influence on the Understanding of Optical Apparatus in General. By **Moritz v. Rohr** 514
Short Original Communications:
Raman Effect of Gaseous Ammonia. By **E. Amaldi and G. Placzek** 521
Dependence of the Solar Constant on Solar Phenomena. By **Franz Baur** 521
Electron Microscope. By **R. Rüdenberg** 522

DIE NATURWISSENSCHAFTEN

VOL. 20, NO. 29 — JULY 15, 1932

On the Discovery of X-ray Interference Twenty Years Ago and Sir William Bragg's Seventieth Birthday. By **P. P. Ewald** 527
On the Significance of X-ray Interference for Metallography. By **E. Schmid** 530
Lattice Forces and the X-ray Spectrum. By **R. Glocker** 536
Importance of X-ray Structure Analyses in the Field of Organic Chemistry. By **J. Hengstenberg and H. Mark** 539

PHYSIKALISCHE ZEITSCHRIFT

VOL. 33, NO. 13 — JULY 1, 1932

Raman Effect and Molecular Anisotropy. By **J. Weiler** 489
Original Communications:
Calculation from Viscosity Measurements of the Influence of a Solid Wall on the State of Aggregation of a Fluid. By **M. Reiner** 499
Determination of the Nature of Cosmic Rays by Coincidence Measurements. By **J. N. Hummel** 503
Method of Testing the Plane Parallelism of Plates and an Interference Arrangement. By **Cl. Münster** 505
Scattering of Cathode Rays from Crystal Surfaces. By **F. Kirchner and H. Raether** 510
Measurements on the Selenium Contact Layer Photocell. By **L. Bergmann** 513

ANNALEN DER PHYSIK

Vol. 14, No. 1 — July 1, 1932

Dia- and Paramagnetism in Metallic Mixed Crystal Series. By **Eckhart Vogt** 1
Existence of Resistance Limits for Mixed Crystals with Irregular Atom Dispersion. By **R. Glocker** 40
Influence on the Threshold of Hearing of the Disturbance in the Sound Field Produced by the Head and the Ear Mechaism. By **Georg v. Békésy** 51
Lower Limit of Sensitivity of Technical Potassium Cells and their Application to the Photoelectric Measurement of α-Preparations. By **G. A. Teves** 57
Excitation of Undamped Vibrations of Decimeter Wave-length in the feed-back Circuit. By **W. Kroebel** 80
Direction Distribution of Electrons Emitted from Potassium Atoms by Ultraviolet Polarized Light. By **A. Kraus** 103
Application of Acoustic Filters as Noise Suppressers. By **K. Schuster and M. Kipnis** 123

COMPTES RENDUS

Vol. 194, No. 26 — June 27, 1932

Investigations of the Optical Density and the Viscosity of Therapeutic Serums. By **Charles Achard, Augustin Boutaric and Madeline Gautrot** 2249
Improvements of Rare Gas Glow Tubes. By **Georges Claude** 2253
Ascending Globular Lightning in Mountains and Elevated Plateaus. By **E. Mathias** 2257
Stability of the General Laminar Motion of an Incomprehensible Viscous Fluid. By **A. Rosenblatt** 2284
Problem of n Bodies of Variable Mass Treated with the Equality of Levi-Civita. By **M. Mendes** 2289
Molecular Surfaces and Volumes in a Superficial Solution. Interpretation and Application to the Determination of Molecular Masses. By **D. G. Dervichian** 2294
Dispersion of Anomalous Magnetic Birefringence. By **René Lucas and Marcel Schwob** 2296
Cabannes-Daure Effect and the Molecular Field in Molecular Diffusion. By **A. Rousset** 2299
Thermal Variation of Magnetic Rotatory Power. Study of Solutions of Nickel Chloride. By **H. Ollivier, J. Pernet and J. Lesne** 2301
Anomalies in Radiographs Obtained by Semi-conducting Cells. By **G. Reboul** 2304
On Radioactive Transformations. By **L. Wertenstein** 2305
Passivity of Electrolytic Iron in an Alkaline Medium. By **A. Travers and J. Aubert** 2308
Biological Action of Monochromatic X-rays of Different Wave-lengths on the Eggs of Ascaris. By **A. Dognon** 2336

PHYSIKALISCHE ZEITSCHRIFT DER SOWJETUNION

Vol. 1, No. 4 — April, 1932

Kinetics of the Oxidation of the Mixtures of CH_4+O_2 and $C_2H_6+O_2$. By **A. Kowalsky, P. Sadownikow and N. Tchirkow** 451
Ultraviolet Absorption Spectrum or Ozone and the Structure of the O_3 Molecule. By **A. Jakowlewa and V. Kondratjew** 471
On the Fundamentals of the Theory of Statistical Equilibrium and Irreversible Processes. By **J. Frenkel** 485
Note on a Relation between the Speed of Crystallization and Viscosity. By **J. Frenkel** 498
On the Formation of Molecules from Atoms under Light Radiation. By **V. Kondratjew** 501
Energy Transfer and the Quenching of the Fluorescence in Iodine Vapor. By **M. Eliaschewitsch** 510
Range of the Thermal Ignition of Mixtures of Methane and Oxygen. By **M. Neumann and A. Serbinoff** 536
Oxidation of Hydrocarbons and the Chain Theory. By **N. N. Semenoff** 546
On the Analogy between the Decomposition Reaction of Cl_2O and the Oxidation of Ethane. By **N. N. Semenoff** 561
Mechanism of the Upper Limit (Pressure Limit for Explosive Reaction). By **A. Kowalsky and P. Sadownikow** 567

On the Question of the Existence of a Critical Temperature of Condensation. By **M. Gen, M. Lebedinsky and O. Leipunsky** 571
On the Mechanism of the Ignition of Mixtures of H_2+O_2. By **F. Dubowitzky** 586
Letters:
Apropos a New Kinetic Law. By **N. N. Semenoff** 589
On the Possibility of Active Absorption on Molecularly Smooth Surface. By **A. Magid and S. Roginsky** 592
On the Active Absorption and Its Role in Catalysis. By **O. Leipunsky and S. Roginsky** .. 593
Combustion Kinetics of Hydrogen. By **A. Kowalsky** 595
Propagation Velocity of Flames in Heated Gas Mixtures. By **A. Sokolik and E. Wetrow** .. 597
About a General Law Concerning Reaction Rates in the Case of Exothermic Reaction. By **N. N. Semenoff** 601

INDIAN JOURNAL OF PHYSICS

VOL. VII, PART 1 APRIL, 1932

Surface Convection and Variation of Temperature near a Hot Surface. By **L. A. Ramdas and S. L. Malurkar** 1
Magnetic Rotations of Liquid Mixtures. By **Ram Narain Mathur and Amar Nath Kapur** . 15
Diamagnetism and Structure of some Compounds of Ethylene, Carbon Tetrachloride and Titanium Tetrachloride. By **V. I. Vaidhianathan and Balwant Singh** 19
On the Performance Test in Statistics. By **S. R. Savur** 27
Diamagnetism of Bismuth. By **S. Ramachandra Rao** 35
X-ray Analysis of the Structure of Diphenyl. By **Jagattaran Dhar** 43
On the Raman Spectra of Piperidine, Ethyl Alcohol and Acetone. By **S. C. Sirkar** 61
Polarization of Raman Lines in Liquids. By **S. Bhagavantam** 79
Note on the Variation of Faraday Effect with Concentration. By **P. K. Pillai** 87
Note on a New Rotating Commutator. By **A. Venkat Rao Telang** 91
Note on the Coefficient of Viscosity of Liquid Sodium Amalgams. By **G. R. Paranjpe** 95
Review—The Physical Properties of the Soil. By **Bernard A. Keen** 99
The Institute of Physics 103

PROCEEDINGS OF THE NATIONAL ACADEMY OF SCIENCES

VOL. 18, NO. 7 JULY, 1932

Concentration of the H_2 Isotope of Hydrogen by the Fractional Electrolysis of Water. By **Edward W. Washburn and Harold C. Urey** 496
Electronic Structure of the Normal Nitrous Oxide Molecule. By **Linus Pauling** 498

BUREAU OF STANDARDS JOURNAL OF RESEARCH

VOL. 9, NO. 3 SEPTEMBER, 1932

New Determination of the Atomic Weight of Osmium. By **Raleigh Gilchrist** 471
"Moisture Expansion" of Ceramic Whiteware. By **R. F. Geller and A. S. Creamex** 472
Infrared Arc Spectra Photographed with Xenocyanine. By **W. F. Meggers and C. C. Kiess** 473
Tensile Properties of Cast Nickel-Chromium-Iron Alloys and Some Alloy Steels at Elevated Temperatures. By **William Kahlbaum and Louis Jordan** 474
Comparison of High Voltage X-ray Generators. By **Lauriston S. Taylor and K. L. Tucker** 475
Structure of the Chromic Acid Plating Bath; the Theory of Chromium Deposition. By **Charles Kasper** 476
Physical Properties and Weathering Characteristics of Slate. By **D. W. Kessler and W. H. Sligh** 477
Radiation from Caesium and Other Metals Bombarded by Slow Electrons. By **C. Boeckner** 478
Simplified Precision Formula for the Inductance of a Helix with Corrections for the Lead-in Wires. By **Chester Snow** 479

Register Studies in Offset Lithography. By **C. G. Weber and R. M. Cobb** 480
Creep at Elevated Temperatures in Chromium-Vanadium Steel Containing Tungsten or Molybdenum. By **William Kahlbaum and Louis Jordan** 481

JOURNAL OF THE FRANKLIN INSTITUTE

VOL. 214, NO. 2 AUGUST, 1932

Development and Use of Talking Motion Pictures. By **H. M. Wilcox** 137
Use of a Thermionic Tetrode for Voltage Control. By **J. C. Street and Thomas H. Johnson** 155
Polychrome Photography. By **Frederic E. Ives** 163
Resources of the Ocean. By **Harden F. Taylor** 167
Red Shift. By **H. E. Buc** 197
Vibrations of Rods and Plates. By **Robert C. Colwell** 199
Magnetic Field Intensity Near a Circular Loop Carrying an Electric Current. By **A. L. Fitch** 215
Method for the Calculation of the Correct and Most Economical Concentrations of Elon and Hydroquinone in a Borax Developer for Motion Picture Film. By **Alan M. Gundelfinger** 223